THE TREATMENT OF VACUUM DISTILLED RESIDUE FROM THE CANMET PROCESS IN ARGON/HYDROGEN PLASMAS

by

Bogdan Zygmunt Dlugogorski, B Sc in Chem Eng.

Department of Chemical Engineering

A thesis submitted to the Faculty of Graduate Studies and Research of McGill University in partial fulfilment of the requirements for the degree of Master of Engineering

McGill University
Montreal, Canada

September 1989

Bogdan Zygmunt Dlugogorski
M Eng.

The Treatment of Vacuum Distilled Residue
in Argon/Hydrogen Plasmas

THE TREATMENT OF VACUUM DISTILLED RESIDUE FROM THE CANMET PROCESS IN ARGON/HYDROGEN PLASMAS

ABSTRACT

The pitch-like carbonaceous material obtained from the CANMET hydrocracking process as vacuum distilled residue was treated in a stationary particle (semi-batch) reactor with argon/hydrogen plasmas. The average plasma temperature was varied between 2190 and 4450 K, and its hydrogen content was changed between 0 and 33 %.

The results indicate that the residue is pyrolysed, and the gas phase reactions lead to the production of acetylene, ethylene, methane, hydrogen, carbon monoxide and trace amounts of ethane and hydrogen sulphide. No liquid hydrocarbons were detected but soot was also produced. Nitrogen is concentrated in the unconverted residue whereas hydrogen and oxygen are preferentially removed. Sulphur is fixed in the unconverted residue by reduction of calcium sulphate to calcium sulphide Because of highly condensed aromatic structure of the residue, the conversion of carbon to light unsaturated hydrocarbons was not higher than 14 % in argon and 24 % in argon/hydrogen plasmas. The production of acetylene was optimized between 2900 and 3400 K. As a result of the high ash content of the residue, the conversion of carbon to carbon monoxide is between 1.5 and 4 5 %.

RESUME

Le résidu de la distillation sous vide dans le procédé d'hydrocracking CANMET, une substance à base de carbone ressemblant à du goudron, a été traité dans une réacteur à particules fixes (semi-continu) avec des plasmas à argon/hydrogène. La température moyenne du plasma a été variée entre 2190 et 4450 K, et le contenu en hydrogène a eté garde entre 0 et 33 %

Le résultats indiquent que le résidu est pyrolysé, et que les réactions en phase gazeuse entrainent la production d'acetylene, d'ethylene, de méthane, d'hydrogène, de monoxyde de carbone et de très faibles quantités d'éthane et d'hydrogène sulfuré. La présence d'hydrocarbures liquides n'a pas été détectée mais de la suie a eté produite L'azote est concentre dans le residu non converti alors que l'hydrogene et l'oxygène sont soutires de façon préférentielle. Le soufre est fixé dans le résidu non converti par la réduction du sulfate de calcium en sulfure de calcium A cause de la structure aromatique condensée du résidu, la conversion du carbone en hydrocarbures légers non saturés n'était pas plus haute que 14 % dans le plasmas à argon et 24 % dans les plasmas à argon/hydrogène. La production d'acétylène a été optimisée à des températures variant entre 2900 et 3400 K. La haute teneur en cendres du résidu entraine une conversion du carbone en monoxyde de carbone se situant entre 1.5 et 4.5 %.

ACKNOWLEDGEMENTS

I would like to take this opportunity to thank all those who helped in the successful completion of this research project

Especially I am indebted to my professors and colleagues for many useful discussions In particular I would like to express my gratitude to Professors Dimitrios Berk and Richard J Munz for their guidance in the course of this work

I owe a special debt to Dr Jean-Luc Meunier whose knowledge in spectroscopy was invaluable Without him the spectroscopic temperature measurements would not have been possible

Mr Andre Dufresne from the School of Occupational Health at McGill University introduced me to the interesting field of the X-ray powder diffraction

It is a pleasure to mention fellow graduate students who assisted in the experimental runs Maysa Habelrih, Peter Patterson, Pritham Ramamurthy and Xuejun Zou. Summer student, Mr. Stanley Fong helped in the development of the suction probe

I would like to express my appreciation to Mr Charles Dolan from the Chemical Engineering Workshop for the construction of the important parts of the apparatus His work was always of the greatest quality

I am particularly thankful to my wife Eve for her ability to understand and support my work on this project For their priceless help special recognition goes to my parents-in-law I say thanks to my little son David who did not mind not to play with his daddy too often

I would indeed be ungrateful if I did not mention a financial support in the form of research scholarships from the National Science and Engineering Research Council of Canada and the Eugenie Lamothe Bequest which I held for the last two years. In addition the cost of the equipment and the analysis was covered by CANMET, Energy, Mines and Resources Canada.

To my mother and father,
Aleksandra and Zygmunt Dlugogorski

TABLE OF CONTENTS

LIST OF FIGURES

LIST OF TABLES

LIST OF SYMBOLS

A_{pq}	Probability of the Transition, s^{-1}
c	Speed of Light in Vacuum, $2.9979 \cdot 10^{8}$ m s^{-1}
c_1	First Radiation Constant, $3.7415 \cdot 10^{-16}$ W m^{2}
c_2	Second Radiation Constant, $1.4388 \cdot 10^{-2}$ m K
c_p	Heat Capacity, cal K^{-1} mol^{-1}
e_1, e_2	Emissivities
$E(\lambda,T)$	Monochromatic Emissive Power of a Black Body, W m^{-3}

E_p	Energy of the Upper Excited State, J
g_p	Statistical Weight of Level p
h	Planck Constant, $6.6262 \cdot 10^{-34}$ J Hz^{-1}
$H(\lambda,T)$	Incident Flux Density, W m^{-2}
I	Intensity of a Spectral Line, W m^{-3}
k	Boltzmann Constant, $1.3807 \cdot 10^{-23}$ J K^{-1}
N(T)	Total Density of Atoms, m^{-3}
n_e	Electron Density, cm^{-3}
$N_p(T)$	Population Density of the Species in the Excited Upper Level p, m^{-3}
p	Upper Energy Level
PP	Plate Power, kW
q	Lower Energy Level
r	Distance from the Symmetry Axis of the Reactor, mm
r	Reaction Rate, s^{-1} (Chapter 7)
t	Time, s
T	Absolute Temperature, K
T_a	Apparent Temperature, K
T_f	Final Quenching Temperature, K
T_o	Initial Quenching Temperature, K
T_t	True Temperature, K
$w_{1/2}$	Half Width of Hβ Hydrogen Line, Å
Z(T)	Partition Function
λ	Wavelength, m^{-1}
R^2	Coefficient of Correlation

(SI Equivalent Units: 1 Å = 10^{-10} m, 1 cal = 4.184 J)

LIST OF ABBREVIATIONS

AC	Alternating Current
CEC	Control Equipment Corporation
DC	Direct Current
EMI	Electromagnetic Interference
GC	Gas Chromatography
LTA	Low Temperature Asher
LTE	Local Thermodynamic Equilibrium
RF	Radio Frequency
RFI	Radio Frequency Interference
SEM	Scanning Electron Microscopy
SER	Specific Energy Requirement, MJ/(kg C_2H_2 and/or C_2H_4)
STP	Standard Temperature and Pressure (100.3 kPa, 293.15 K)
TCD	Thermal Conductivity Detector
THF	Tetrahydrofuran
XRD	X-Ray Powder Diffraction
XRF	X-Ray Fluorescence

1.0 Introduction

Since the end of the previous century western civilization has progressively become more dependent on energy sources derived from fossil fuels. Initially, coal, which is in the greatest supply, was the most widely used fuel. However, over the last 50 or 60 years, in all highly industrialized countries, crude oil and natural gas have emerged both as the principal sources of energy and very important feedstocks in the chemical industry. This contrasts with the fact that most of those countries have only small and relatively isolated deposits of liquid fuels. Hence, processes for conversion of coal and natural gas into the liquid petroleum have gained substantial interest from several governments. However, it appears that there is no unique solution, and depending on the regional conditions, every country has developed different technologies. For example, New Zealand, having large deposits of natural gas, converts it to gasoline via methanol. On the other hand, the Republic of South Africa, wishing to remain independent of imported oil, has successfully improved Fischer-Tropsch process for conversion of coal into liquid hydrocarbons.

Canada, which possesses some of the world's most important sedimentary deposits of coal and heavy oil, has been involved in the development of a hybrid process. The concept has been to mix finely ground coal particles with the heavy oil or heavy oil vacuum bottoms and an additive (functioning as a catalyst), and then to hydrogenate the resulting mixture. Details about the (CANMET) process may be found elsewhere (Menzies *et al.* 1981). Here, only the relevant points will be described.

The additive, which until recently was iron sulphate (Rahimi *et al.* 1989) or other metallic salts, comprises 0.5 to 5 mass % of the feed. Together with the undistilled hydrocarbons and the ash derived from coal and heavy oil it represents the residue. Since such residue, contains relatively large amounts of iron, sulphur (from the catalyst, coal and heavy oil), oxides of aluminum, silicon and calcium (from coal) it has no commercial value and it may be discarded. In 1981, it was estimated that the CANMET additive would cost $10,200/day whereas the initial capital and operating costs for the hydrotreaters charge would be $3,400,000 and $6,300/day respectively (Menzies *et al.* 1981). If, however, a newly developed catalyst is based on more expensive metals, such as nickel or tungsten and molybdenum sulphides, its regeneration may determine the economic feasibility of the process.

Several possible traditional schemes for recovery of spent catalyst can be investigated. For instance, the entire residue can be burnt and the catalyst can be recovered from the resulting fly ash. Such an approach would be associated with large capital investments.

An alternative process is treating the residue with a hydrogen plasma. In contrast to the traditional technology, where only the catalyst is recovered, the production of sizeable quantities of light unsaturated hydrocarbons, especially acetylene, might be expected. In the Province of Quebec with its cheap electricity a similar process for the conversion of the natural gas to acetylene has been found to be economically viable (Cooke *et al.* 1987).

The general objective of the research project was to assess the technical feasibility of a CANMET residue to acetylene process. Specific objectives were (1) to build laboratory scale equipment including a reactor and sampling train, (2) to develop experimental and analytical techniques which could be used for studying the treatment of the residue in argon/hydrogen plasma, (3) to investigate the effect of different operational conditions, such as temperature, concentration of hydrogen or residence time, on the product distribution and finally (4) to understand the governing mechanisms during the production of acetylene from the CANMET residue in argon/hydrogen plasmas.

The thesis is organized as follows: Chapter 2 reviews the literature of the plasma treatment of fossil fuels and Chapter 3 presents the results of a thermodynamic analysis on which the design of the equipment and experiments were based. The apparatus is described in Chapter 4 while the results of residue characterization experiments are described in Chapter 5. The characterization of the plasma and reactor system by calorimetry, spectroscopy and thermocouple probes is discussed in Chapter 6. Finally, the experimental results of the plasma treatment of the residue are given in Chapter 7.

2.0 LITERATURE REVIEW OF PLASMA OF FOSSIL FUELS

2.1 Introduction

Very extensive literature is available on the subject of the plasma chemistry of fossil fuels. Venugopalan *et al.* (1980) have compiled the most comprehensive review of the topic ever published Several authors have devoted separate chapters to plasmas in hydrocarbons. These include papers by Kevorkian (1962) and Vurzel and Polak (1965b) who have summarized plasma research prior to 1961. Brzeski *et al.* (1983) and Drost (1978) have examined the recent progress in plasma experimentation and theory over last three decades

Although several classifications, to describe plasma reactions in hydrocarbons, have been developed, the following scheme appears to be the most practical: according to the type of substrate Venugopalan *et al.* (1980) distinguish among reactions in (1) natural gas and methane plasmas, (2) petroleum plasmas, (3) plasmas in coal, (4) other fossil fuel plasmas. In addition, they divide each group into reactions in non-equilibrium glow discharges and equilibrium arcs and jets. They describe separately the desulphurization of petroleum and coal, flash heating and reactions initiated by laser irradiation

Ir the field of chemical processing Baddour and Timmins (1967) define plasma as "a gaseous system sufficiently ionized to be electrically conductive but still electrically neutral." For purposes of this work there is no need to accept a more restrictive definition. Non-equilibrium plasma is defined as one for which the inequality Te > Ti > Tg holds (Te, Ti, and Tg denote temperatures of electrons, ions and neutral particles). Conversely equilibrium plasma exists when the average kinetic energy of electrons, ions, and neutral particles remains similar (Brzeski *et al* 1983). In the Western literature the equilibrium plasma is denoted as hot or thermal whereas cold plasma implies lack of thermal equilibrium. However, in the Eastern Europe another term - low temperature plasma - is also used; it includes both equilibrium and non-equilibrium plasmas below 15 000 K (Brzeski *et al.* 1983, Vurzel and Polak 1970). An exhaustive description of the meaning of plasma chemistry is given by Drost in the introduction to his book (Drost 1978).

Descriptions of an electric arc discharge and a plasma jet may be found in the literature, for example Boulos *et al.* (1986) or Kevorkian (1962). In general, a plasma jet incorporates an arc discharge whose cross-sectional area is artificially constrained. Since higher temperatures are possible with plasma jets, a hydrocarbon gas may be mixed with a plasma gas outside of an arc discharge (plasma pyrolysis). This procedure eliminates some inherent disadvantages (high conversion of feed to soot rather than to acetylene, Brzeski *at al.* 1983) of passing hydrocarbons through an arc (electrocracking).

The space which may be devoted to the literature review is rather limited. Hence I was faced with a necessity to confine the scope of this survey. Although the investigation of non-equilibrium reactions of fossil fuels has been an important research area, during the last century, these reactions have not been used in industrial hydrocarbon processing On the other hand, plasma reactions in arcs and jets, satisfying the equilibrium conditions, ie. $Te \approx Ti \approx Tg$, have been successfully employed in several practical applications. The equilibrium reactions will be covered here in more detail. The chemical reactions taking place in non-equilibrium plasmas, which are important in chemical processing, have been reviewed by Vurzel and Polak (1970). Reactions of hydrocarbons in glow discharges have been examined by Venugopalan (1980).

2.2 Comparison of Homogeneous and Heterogenous Systems

It has been shown that fundamental differences exist between homogeneous and heterogeneous reactions in plasmas (Fauchais *et al.* 1980). For example, the research published by Graves *et al* (1966) proved that as a result of heat transfer limitations between a hot plasma gas and coal particles, a complete thermal decomposition did not take place. In addition, Honda *et al.* (1985) reported results from a simulation study on decomposition of coal in argon plasma. Assuming that the decomposition rate was limited by heat transfer and using an energy balance, they could correlate conversion with the argon flow rate, electric input power and residence time. It is well known that the addition of even 10 percent of hydrogen to argon plasma may dramatically change its transport properties, especially its thermal conductivity. Several experimental investigations have confirmed that conversion of coal to light unsaturated hydrocarbons was enhanced in argon/hydrogen plasmas, and this improvement was not due to a direct reaction between hydrogen and coal (Anderson *et al.* 1968, Beiers *et al* 1985, Chakravartty *et al.* 1984)

Moreover, there is an interaction between plasma and cooled reactor walls. As reported by Szymański *et al.* (1978b) part of hydrocarbons, fed in liquid phase, does not evaporate in the plasma but rather forms a flowing film on reactor walls; this results in the lower overall conversion. Furthermore, coal particles may agglomerate (coke), during the injection into a plasma flame, forming clinkers and eventually choking the injection nozzle. This phenomenon was observed by Chakravartty *et al.* (1976)

Gas phase reactions avoid many of these technical difficulties. Since there are fewer independent variables these reactions may be experimentally optimized and even the yield, product distribution, and specific energy requirement (SER), may be estimated from thermodynamic and kinetic calculations (*e.g.* Gulyaev and Polak 1965, Melamed *et al.* 1965) (SER is defined as the amount of energy required to produce one kilogram of acetylene, it is measured in MJ/kg). On the other hand, reactions of solid or liquid hydrocarbons (*i.e.* hydrocarbons injected in liquid phase) in plasma are poorly understood phenomenologically although an interesting reaction mechanism has been reported in recent literature (Baumann and Bittner 1988, Baumann *et al.* 1988)

As a result of the above-stated dissimilarities homogeneous and heterogeneous systems will be discussed separately

2.3 Homogeneous Systems

2.3.1 Optimum Conditions for Methane Decomposition in Plasma

The first industrial process for the plasma production of acetylene, known as Huls process, was developed using an electric arc discharge (Baumann 1948) and therefore it was rather energy inefficient Since the advent of plasma jets, at the end of 1950's, hydrocarbon plasma processing has undergone a rapid expansion.

As early as 1961, Leutner and Stokes have reported that methane can be converted to acetylene at 80 % yield by feeding methane into the tail flame of an argon plasma jet. Subsequently, their experiments were duplicated in the U.S.S.R. for higher flows of methane (Gulyaev *at al.* 1963). Initial thermodynamic and kinetic analysis of CH_4 decomposition in plasma were performed by Anderson and Case (1962); in the calculations they included CH_4, C_2H_2, H_2, H. Gulyaev and Polak (1965) proved that results from thermodynamic calculations remain in a close agreement with experimental results They ensured that mixing between cold feed (CH_4) and hot plasma gas was approximately 15 times faster than acetylene formation. In addition they maintained quenching rates above 10^6 K/s preventing acetylene decomposition. It is worthwhile to mention that the rate of soot formation is much slower than the rate of acetylene generation and hence thermodynamic calculations ought to be performed only in the gas phase; some researchers use the term quasi-equilibrium as opposed to full equilibrium when both phases are included. Soot consists mainly of carbon but it may contain very small amount of hydrogen.

Gulyaev and Polak's elegant analysis spurred many papers. Plotczyk (1983,1985) has verified, experimentally and numerically, that conversion of methane depends on the quenching temperature. Methane transformation is essentially complete above 1900 K, however conversion to acetylene is maximized between 1900 and 2600 K. His results further corroborate Gulyaev and Polak's conclusion that the highest energy efficiency is achieved at 1900 K.

2.3.2 Decomposition of Other Gaseous Hydrocarbons in Plasma

In the paper, originally published in 1961, Tsentsiper *et al* (1962) indicated that in an arc in addition to methane, ethane, propane, ethylene and propylene can be cracked to acetylene. They noted that conversion of these hydrocarbons to acetylene is associated with improved yields and lower energy consumption.

Vurzel and Polak (1965a) reported results from several experiments conducted both in homogeneous and heterogeneous systems Investigating pyrolysis of n-heptane and gasoline they determined that liquid hydrocarbons should enter a reactor in the vapour state. They also showed that for heterogeneous reactions the conversion diminishes, for example for n-heptane from 79 to 58 %.

Il'in and Eremin, in 1962, performed pyrolysis of gasoline by mixing a hydrogen plasma and gasoline vapour in the reactor (Il'in and Eremin 1962). In another investigation, the same authors (Il'in and Eremin 1965), pyrolysing hexane, heptane, and n-octane determined that the product distributions are similar to those obtained from the previous study. Polak *et al.* (1969) drew analogous conclusions for the pyrolysis of vapours of crude oil in a hydrogen plasma. Their experiments were conducted below 1600 K to avoid formation of soot. As determined by Rozanova and Sidorov (1976) substitution of Diesel oil for gasoline tends to decrease conversion to acetylene and to ethylene Conversion of gaseous or vaporized hydrocarbons in plasma was also investigated by other authors (*e g.* Endyus'kin *et al.* 1974, Gehrmann and Schmidt 1971, Gladisch 1969), and more recently by Beiers *et al.* (1988).

Small amounts of liquid hydrocarbons may be produced during plasma pyrolysis. For example, in Huls process (Baumann 1948) 23 kg of benzol (benzol denotes a mixture distilling below 100 °C and containing 70 % benzene) are manufactured for every 1000 kg of acetylene, whereas in modified Huls process (Gladisch 1969), approximately 1 6 % of cracked propane is converted to benzene. Similarly the pyrolysis of long chain paraffins in a H_2/CH_4 plasma results in about 2 % conversion to liquids However the pyrolysis of high molecular weight cycloalkanes and aromatics (decalin, dodecylbenzene) in a H_2/CH_4 plasma yields up to 12 % of liquid hydrocarbons (Baronnet *et al* 1987).

Apart from processes described above, other interesting investigations include a paper by Il'in and Eremin (1963) about pyrolysis of gasoline vapour in a water vapour plasma, a report by Kerker and Muller (1984) of using a water vapour/methane plasma to produce synthetic gas and lastly a publication by Bonet (1976) who reduced ilmenite in a methane plasma.

2 3.3 Quenching Techniques

If a reacting mixture of hydrocarbons is not cooled rapidly acetylene would participate in a chain reaction leading to the formation of soot (Spangenberg 1981).

$C_2H + C_2H_2 \rightarrow C_4H_3 \rightarrow C_4H + H_2 \rightarrow C_4H_2 \rightarrow .. \rightarrow C_6H_2 \rightarrow . \rightarrow C_8H_2$ *etc.*

However, if the mixture is quenched the C_2H radical may enhance the yield of acetylene (Plooster and Reed 1959) Krukonis and Gagnon (1974), using deuterium and ^{13}C, investigated mechanism of the hydrogen quench. They determined that hydrogen is a more efficient quenching medium than an inert gas as helium, argon or nitrogen. However, they were not able to explain this difference by variations in the conductivity, diffusivity or heat capacity of the mentioned gases. Eventually they suggested a chain mechanism that was initiated by acetylene fragmentation into C_2H, C_2, CH and H. At lower temperatures, the chain reactions were terminated by recombination of C_2H and H or two CH radicals.

Sundstrom and DeMichiell (1971) performed a numerical study to evaluate different quenching techniques: mixing with a cold gas, injection into a fluidized bed, contact with a cold surface or evaporation of a liquid spray. The first two techniques provide the fastest rate of quench - above 10^7 K/s. Quenching by contact with a cold surface with the rate of quench greater than 10^6 K/s is commonly used in a laboratory scale equipment. There are several publications on theoretical and numerical aspects of these quenching techniques (Bukhman *et al.* 1965a&b, Khait 1965, Kurowski and Lesiński 1978); quenching by an adiabatic expansion is described by Spangenberg (1981) and Dessau *et al.* (1985). An experimental comparison of some of quenching techniques may be found in (Drost *et al.* 1985a); quenching by injection into a fluidized bed was studied by Goldberger and Axley (1963).

An increase in the concentrations of acetylene and ethylene in the product gases as well as an improvement in thermal efficiency is achieved by quenching in two stages (Polak 1971). In the first stage gaseous or liquid hydrocarbons are mixed with hot reacting gases. The temperature is decreased due to the evaporation of liquid and heating up of gaseous hydrocarbons. Also, quench hydrocarbons are decomposed in endothermic reactions to C_2H_2, CH_4, H_2 and especially to C_2H_4 This results in further temperature decrease (Plotczyk *et al.* 1986) and it may be described as a chemical quench. The second stage is realized by utilizing one of the standard quenching techniques.

2.3.4 Reaction Mechanism and Catalytic Effects

Kassel (1932,1935), who studied the thermal decomposition of methane in quartz bulbs between 700 and 850 °C, concluded that the primary rupture may be represented as $CH_4 \rightarrow CH_2 + H_2$. This result was soon disputed by Rice and Dooley (1934) who did not detect methylene radicals (CH_2) but instead observed methyl groups (CH_3); they represented the primary step as $CH_4 \rightarrow CH_3 + H$ Nevertheless the Kassel's mechanism, slightly updated (Shantarovich and Pavlov 1956), has been repeatedly applied, for over forty years, in simulation of methane decomposition in plasma (Vurzel and Polak 1975, Kurowski and Lesiński 1978).

The kinetics of thermal decomposition of ethane, ethylene and acetylene, between 1000 and 1600 K, were investigated by Towell and Martin (1961). Ostroff and Miller (1971) determined an Arrhenius expression for decomposition of benzene between 1400 and 2200 K.

Since the invention of a shock tube, described by Kevorkian (1962), there has been a substantial progress in the understanding of the reactions of formation and decomposition of light unsaturated hydrocarbons at high temperatures (Frenklach *et al.* 1984, Klotz *et al.* 1983, Koike and Morinaga 1981, Spangenberg *et al.* 1986, Tanzawa and Gardiner 1978). Borger *et al.* (1982) and Spangenberg *et al.* (1985,1986) showed that decomposition of methane is of the first order (in methane) below 1850 K and it changes to the second order above 2200 K; formation of methyl radicals was taken as the primary step. Their experiments included measurements in plasma jets and behind reflected shock waves. The same authors studied the kinetics of formation of higher acetylene derivatives (Spangenberg *et al.* 1978) and creation of soot particles (Spangenberg *et al.* 1983).

It is worthwhile to mention that although thermodynamic calculations were successfully applied by Gulyaev and Polak (1965) to methane, this approach may not be as accurate for other hydrocarbons For instance, Il'in and Eremin (1965) demonstrated that due to the distinct kinetic mechanisms the plasma decomposition of n- and i-octane showed different product distributions. A variation in the product distribution was also observed by Beiers *et al.* (1988), who maintained C/H ratio, temperature and pressure constant but changed feed hydrocarbons, C/H = C in hydrocarbon / (H in plasma + H in hydrocarbon). This is yet another proof that reactions in plasma are kinetically controlled

Conversion of propane to acetylene in an argon plasma may be increased with the presence of aluminum, tungsten or iron vapours, as investigated by Meubus (1975a&b). The introduction of nickel particles during the pyrolysis of C_1-C_4 hydrocarbons changes the product distribution (Moisyeyev *et al.* 1986) The acetylene yield could be as high as 100 % for iron, 93 % for aluminum and 87 % for tungsten vapours. In the absence of metals similar yield is around 70 %. Also, the metals vapours tend to decrease the reaction temperature required for maximum yield. Meubus attributes these phenomena to catalytic effects taking place on surfaces of minute metal crystals which condense during quenching In addition in the presence of aluminum, C_2H radicals are preserved by energy transfer from excited Al atoms during the quenching process The effect of irradiation by UV light, during cracking of propane in an argon plasma gas, is investigated in yet another paper by the same author (Meubus 1985).

Drost *et al.* (1985a), performing experiments in a single pulse shock tube, found that even small addition of ethane (less than 5 %) to methane may improve yields of acetylene and particularly ethylene - up to eight fold at 1500 K From the decay curves they concluded that ethane is pyrolysed faster than methane. They theorized that C_2H_5 radicals were responsible for a better conversion to ethylene.

2.3.5 Plasma Reactors

In initial experiments Leutner and Stokes (1961) attempted to use an argon/methane plasma jet to produce acetylene. However, they were not able to control heat transfer to the tungsten cathode which melted instantaneously. Gulyaev and Polak (1965) were not only capable of operating their torch with a pure hydrogen plasma but also they succeeded in designing a reactor in which the mixing time between hydrogen and methane was 10^{-5} s.

Processing of hydrocarbons in thermal radio frequency (RF) reactor, inductively coupled, was investigated by Ibberson and Christofides (1977,1983). The residence times were between 6-8 ms, over 40 times longer than optimum, resulting in severe decomposition of acetylene to soot. Furthermore, mean exit temperatures were between 3000 and 4000 K, the optimum temperatures calculated from full thermodynamic equilibrium. It is clear that RF reactor is not well suited for production of acetylene but may be successfully employed in manufacturing of acetylene black (Bolouri 1983).

Application of a capacitatively coupled RF plasma for thermal pyrolysis of methane and heavy oils was studied by Kovener (1983). He concluded that RF plasma jet pyrolysis of hydrocarbons may not compete with AC or especially DC devices in industrial applications. It is known that capacitatively coupled RF plasma torches have efficiency of only 20-30 % (Brzeski *et al.* 1983). Iberson and Christofides (1977) reported 49 % efficiency for their torch. In spite of these drawbacks RF torches are ideal laboratory tools since they do not contaminate the plasma gas.

An interesting reactor for hydrocarbon processing is described in a recent patent (Hoffmann *et al* 1983). The reactor chamber is lined with graphite through which several holes are drilled, parallel to the axis of the reactor. Liquid or liquefiable hydrocarbons are fed into the graphite lining at the bottom of the reactor. As they flow upwards they are vaporized and are eventually injected into the reactor chamber.

Some aspects of the design of a plasma reactor, including selection of its shape and scaling up equations, are discussed by Szymański (1978).

2.3.6 Specific Energy Requirement

Any industrial process of plasma production of acetylene, to be commercially successful must minimize the consumption of electricity. The following discussion will be based in part on a paper by Krukonis and Schoenberg (1968) Decomposition of methane to acetylene is an endothermic reaction with energy consumption of 354.4 kJ/(mol of acetylene) or SER = 13.6 MJ/kg. Assuming 80 % conversion of methane to acetylene and including the sensible heat for heating a plasma gas and methane to 2000 K one obtains SER of around 17 5 MJ/kg. Energy losses from a reactor and from torch electrodes tend to increase minimum SER further to 23 - 25 MJ/kg However decomposition of higher hydrocarbons is not as endothermic. Additionally, more acetylene and ethylene may be produced during the two stage quench. For example, newly developed AVCO process (Patrick *et al*. 1985) for conversion of coal to acetylene and ethylene is credited with SER of 22 MJ/(kg of C_2H_2 and C_2H_4).

A more refined analysis of SER for methane conversion to acetylene in a plasma process was performed by Szymański (1977) and by Szymański *et al* (1978c).

2 3.7 Industrial Applications

A comparison among existing industrial processes as Huls (Baumann 1948), Westinghouse (Fey *et al*. 1985), Du Pont, modified Huls (Gladisch 1969), Hochst (Gehrmann and Schmidt 1971), and WLP (Knapsack-Griesheim) (Sennewald 1963) may be found elsewhere (Brzeski *et al*. 1983, Drost 1978, Fauchais *et al*. 1980). In general Huls, Westinghouse and Du Pont utilize electrocracking technology whereas modified Huls, Hochst and WLP employing plasma pyrolysis process, accept liquid and gaseous feed. The Huls process has been in operation in Germany since 1928 (Foster 1985). The Du Pont plant in Montague in the U S.A., came on stream in 1962 but it had to shut down in 1968 due to the contracting market for acetylene (Kushner 1985) and reduced cost of calcium carbide. Manufacturing costs of acetylene in the Huls or the Du Pont plant were approximately equal (Polak 1967).

Drost (1978) and Brzeski *et al.* (1983) give information about pilot plants in Romania (in Borzesti, 20 kW), in Czechoslovakia (Brunn process, 35 kW) and in Poland (in Tarnów, 100 kW), nevertheless it is not certain if these installations are still in operation. There are no detailed data on pilot plants in the U.S.S.R. although it appears that the research is conducted not only in Moscow but also in Azerbaijan (Melik-Zade *et al.* 1975), in Byelorussian (Zabrodin *et al.* 1973), in Kirghiz (Kolobova *et al.* 1984 and 1985), and in Tajik (Novikova *et al.* 1984) Soviet Republics.

2.4 Heterogeneous Systems

2.4.1 Reactions of Graphite and Coal in High Intensity Arcs

Several kinetic and thermodynamic studies, on reactions between carbon and hydrogen at high temperatures were reviewed by Clarke (1967). They included papers on graphite rods and tubes, on fixed beds, on graphite filaments and on high intensity arcs.

Baddour and Blanchet (1964), and Baddour and Iwasyk (1962), using a consumable anode in a high intensity arc, produced acetylene and condensed carbon. The concentration of acetylene was as high as 26 % in a hydrogen/inert gas plasma, and 52 % with methane feed, supporting Plooster and Reed's hypothesis (1959) that C_2H radicals improve the acetylene yield.

Leutner and Stokes (1961) produced small amount of acetylene by feeding powdered carbon into an argon/hydrogen jet. This confirms the conclusion by Baddour and coworkers that a plasma jet reactor is inferior to a high intensity arc reactor for investigations of the kinetics of reactions between carbon and hydrogen at high temperatures. Subsequently, Amman *et al.* (1964), Krukonis and Gagnon (1974) as well as Krukonis and Schoenberg (1968) used an arc reactor in decomposition of coal whereas Sheer and Korman (1974) employed a carbon anode for arc synthesis of hydrocarbons.

2.4.2 Inorganic Matter in Coal and Addition of Catalysts

Certain interesting results were obtained by processing coal with high ash content in an argon plasma (Kozlova *et al.* 1977). It was shown that for the coal particles between 63 and 160 μm, 20 % of the SiO_2 was converted into SiC. On the other hand, the product gases contained mostly hydrogen (47.7 %), carbon monoxide (45.0 %), and small amounts of oxygen (3.4 %) and acetylene (4.0 %).

The mount of inorganic matter contained in coal may have a significant effect on the overall conversion and on the yield of acetylene in particular. This was experimentally verified by Bittner *et al.* (1985) for South African, German and American coals, as well as by Chakravartty (1976,1984) for Indian coals. In general, decomposition of coals with higher ash content increases the conversion to carbon monoxide at the expense of the conversion to acetylene, *i.e.* metal oxides are reduced by the carbon content.

The effect of some catalysts (cobalt molybdenite, zinc chloride and calcium chloride) was studied by Anderson *et al.* (1968). An addition of $CaCl_2$ to coal, during processing in an argon/nitrogen plasma, resulted in an increase in production of H_2, CH_4, C_2H_2 and HCN. However, in an argon/hydrogen plasma the presence of catalysts decreased production of C_2H_2 and HCN by as much as 50 %.

Some coals may contain sulphur bearing minerals as pyrite (FeS_2) and pyrrhotite ($Fe_{1-x}S$). At high temperatures, sulphur from the decomposing sulphides reacts with carbon and hydrogen to form H_2S and COS Sulphur absorbing compounds (calcium carbonate or potassium carbonate) may be added to the feed; during processing they form CaS and K_2S (Bozzuto 1984). It appears likely, however, that application of either carbonate could result in decrease of acetylene and in increase of carbon monoxide yields.

Finally, heterogeneous reactions between reactor walls and a plasma gas are considered to be not important (Szymański 1979).

2 4 3 Effect of Grain Size and of Volatile Content

A summary about different processing parameters and their importance on conversion of coal to acetylene was given by Kulczycka (1978) Since the size of coal particles, the amount and type of volatiles present in coal as well as plasma gas appear to be extremely significant they will be covered here in more detail

It is universally accepted that higher conversions to acetylene are achieved with decreasing grain size of coal, below 10 μm coal particles tend to agglomerate. Conversion of coal to acetylene may be increased by proper selection of size distribution of coal particles which would burst in the plasma jet due to a fast liberation of volatile material (Baumann *et al* 1988, Bond *et al.* 1966, Kozlova and Kukhto 1976, Kulczycka 1978) This process is aided by lowering the pressure in a reactor

The maximum conversion of coal is constrained by the amount of hydrogen initially present in coal (C/H ratio) and its distribution among aliphatic, alicyclic and aromatic hydrocarbons (Chakravartty *et al* [illegible]) Bittner *et al.* (1985) reported that "the maximum acetylene yield will be obtainable in the transitional range between high and medium volatile bituminous coals "

It was determined that addition of hydrogen to an argon plasma enhances conversion of coal to acetylene by roughly two times (Bittner *et al* 1985, Nicholson and Littlewood 1972, Szymański *at al* 1978a, and in case of coal extracts by even three times (Kulczycka 1974) The yield of acetylene increases rapidly between 0 and 10 % of hydrogen in plasma, however it levels off for higher hydrogen concentrations For example, Nicholson and Littlewood (1972) were able to obtain a maximum acetylene yield of 74 %, on a carbon basis, with 10 % hydrogen plasma Low feeding rates of coal, in those experiments, might have allowed a complete pyrolysis of the fed coal Similarly, Kawana *at al* (1967), obtained 52 % conversion to acetylene in an argon plasma, at very high SER of 486 MJ/kg

Reaction of coal with a hydrogen plasma involves two phenomena pyrolysis and hydrogenation in the gas phase ([illegible] and [illegible] 198[illegible]) According to a theory put forward by Baumann and coworkers ([illegible]) a rate limiting step is pyrolysis of the coal itself which requires approximately 4 ms. Primary volatiles which are formed consist mostly of tars and small amounts of low molecular weight gases. These tars undergo very fast reactions (reaction time less than 0.4 ms) leading to the formation of acetylene. The reaction temperature should be high enough to promote bursting of coal particles but not so high as to result in the formation of soot

2.4.4 Gasification of Petroleum, Coal and Other Fuels in Water Plasmas

If a carbonaceous material is reacted with a water plasma H_2, CO, CO_2 and small amount of hydrocarbons are formed. This method is suitable for production of reducing gases. For example Gauvin *et al.* (1983) and Stuart *et al.* (1984) were able to produce a synthesis gas with H_2/CO ratio of 1.8 from dried and ground peat Since they obtained a carbon conversion of 89 % they concluded that their process, with slight modifications, could be indirectly used for methanol production. Production of the synthesis gas, from a variety of substrates, was reported by Camacho (1985). A similar study but with an argon plasma was performed by Huczko *et al.* (1987). Muller *et al.* (1987a) demonstrated the feasibility of using the Huls process for the production of H_2

Kubanek *et al.* (1985,1986) reported conversion of up to 100 % of Alberta heavy oil in simulated steam plasmas. Other researchers investigated gasification of coal (Belov and Romas' 1978, Dobal 1978, Kolobova *et al* 1985) or oil shale (Nursultanov *et al* 1974) in true water plasmas Decomposition of coal and liquid hydrocarbons in water/air plasmas was reported by Kolev and Georgiev (1987) and Yakovlev *et al.* (1982) Papers, on simple models (Dobal 1978), engineering correlations (Kolobova *et al* 1984) or simulations (Lesiński *et al.* 1985) involving chemical reactions in water plasmas, were published

2.4 5 Plasma Reactors

Reactors used for gaseous systems are also applied in processing of liquids and solids Additionally, there are several reactors developed only for heterogeneous systems For example, Venugopalan *et al* (1980) review submerged arcs in petroleum and liquid hydrocarbons Fedoseyev *et al* (1965) described a stationary reactor in which argon jet is directed at the surface of kerosene Zabrodin *et al* (1973) compared concurrent and countercurrent modes of petroleum injection into nitrogen and methane/hydrogen plasma jets They concluded that, for heterogeneous systems, both the overall conversion and acetylene yield are improved in countercurrent arrangement The countercurrent technique was first developed by Mosse *et al* (1971) To a smaller extent, arc reactors are also used in liquid hydrocarbon processing, an example of such a reactor is given by Drost *et al* (1985b)

In general, the processing of coal is performed either in stationary or in flow reactors. Stationary reactors, involving carbon electrodes or compacted beds, were used by Amman *et al* (1964), by Baddour and coworkers (1962,1964) as well as by Leutner and Stokes (1961) A stationary spouted bed reactor was operated by Bal *et al* (1971) Szymanski and Galska Krajewska (1971) studied operation of another stationary reactor - fluidized bed reactor Also, Szymanski *et al.* (1983) studied pyrolysis of brown coal in spouted bed and fluidized bed reactors As in the case of liquid hydrocarbons, flow reactors may be operated in concurrent or countercurrent modes Although, the countercurrent method yields promising results (1985), at this time, the concurrent technique seems to be utilized more often (e g Baumann and Bittner 1988, Bond *et al* 1966, Graves *et al* 1966, Nicholson and Littlewood 1972)

2 4 6 Production of Acetylene from Coal

Based on the literature survey it appears that there are two processes that achieved economical and technical maturity and may be used in a full scale industrial plant, those are Huls process in Germany (Muller and Peuckert 1983, Muller and Kaske 1984, Peuckert and Muller 1985, Muller et *al.* 1987b&c) and Avco process in the U.S.A. (Kushner 1985, Patrick *et al.* 1985). Both were tested in pilot plants, Huls in 500 kW unit and Avco in 1 MW reactor. Similarly, they employ a hydrogen plasma with hydrocarbon quench, they operate at pressures below atmospheric. Huls D.C. reactor is stabilized by vortex while Avco utilizes a D.C. rotating arc reactor. They both claim analogous conversion to acetylene of around 50 %. According to a financial study, in 1981, a total cost of a kilogram of acetylene produced in AVCO process was estimated to be 44.4 ¢ (Patrick *et al* 1985). However, the net cost of production of C_2H_2 from AVCO pilot plant was evaluated to be 24 % higher than from thermal decomposition of hydrocarbons in a Wulff furnace (Fauchais *et al.* 1980).

2.5 Some Economic Considerations

One should realize that it is highly unlikely that acetylene may substitute ethylene as a basic feed stock for the petrochemical industry, at least not in the near future. Although U.S. production of acetylene increased by 43 % in January and February 1989 compared to the same period last year, it should be remembered that acetylene production is only 1.8 % of the total U.S. output of ethylene (Anonymous 1989). Moreover, according to Hunter (1989), ethylene production capacity in the U.S.A and in Canada will increase by 6.4 billion kg/year between 1990 and 1993.

Lastly, predictions that plasma processing of hydrocarbons would become important were based on two assumptions. (1) cost of fossil fuels would increase and (2) cost of electricity would tend to decrease. Neither of those predictions was fulfilled over last decade; according to Nelson-Farrar Cost Index (published in Oil & Gas Journal) cost of fuel actually decreased by more than 50 % between July 1981 and January 1989. Over the same period cost of ethylene increased marginally from 61.7 ¢/kg (Patrick *et al.* 1985) to 70.5 ¢/kg (as given in Chemical Marketing Reporter, 12 June 1989).

3.0 THERMODYNAMIC INVESTIGATION

The consideration of the equilibrium composition of plasma systems provides useful information about the optimum operating conditions. Because of the kinetic limitations the exact product distribution from the pyrolysis of complex hydrocarbons in the plasma cannot be determined from thermodynamic calculations (Chapter 2). The objective of this study was to assist in planning an experimental program for the treatment of the CANMET residue in hydrogen plasmas, and especially (1) to determine the maximum yield of the unsaturated hydrocarbons as a function of the quenching temperature and (2) to investigate the concentration of potentially lethal gases in the products.

In general, the equilibrium composition may be calculated either by the classical equilibrium constant method or by the direct free-energy minimization method. The latter, which is now commonly used, was developed by White *et al* (1958) and it was extended to plasma systems by Zeleznik and Gordon (1966). In brief, it is based on the minimization of the Gibbs free energy at constant temperature and pressure to determine the composition subject to the element balance constraint. In other words, given a certain C/H ratio, temperature and pressure, and assuming a set of compounds for which the Gibbs free energy of formation is known the equilibrium composition can be uniquely calculated. Numerical algorithms for the calculation of chemical equilibrium were extensively reviewed by Smith and Missen (1982).

The thermodynamic calculations were based on the chemical composition of the CANMET residue as given in Table 5.1 or on a molar basis as $CH_{1.0601}N_{0.0135}S_{0.0172}O_{0.0412}$ with a molecular weight of 14.46 g/mol. Small amounts of metal oxides (Table 5.2) were not included in the calculations. The computation of the distribution of the metals among a large number of solid phases was not justified in view of the approximate character of the thermodynamic calculations. In addition the cost of the calculations would have been substantially increased.

Duff and Bauer (1962) calculated thermodynamic functions for a large number of C-H molecules. They showed that acetylene and hydrocarbon radicals, but not alkanes are important in characterizing the equilibrium composition above 2000 K. The thermodynamics of C-H-N systems was analyzed by Marynowski *et al.* (1962) and Spangenberg *et al.* (1974) to investigate the production of hydrogen cyanide, cyanogen and acetylene. Finally, Pustovoytenko (1979) examined thermodynamic quasi-equilibrium (no solid phase included in the calculations) of C-H-N-S-O system using an example of a fossil fuel with the formula $CH_xN_{0.01}S_{0.004}O_{0.065}$, where x was varied between 0.1818 and 1.4286.

The thermodynamic calculations were performed on the F*A*C*T program (Facility for the Analysis of Chemical Thermodynamics) available on the McGill computer system. Boulos and Fauchais (1986) concluded that for calculations of the composition of the plasma and its thermodynamic properties, data coming from the same source should be used or serious errors may arise Consequently the thermodynamic data necessary for the computation such as standard heat of formation (at 298 K), absolute entropy (at 298 K), and the heat capacities were all taken from the JANAF Thermochemical Tables (1971)

The functional relationship between the absolute temperature and the heat capacity was computed by curvefitting the data from the JANAF Tables into the form;

$$c_p = a + b \cdot 10^{-3} \cdot T + c \cdot 10^{5} \cdot T^{-2} + d \cdot 10^{-6} \cdot T^{2} \qquad (3.1)$$

where a, b, c and d are constants, T is absolute temperature in K and c_p is heat capacity expressed in cal K^{-1} mol^{-1}.

The entire temperature range was subdivided into two intervals 298 to 2000 K and 2000 to 6000 K. The coefficients of the equation (3.1) are presented in Tables 3.1 and 3.2. The accuracy of the least squares calculations is good with a maximum error of 2 7% for 298 - 2000 K and 0.3% for 2000 - 6000 K. The heat capacities at high temperatures are easier to fit since they do not change rapidly. The coefficients a, b, c, d were used to create a private file on the F*A*C*T system.

The Tables 3.1 and 3.2 do not contain aromatic and higher unsaturated hydrocarbons. Due to kinetic considerations (low rates but high thermodynamic stabilities), those compounds were not included in the computations

Simple calculations were performed to verify the EQUILIB program (a part of the F*A*C*T system) The equilibrium composition of a mixture containing CH_4, CO, CO_2, O_2, H_2 and H_2O was calculated directly from the free energy values by using the programs from Appendices A.2 1 and B.2 2 of Smith and Missen (1982) The agreement between these calculations and the EQUILIB results was within three percent

Table 3.1 Heat Capacity at Constant Pressure for C-H-N-S-O Compounds in cal K^{-1} $mole^{-1}$; Range 298-2000 K (curvefitted from JANAF Tables)

no		compound	a	b	c	d
1	C	carbon graphite	2 54496	3 76062	-1 40453	-1 06390
2	C	carbon monatomic	5 00382	-0 07271	-0 00466	0 03656
3	CH	methylidyne	5 77979	2.24097	0 51166	-0 41040
4	CH_2	methylene	6 03657	6 55366	-0 34108	1 44282
5	CH_2O	formaldehyde	4 97794	12 99740	-0 14479	-3 26270
6	CH_3	methyl	5 35168	12 01646	0 06440	2 90778
7	CH_4	methane	2.90432	18 46863	0 39229	-4 36814
8	CN	cyano	6 04789	2 33267	0 22558	-0 44529
9	CN_2	CNN radical	9 87687	4 08269	-0 81449	-0 97025
10	CN_2	NCN radical	11 67918	3 38549	-1 89493	-0 96691
11	CO	carbon monoxide	5 76104	2 78658	0 38372	-0 67723
12	CO_2	carbon dioxide	8 78884	5 74042	-1 36243	-1 47664
13	COS	carbon oxide sul	10.50338	4 33886	-1 60994	-1 11135
14	CS	carbon monosulph	7.02220	2 07721	-0 43943	-0 57783
15	CS_2	carbon disulphid	11 84482	3 19038	-1 66966	-0 88516
16	C_2	carbon diatomic	7 49641	0 85508	2 31922	0 0017[illegible]
17	C_2H	CCH radical	8 52467	4 62995	-0 85969	-0 92629
18	C_2H_2	acetylene	10.42363	7 57657	-1 79241	-1 51452
19	C_2H_4	ethylene	7.11547	20 31574	-2 30270	-4 90956
20	C_2H_4O	ethylene oxide	9.34893	24 44838	-4 28081	6 11900
21	C_2N	CNC radical	12 21787	2 91500	-1 88692	-0 84509
22	C_2N_2	cyanogen	13 36476	6 63002	-1 46898	-1 76013
23	C_2O	CCO radical	9 63186	5 67788	-0 82297	-1 48283
24	C_3	carbon trimeric	9 32810	5 27370	-1 26642	-1 39731
25	C_3O_2	carbon suboxide	16 23343	9 82456	-2 65266	2 56632
26	C_4	carbon tetratomi	13 01649	7 36745	-2 02986	1 94026
27	C_4N_2	tetracarbon dini	20 61424	10 98724	-2 80941	2 81242
28	C_5	carbon pentatomi	16 70489	9 46119	-2 79329	2 43320
29	H	hydrogen monatom	4 96800	0 00000	0 00000	0 00000
30	HCN	hydrogen cyanide	7 93470	5 26679	0 74630	1 13890
31	HCO	formyl	6 54668	6 09520	0 01645	-1 47630
32	HNCO	isocyanic acid	10 65539	7 35941	-1 77[illegible]	1 73199
33	HNO	nitroxyl hydride	6 51547	6 14069	-0 23[illegible]	1 53405
34	HNO_2	cis-nitrous acid	11 43753	6 97504	-2 14896	1 71240

35	HNO_2	trans-nitrous ac	19.31528	0.15793	-40.00383	-0.01266
36	HNO_3	nitric acid	14.05816	10.54997	-3.83503	-2.73746
37	HS	sulphur monohydr	6.40026	1.62150	0.83593	-0.23662
38	H_2	hydrogen	6.75908	0.22469	0.05311	0.25860
39	H_2O	water	6.15630	4.29092	0.58747	-0.62740
40	H_2S	hydrogen sulphid	5.81754	6.50373	0.48434	-1.45415
41	H_2SO_4	sulphuric acid	22.71293	12.51363	-6.24166	-3.10009
42	N	nitrogen monatom	4.96941	-0.00261	-0.00069	0.00116
43	NH	imidogen	5.99408	1.65883	0.45748	-0.20535
44	NH_2	amidogen	5.72274	5.48065	0.69097	-1.08542
45	NH_3	ammonia	5.39016	10.20414	0.23566	-2.15439
46	NO	nitric oxide	5.94351	2.84355	0.35146	-0.73089
47	NO_2	nitrogen dioxide	8.51564	5.51761	-1.10667	-1.53917
48	NO_3	nitrogen trioxid	14.14342	6.27127	-4.21195	-1.82795
49	N_2	nitrogen diatomi	5.72016	2.64661	0.45389	-0.61022
50	N_2H_2	cis-diimide	6.36744	11.14704	-0.68535	-2.70303
51	N_2H_4	hydrazine	11.56806	15.12384	-3.29336	-3.40295
52	N_2O	dinitrogen monox	9.27316	5.32439	-1.37194	-1.41107
53	N_2O_3	dinitrogen triox	16.40950	8.47325	-2.78987	-2.33895
54	N_2O_4	dinitrogen tetro	20.19922	11.88457	-4.54546	-3.32081
55	N_2O_5	dinitrogen pento	28.45555	8.39177	-7.00075	-2.50485
56	O	oxygen monatomic	5.02434	-0.06487	0.20599	0.01992
57	OH	hydroxyl	6.30934	1.00461	0.48627	-0.00133
58	O_2	oxygen diatomic	6.49137	2.39112	-0.13951	-0.57458
59	O_3	ozone	10.69062	3.58975	-2.09353	-0.99039
60	S	sulphur monatomi	5.71094	-0.85477	0.16813	0.27386
61	SN	monosulphur mono	7.28675	1.81844	-0.18536	-0.50275
62	SO	sulphur monoxide	7.37899	1.74161	-0.59413	-0.48595
63	SO_2	sulphur dioxide	9.97309	4.31686	-1.49269	-1.18919
64	SO_3	sulphur trioxide	13.62389	6.61075	-3.02835	-1.88537
65	S_2	sulphur diatomic	8.44106	0.62904	-0.76971	-0.16798
66	S_2O	disulphur monoxi	11.81364	2.28260	-1.71408	-0.66292
67	S_8	sulphur octatomi	42.76133	1.10011	-5.14489	-0.33032

Table 3.2 Heat Capacity at Constant Pressure for C-H-N-S-O Compounds in cal. K^{-1} $mole^{-1}$; Range 2000-6000 K (curvefitted from JANAF Tables).

no.		compound	a	b	c	d
1	C	carbon graphite	6.09011	-0.04583	-8.94461	0.02267
2	C	carbon monatomic	3.98941	0.46515	9.14459	-0.03527
3	CH	methylidyne	8.70919	0.19034	-17.88466	-0.00540
4	CH_2	methylene	14.27550	0.17934	-47.16951	-0.01444
5	CH_2O	formaldehyde	19.34893	0.15023	-60.49549	-0.01215
6	CH_3	methyl	19.26657	0.17218	-65.28157	-0.01381
7	CH_4	methane	24.64087	0.34110	-106.63616	-0.02752
8	CN	cyano	5.84451	1.97479	-4.20185	-0.18633
9	CN_2	CNN radical	14.66115	0.06940	-24.01149	-0.00560
10	CN_2	NCN radical	14.88128	0.00647	-10.02070	-0.00052
11	CO	carbon monoxide	8.86151	0.05742	-12.55877	0.00007
12	CO_2	carbon dioxide	15.03500	0.00014	-27.21928	0.01553

13	COS	carbon oxide sul	14 83685	0 17642	-16 61336	-0 00152
14	CS	carbon monosulph	8 93191	0 05183	-5 22287	-0 00027
15	CS_2	carbon disulphid	14.87712	0 04300	-9 90428	-0 00064
16	C_2	carbon diatomic	8 56815	0 66540	-17 36162	-0 05511
17	C_2H	CCH radical	12 10897	1 67896	-29 42955	-0 16577
18	C_2H_2	acetylene	19 93691	0 58435	-61 17033	-0 02116
19	C_2H_4	ethylene	30 52274	0 36322	-114 09419	-0 02926
20	C_2H_4O	ethylene oxide	36 49157	0 36133	-123 68802	-0 02911
21	C_2N	CNC radical	15 17406	-0 12649	-11 60619	0 01622
22	C_2N_2	cyanogen	20 66531	0 05771	-30 87875	-0 00466
23	C_2O	CCO radical	16 98919	-0 38215	-4[illegible] 79277	0 02089
24	C_3	carbon trimeric	14 79633	0 03141	20 15039	0 00256
25	C_3O_2	carbon suboxide	26 60451	0 56439	-40 26314	-0 00523
26	C_4	carbon tetratomi	20 70796	0 04637	-28 95976	-0 00382
27	C_4N_2	tetracarbon dini	32.58233	0 04739	-49 76798	-0 00285
28	C_5	carbon pentatomi	26 61959	0 06134	-37 76912	-0 00507
29	H	hydrogen monatom	4 96800	0 00000	0 00000	0 00000
30	HCN	hydrogen cyanide	14 15677	0 38269	-34 71807	-0 03336
31	HCO	formyl	13 57863	0 09456	-32 81741	-0 00759
32	HNCO	isocyanic acid	19 27043	0.17113	-45 64356	-0 01375
33	HNO	nitroxyl hydride	13 64005	0 07792	-29 45828	-0 00633
34	HNO_2	cis-nitrous acid	19.31528	0 15793	-40 00383	-0 01266
35	HNO_2	trans-nitrous ac	11 43758	6 97594	-2 14890	-1 71230
36	HNO_3	nitric acid	25 27205	0 15965	-49 63293	-0 01282
37	HS	sulphur monohydr	8 86766	0 11253	-16 78771	-0 00235
38	H_2	hydrogen	7 66257	0 50969	-16 79177	-0 01587
39	H_2O	water	12 80011	0 45985	56 52941	-0 02761
40	H_2S	hydrogen sulphid	13 50928	0 27591	-38 67037	-0 00931
41	H_2SO_4	sulphuric acid	36 72917	0 29051	-73 74549	-0 02326
42	N	nitrogen monatom	5 11943	-0 27586	4 91080	0 07349
43	NH	imidogen	8 57852	0 22062	-20 49718	-0 00784
44	NH_2	amidogen	13 19963	0 20240	-47 57982	-0 01623
45	NH_3	ammonia	16 79314	1 04894	-64 57130	-0 02605
46	NO	nitric oxide	8 88638	0 06408	-10 02333	-0 00137
47	NO_2	nitrogen dioxide	13 86265	0 01403	-15 87568	0 00116
48	NO_3	nitrogen trioxid	19 85359	0 00507	-16 78257	0 00038
49	N_2	nitrogen diatom.	8 92185	0 02282	-15 42724	0 00305
50	N_2H_2	cis-diimide	19 16572	0 20087	-61 68049	-0 01613
51	N_2H_4	hydrazine	20 20596	0 45211	-109 04638	-0 03634
52	N_2O	dinitrogen monox	14 79709	0 03066	20 52950	-0 00246
53	N_2O_3	dinitrogen triox	24 75281	0 02496	-27 28276	-0 00199
54	N_2O_4	dinitrogen tetra	31 69017	0 03052	-36 11062	-0 00247
55	N_2O_5	dinitrogen pento	35 68256	0 03372	-17 84406	-0 00318
56	O	oxygen monatomic	4 55535	0 11746	7 59649	0 00134
57	OH	hydroxyl	8 41590	0 24089	22 96332	0 01192
58	O_2	oxygen diatomic	7 70033	0 82585	-2 77610	0 06674
59	O_3	ozone	13 89579	0 15021	-9 31222	0 00635
60	S	sulphur monatomi	4 12424	-0 [illegible]	[illegible] 6691	0 [illegible]
61	SH	monosulphur mono	8 [illegible]	0 [illegible]	[illegible]	[illegible]
62	SO	sulphur monoxide	9 [illegible]	0 [illegible]781	-[illegible]	[illegible]
63	SO_2	sulphur dioxide	13 [illegible]	0 [illegible]	-11 [illegible]	[illegible]
64	SO_3	sulphur trioxide	19 93[illegible]	[illegible]	13 [illegible]	[illegible]

65	S_2	sulphur diatomic	8.94253	0.06358	-1.77747	-0.00001
66	S_2O	disulphur monoxi	13.90231	0.00244	-6.39696	-0.00019
67	S_8	sulphur octatomi	43.71730	0.00068	-6.85870	-0.00005

The results of two sets of calculations, with and without solid phase are presented in Figures 3.1, 3.2 (without solid phase) and 3.3 (with solid phase). The simplicity of the figures was preserved by not including compounds nor radicals whose concentrations were below 1%. Ions were found to exist at temperatures below 6000 K, however their combined volume was not higher than 0.002%

Figure 3 1 shows the pyrolysis of the residue in a hydrogen plasma when one molecule of H_2 is added to every pseudo-molecule of the CANMET residue. Since the operation with the pure hydrogen plasma was not possible in the experimental equipment, the decomposition of the residue in an argon/hydrogen plasma was also investigated (Figure 3.2). Because of the dilution by argon the maximum concentrations of hydrocarbons decrease; however the shapes of the concentration curves remain unchanged. At temperatures below 1500 K familiar stable molecules (such as CH_4, C_2H_4, CO) predominate whereas formation of acetylene and its precursor (C_2H) is important between 1500 and 3500 K. Above 4000 K the concentration of monatomic gases as C and H becomes significant.

The full equilibrium calculations were performed to determine the effect of the presence of solid carbon (graphite) on the production of acetylene (Figure 3 3). Below the sublimation temperature of carbon, (3400 K) the gaseous phase consists almost exclusively of argon, hydrogen, carbon monoxide and methane at low temperatures. The fraction of the initial carbon that goes to the solid phase is 0.26 at 500 K, but it increases to 0 95 at 1000 K, then it stays approximately constant to decrease rapidly above 3000 K (Figure 3.3) The production of acetylene attains a maximum at 3500 K and it is mostly due to the C_2H radical. Since the conversion to acetylene and C_2H radical is higher for the quasi-equilibrium calculations (95%) one can conclude that the residence time of the gases in the reactor should be maintained between 10^{-4} and 10^{-3} s to allow the formation of acetylene and to avoid the generation of soot (Baumann *et al.* 1988).

Figure 3.4 shows that the maximum conversion of carbon to acetylene is

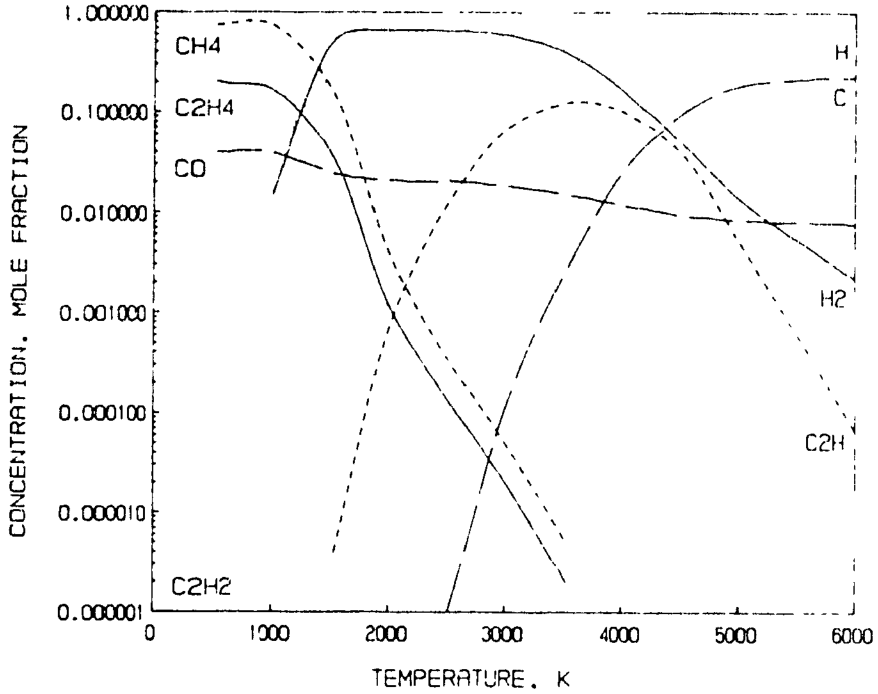

Figure 3 1 Decomposition of the CANMET Residue in a Hydrogen Plasma, Quasi-Equilibrium Calculations (Pressure = 101 3 kPa, Residue Hydrogen = 7 23 1 mass ratio)

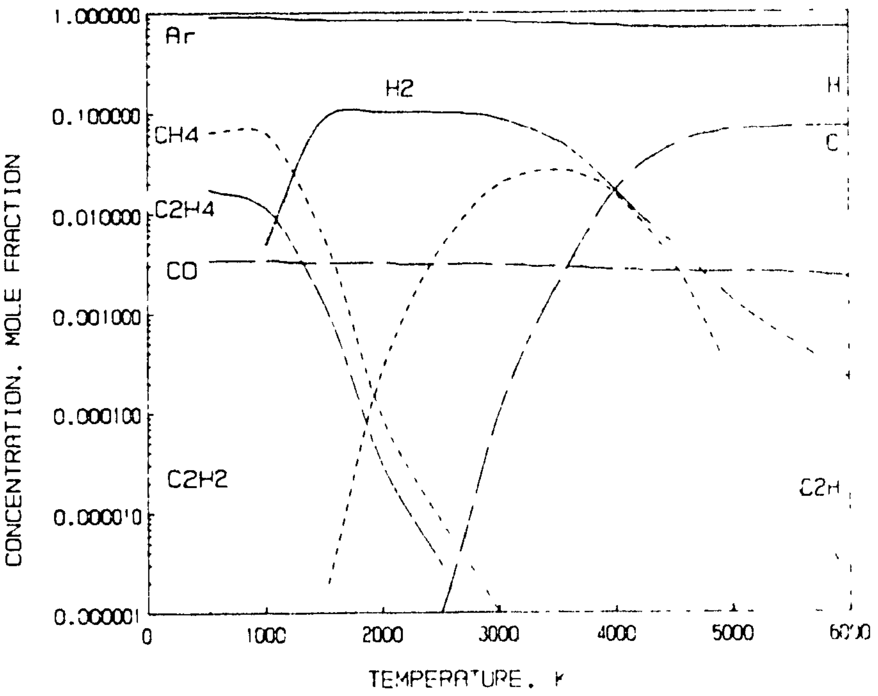

Figure 3 2 Decomposition of the CANMET Residue in an Argon/Hydrogen Plasma, Quasi-Equilibrium Calculations (Pressure = 101 3 kPa, Residue Hydrogen Argon = 7 23 1:180 mass ratio)

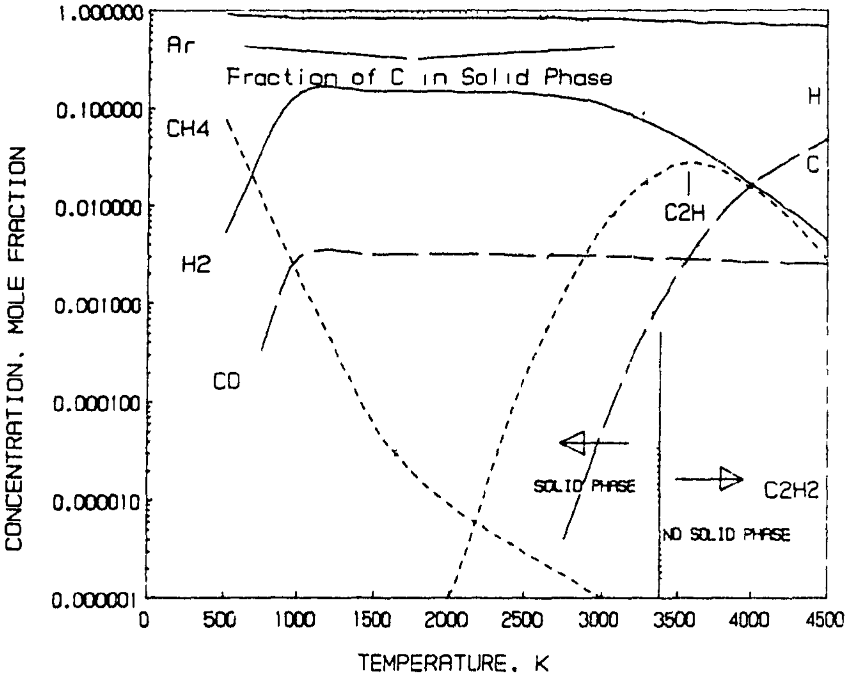

Figure 3.3 Decomposition of the CANMET Residue in an Argon/Hydrogen Plasma, Equilibrium Calculations (Pressure = 101 3 kPa, Residue.Hydrogen.Argon = 7 23:1:180 mass ratio)

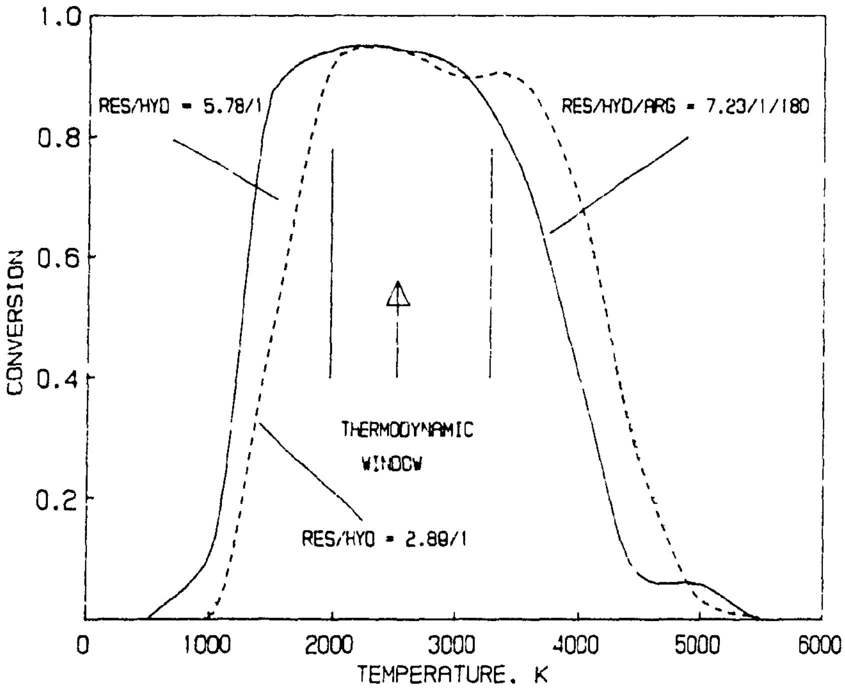

Figure 3.4 Conversion of Carbon in the Residue to C_2H_2 and C_2H in Hydrogen and Argon/Hydrogen Plasmas, Quasi-Equilibrium Calculations (Pressure = 101.3 kPa)

between 1800 and 3300 K and this is quite insensitive to plasma composition.

Finally, it is expected that the production of some toxic gases will exceed the safety limits. For example the maximum allowed contamination of air by HCN is 4.7 ppm, by H_2S is 50 ppm (peak) and by C_2N_2 is 10 ppm (Sitting 1985). The equilibrium calculations indicate that concentrations of these compounds in the exit gas during the experiments may be 100-1000 times higher. The exit gas must thus be either diluted or scrubbed before being exhausted to the atmosphere.

4.0 APPARATUS

The main components of the apparatus are a high frequency power supply, an induction plasma torch, a single particle reactor system and a sampling train (Figure 4 1).

4.1 Power Supply and Control Console

The induction power supply is a self contained radio frequency oscillator. It rectifies 3 phase, 60 Hz power (575 V, 36 kW) into DC power (also called plate power) and then converts it into 4 MHz AC which is delivered to the torch A Lepel High Frequency Laboratories model 32-30MC was used. It is able to deliver plate powers of up to 30 kW The power supply contains a grid control to match the oscillator circuit to the plasma gas Munz (1974) gave a more detailed description of the power supply.

The gas flow rates were measured with (±2%) precision rotameters Those were calibrated with a wet test meter between 2 and 56 l/min and, if necessary, below 2 l/min by a bubble meter. Argon and carbon dioxide rotameters were calibrated directly with those gases but the hydrogen rotameters were calibrated with helium and an appropriate correction for molecular weight applied. The flow of argon delivered to the torch was metered and controlled by a TAFA Model 47-10A control console; see Munz (1974) for more details. Separate rotameters were added to regulate the flow of hydrogen to the torch and to the argon tailflame as well as to control the flow of argon which was used as a shroud gas in the reactor and the flow of carbon dioxide which was required for the spectroscopy measurements (Section 6 2)

4.2 Plasma Torch

The induction plasma torch used in this investigation was manufactured by TAFA as model 56 (Figure 4.2). The plasma was sustained within the water cooled quartz tube by the vortex stabilization technique. Argon which formed the plasma was fed to the back of the torch through a gas distributor nozzle

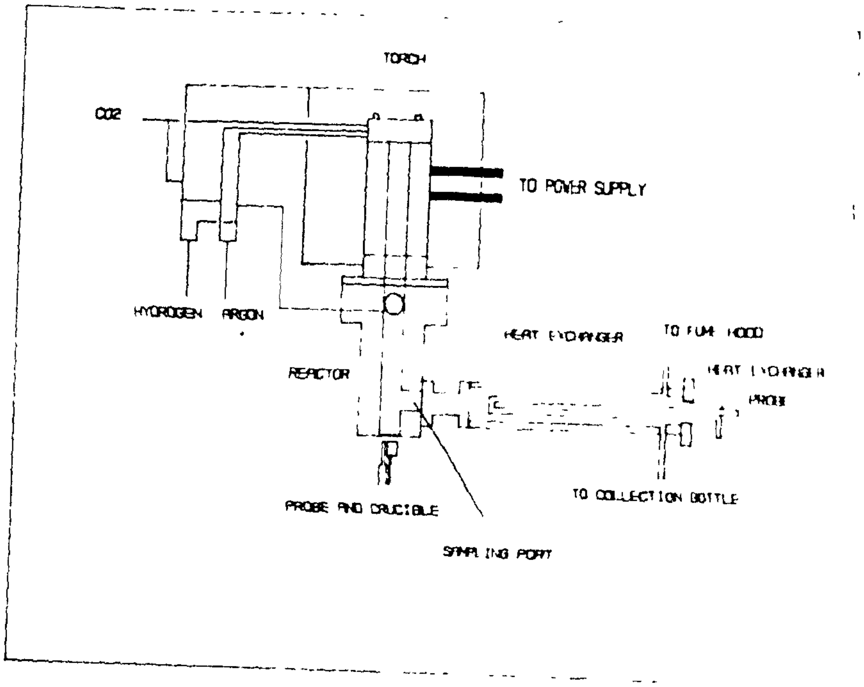

Figure 4.1 Experimental Apparatus

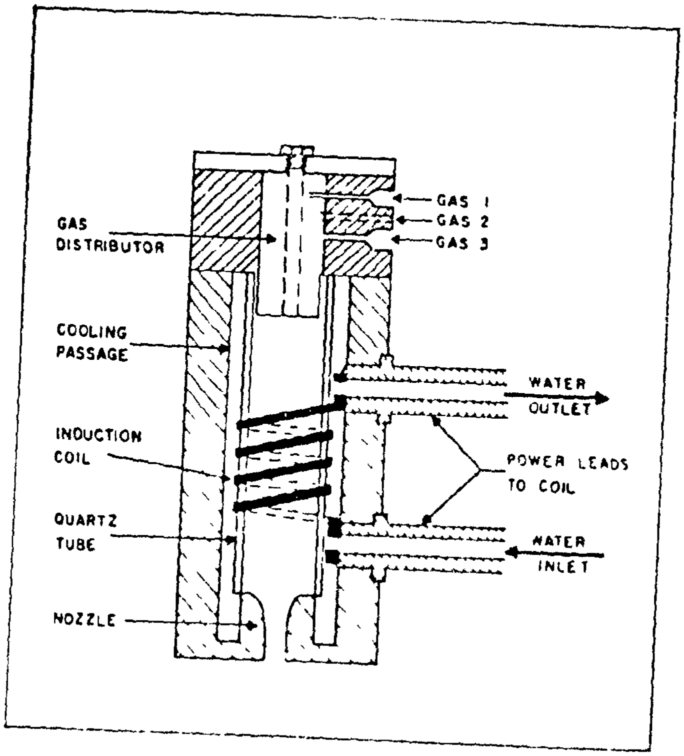

Figure 4.2 The Plasma Torch

that allowed axial, radial and tangential directions of injection. Once the torch was ignited, argon was delivered to the radial and tangential (swirl) injection ports.

4 2.1 Operation with Hydrogen

Thorpe (1966) was able to sustain 70 % hydrogen flame at 52 1 kW plate power in an induction plasma torch. Thorpe and Scammon (1968) reported the operation with pure hydrogen at plate powers between 60 to 185 kW Analysis of the thermal pinch effect (Thorpe and Scammon 1968) suggests that it should be feasible to maintain a stable plasma of 10 % of hydrogen in argon in TAFA model 56 torch at 30 kW and 4 MHz The experimental results (Thorpe 1966) indicate that 35 % hydrogen should be possible at 5 MHz or, after adjusting for the lower frequency of the 32*30MC power supply, 29 % hydrogen at 4 MHz.

A series of experiments was performed to evaluate the operation with hydrogen which was added primarily into the radial but also into the axial and in some instances into the tangential injection ports in the torch. Stable operation was attained with maximum 32 % hydrogen in argon under the following conditions. argon flow 32 l/min. hydrogen flow 15 l/min, plate current 4.2 A, and plate voltage 7 6 kV, this corresponds to almost 32 kW plate power, slightly above the specifications of the power supply. However the range of stable operation is not as broad as with pure argon which could be maintained between 4 0 and 15 kW plate power (Figure 6.1 and 6.2) For example, during the operation with 11 % hydrogen the flame extinguished below 23.4 kW and the quartz tube fractured above 28.4 kW. For higher concentrations of hydrogen the range of stable operating power was even smaller.

In 1968 Thorpe noted that at hydrogen concentrations above 50 %, the convective and the conductive heat transfer from the plasma "on the quartz tube became so high that the devitrification occurred after one or two minutes of operation". The same difficulties were experienced during this investigation with devitrification developing in between 2 and 30 minutes of operation depending on the experimental conditions The cost of a single quartz tube is more than $60

In principle, one may attempt to use a segmented metal wall or to operate the torch with the fireball surrounded by cold sheath gas. However, substantial changes in the equipment would have been required.

Instead it was decided to inject hydrogen into the argon tailflame i.e. into the base of the torch below the coil. This had the advantage of requiring only the addition of a few fittings to the equipment and extending the stable operation limits of the torch since now the hydrogen bypassed the torch. The concentration of hydrogen was limited by the extent of mixing between the hot argon plasma tailflame and the cold injected hydrogen. It was determined by visual observations and probe sampling (Section 4.3) that up to 27 % hydrogen could be used while maintaining a maximum deviation of local and mean hydrogen concentrations of 5 %. The injection of 33.5 % hydrogen gave deviation of 13 %. A second problem associated with tailflame injection was the fact that the temperature of the plasma gas was decreased by the hydrogen addition.

Although an argon plasma can be sustained above 4.0 kW the tailflame assumes a cone like shape only above 7.0 kW. Between 4.0 and 7.0 kW an inverted flame characterized by a relatively cold central part and hot flame fringes (Figure 4.3) is formed. If a crucible is placed inside such an inverted cone, the gas temperature is poorly defined.

The above discussion is summarized in Figure 4.3. Most of the experiments were performed in "the preferred region of operation," that was defined as 7.0 kW < Plate Power < 14.0 kW and 0.0 % < H_2 < 27.0 %.

4.3 Reactor and Auxiliaries

The reactor (Figure 4.4) initially designed by Biceroglu (1983) was adapted for investigation of the plasma treatment of the CANMET residue. The inner part of the reactor, fabricated from a single piece of monel, houses a reaction chamber and the crucible containing residue. Optical pyrometry and spectroscopy measurements were performed through a window in the upper section of the reaction chamber. The upper part of the reactor was 5.08 cm in inside diameter and 11.4 cm in length. The diameter could be decreased

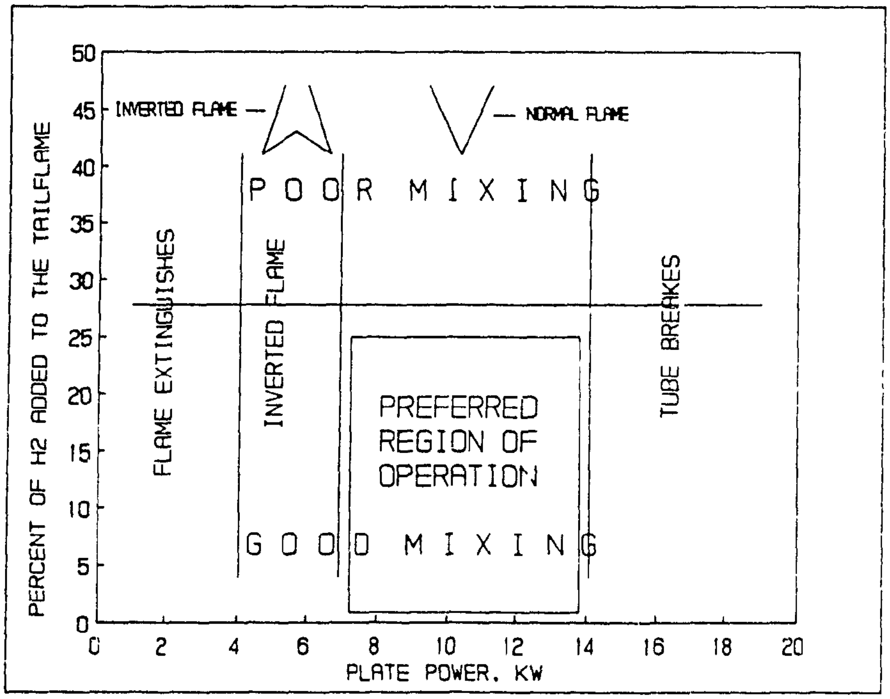

Figure 4 3 Operation with Argon Plasma and with Hydrogen Added to the Tailflame (Argon Flow = 20 81 g/min **Axial** and 37.22 g/min Swirl)

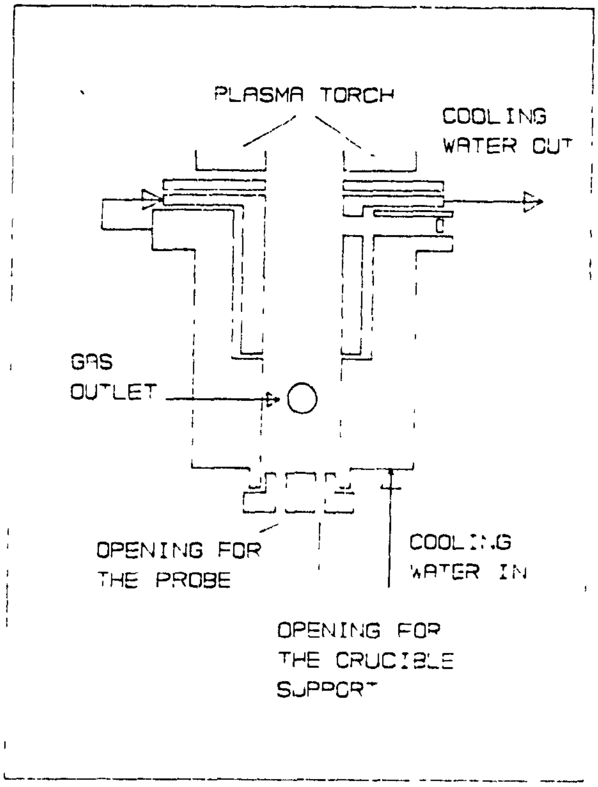

Figure 4.4 Cross-Sectional View of the Reactor

to 2.54 cm by adding a water cooled insert The lower part of the reactor (2.54 cm in diameter and 5.08 cm in length) contains the reactor outlet (1 9 cm in diameter) and below that a cool stagnant region which accommodates the crucible prior to reaction.

The molybdenum crucible (1.9 cm in length, 1 3 and 1 4 cm in inside and outside diameters) was mounted on a 0 32 mm alumina rod which moved vertically through a nylon male connector. The alumina rod was placed slightly off the reactor centre line to permit installation of the suction probe. During experiments the crucible remained within the plasma flame, and it was placed 7 8 cm below the torch coil, this corresponds to 2 5 cm below the torch exit

The reactor was connected to the torch by an uncooled stainless steel adaptor 6.3 mm thick. A water cooled flange was installed between the reactor outlet and the heat exchanger. The heat exchanger (61 cm in length) was made from an outside brass tube and inside 2 54 cm in diameter copper tube with spiral fins supplied by Noranda Metal Industries Inc A water cooled probe was placed inside the heat exchanger to improve cooling (Figure 4.1). The gas leaving the heat exchanger was diluted by more than 200 times with air and exhausted to the fume hood; thus a scrubber was not necessary

4 4 Sampling and Collection Train

The gas samples were withdrawn from two locations (1) from the exhaust gas stream leaving the reactor and (2) from the reactor chamber through the suction probe Since the suction probe could be moved vertically the samples were taken at different positions but usually 5 5 cm below the top of the crucible The gases were cooled either inside the probe or by passing through 12 2 m of stainless steel tubing (with diameter of 0 32 cm) submerged in an ice-water mixture, if samples were withdrawn at the reactor outlet. After passing through a small condenser, designed to trap water and liquid hydrocarbon vapours, the gas was directed to the gas filter where soot particles were deposited (Figure 4 [illegible])

The gas stream was then passed through a pump to increase its pressure to maximum of 135 kPa and to sampling ports. It then passed through a

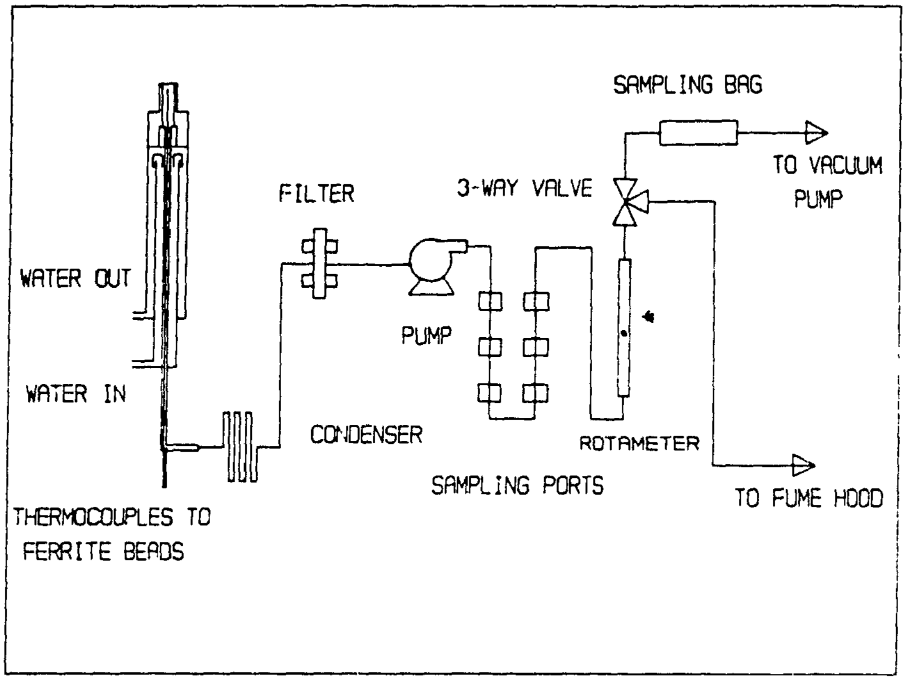

Figure 4.5 Probe and Sampling Train

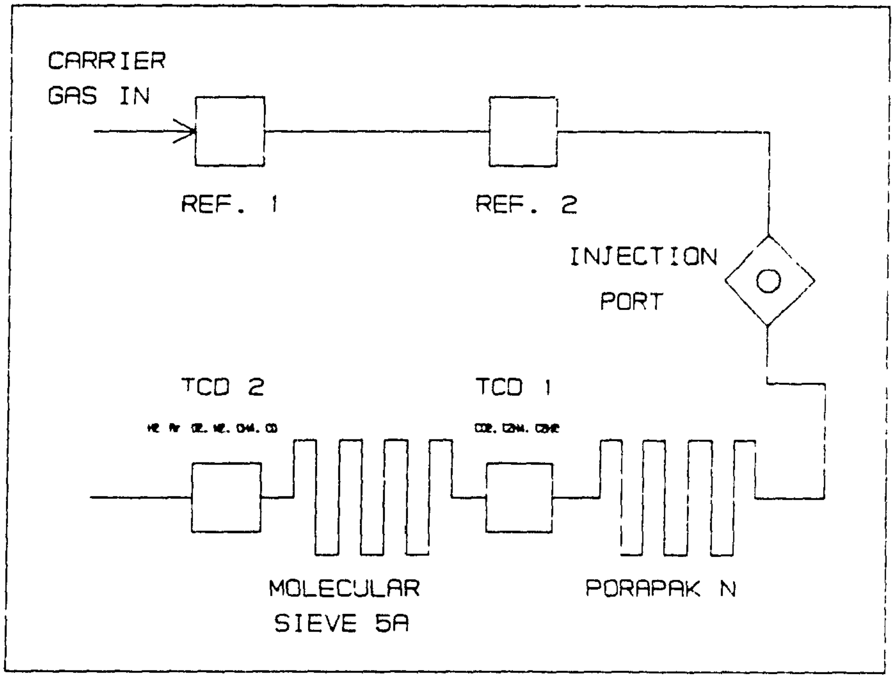

Figure 4.6 Standard Configuration of Fisher Gas Partitioner 1200

rotameter to verify that the flow was constant, and was either exhausted to the fume hood or collected in a plastic bag as an integral sample

4.4.1 Suction Probe

The water cooled suction probe was designed to withdraw the hot gas from the reactor chamber and quench it at a rate of at least 0 $4 \cdot 10^6$ K/s to reduce acetylene decomposition and at the same time to measure the gas inlet temperature using a W-5%Re/W-26%Re thermocouple (Figure 4 [illegible]) The gas flow rates through the probe were usually around 250 cm^3/min The probe was constructed of three concentric stainless steel tubes with diameters of 1 6 mm, 3.2 mm and 6 4 mm and had a length of 60 cm Stainless steel was chosen for its rigidity and inertness The cooling water flow was 0 7 l/min The tip of the probe was not water-cooled and it was made of molybdenum The bare wire (0 13 mm in diameter) thermocouple was passed through alumina thermocouple insulation and placed inside the innermost tube To minimize the conduction losses from the thermocouple junction, the top 1 cm of the thermocouple wires was not insulated

4 5 Experimental Procedure

Before an experimental run, approximately 1 20 g of the residue was packed in the crucible and melted to eliminate trapped air The amount of the residue was determined by taring the empty crucible Normally, the sample of the residue weighed 1 210 ± 0 017 g and its mass was resolved with a precision of 0 0001 g

The crucible was mounted on the alumina support rod and placed in the lower part of the reactor below the gas exit As verified from a few "blank" experiments the temperature in this part of the reactor reached about 210 °C, which was enough to melt the sample but it was too low to permit chemical reactions The suction probe was positioned in the reactor and was not moved during the experiment The reactor was attached to the torch and the cooling water was [illegible] the apparatus was [illegible] and it was verified that the [illegible] care was taken to ensure that there were no gas leaks from the exhaust line and that the fume hood was in operation. The reactor was purged with argon to remove any residual oxygen (for 5 minutes and by injecting 150 l of argon).

After the power supply was allowed to heat up for 25 minutes the plasma was initiated, and the discharge was stabilized by adjusting the grid setting and the argon flow. The plate power was adjusted as required (Section 6.1). Extra argon was added through the reactor window shroud to prevent the deposition of soot. A specified amount of hydrogen was injected into the argon tailflame. At this point, the alumina rod supporting the crucible was moved up and a stopwatch was started. Gas samples were taken in 1 ml syringes every 3 to 15 seconds depending on the operational conditions. The syringes were fitted with locks to minimize the diffusion of gas. After 2 to 4 minutes the torch was turned off, the argon and hydrogen flows were stopped and the crucible was allowed to cool.

Immediately following an experimental run the composition of gas samples was determined on the gas chromatograph. The unreacted residue was removed from the reactor, separated into an upper and lower part, weighed, ground and prepared for further analysis. Soot samples were also taken.

4 6 Gas Analysis

Mixtures of permanent gases (H_2, CO_2, Ar/O_2, N_2, CO) and hydrocarbons (CH_4, C_2H_6, C_2H_4, C_2H_2) were separated isothermally using a two column system which consisted of a Porapak N followed by a Molecular Sieve 5A column. The Molecular Sieve 5A column (pore size 5 Å) can be used to separate hydrogen, argon/oxygen, nitrogen, methane and carbon monoxide (argon and oxygen can only be separated at sub-ambient temperatures or by using a very long column) However carbon dioxide, ethane, ethylene and acetylene are absorbed by the Molecular Sieve 5A column. Porapak N is specifically recommended for separation of ethylene and acetylene (other such as Chromosorb 107 and Chromosorb 108 provide less adequate separation). Thus the Porapak N followed by the Molecular Sieve 5A were found to give satisfactory separation. Their lengths and diameters (1.98 m and 0 32 cm for Porapak N, 2.74 m and 0.32 cm for Molecular Sieve 5A) were determined by trial and error.

The thermal conductivity detector (TCD) was used for the quantitative determination of the gas concentration. The detector was sensitive enough to determine concentrations of hydrocarbons in argon with a precision of 100 ppm. The carrier gas used was a mixture of 8.5 % hydrogen in helium. With this carrier gas the detector response to hydrogen in the analyzed sample is always negative. Therefore in this investigation, the signal from the gas chromatograph which corresponded to the hydrogen peak was inverted before being fed into the Hewlett-Packard integrator. The inversion was accomplished by switching the polarity of the cables that connected the gas chromatograph with the integrator.

The gas separation was performed in the Fisher Gas Partitioner 1200 that could be operated isothermally at ambient or higher than ambient temperatures. Initially it was provided with a Dual Thermal Conductivity Detector. The carrier gas flowed through the reference sides of the first and second TCDs, injection port and the Porapak N column (Figure 4.6). CO_2, C_2H_4 and C_2H_2 were determined on the first TCD and subsequently absorbed on the Molecular Sieve 5A column. The remaining fixed gases and methane were separated in the Molecular Sieve 5A column and were resolved on the second TCD. The output from both detectors was directed to the same integrator often resulting in overlapping of peaks or, if this was avoided, in a long retention time for acetylene.

Figure 4.7 depicts changes made to the standard configuration of the gas chromatograph. These include installation of the six port valve with restrictor in the series-by-pass configuration. After passing through the reference sides of both detectors, the carrier gas proceeds through the first TCD (which is not used), the injection port and it enters the Porapak N column. As soon as hydrogen moves through both columns reaching the detector and the fixed gases and methane leave the Porapak N column entering the Molecular Sieve 5A column, the six port valve is switched and the hydrocarbons are allowed to elute from the Porapak N column bypassing the Molecular Sieve 5A column. After acetylene is detected on the TCD, the valve is switched again and the gases trapped in the Molecular Sieve 5A column

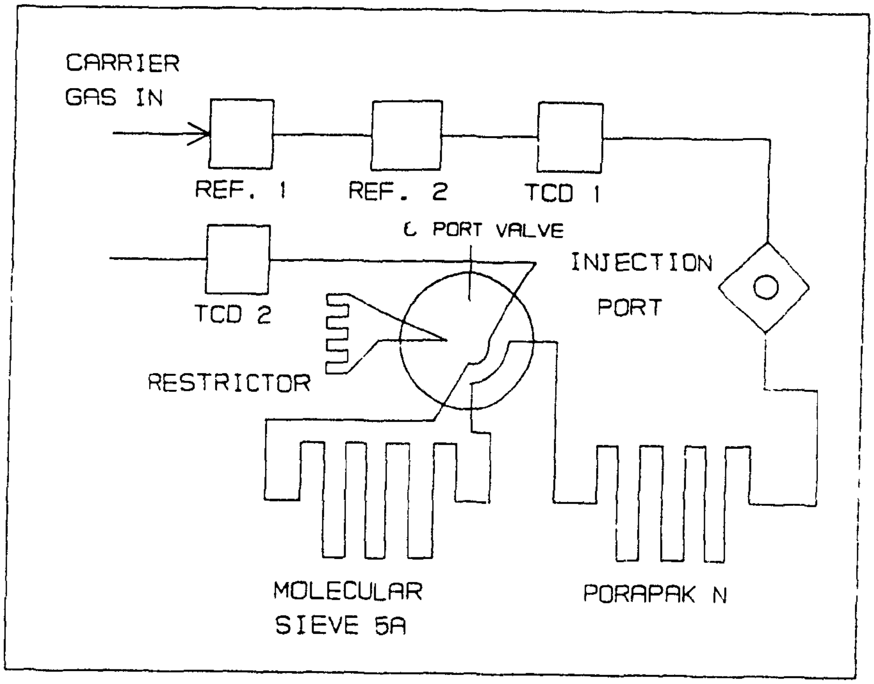

Figure 4 7 Series-By-Pass with Restrictor Configuration of Fisher Gas Partitioner 1200

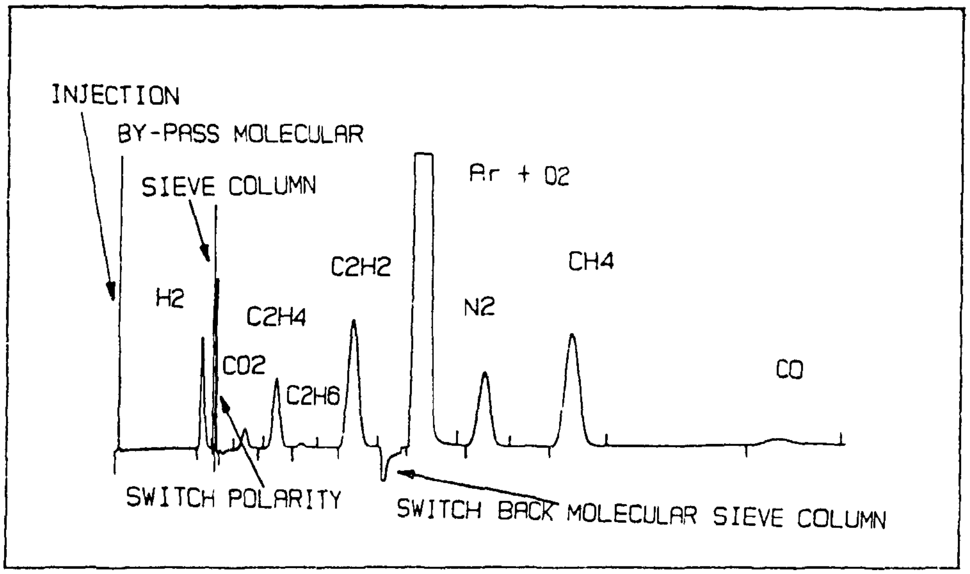

Figure 4.8 Elution Order Using Series-By-Pass Configuration (Parameters. 1.98 m Porapak N. 2.74 m Molecular Sieve 5A, Temperature 80 °C, 0.5 ml Injection, 8.5 % Hydrogen/Helium Carrier Gas at 26 cm^3/min)

such as argon together with oxygen, nitrogen, methane and carbon monoxide elute.

An example of a gas chromatogram obtained by injecting 0 5 ml of the calibration mixture is given in Figure 4.8. The gases elute in the following order. the concentration (in %) and the elution time (in min) are given in brackets H_2 (24 788, 1.97), CO_2 (0 102, 3.02), C_2H_4 (0 464, 3 72), C_2H_6 (0 027, 4.30), C_2H_2 (1 404, 5 56), Ar (70 409, 6 98), N_2 (0 568, 8 59), CH_4 (2 040, 10.68) and CO (0 198, 15.53) Nitrogen was not present in the reactor but was seen on gas chromatograms due to the air diffusion into the syringes. Consequently, it was included in the calibration Oxygen could not be separated from argon and its percentage was estimated from the nitrogen content The elution time of carbon monoxide was long but it could not be decreased due to the isothermal operation of the gas partitioner

5.0 ANALYSIS OF THE CANMET RESIDUE

The CANMET residue is the pitch like substance remaining after the vacuum distillation of the product obtained from the coprocessing of coals and bitumens or petroleum resids in the CANMET process. As reported by Rahimi *et al.* (1989), the most recent feedstocks to the CANMET process were Forestburg coal and Cold Lake vacuum bottoms whose compositions are given in Table 5.1. Slurry products from the CANMET process are distilled up to 525 °C yielding C_1-C_4 gases, naphtha, light and heavy gas oil as well as the residues which in this investigation are denoted as the CANMET residue.

The residue starts to flow at 160 °C and it may be pumped at 230 °C. At this temperature its viscosity is estimated to be 1200 mPa s. Prior to the analysis the residue was homogenized by heating (to above 200 °C) in an oil bath and stirring. Precautions were taken to conform with ASTM D 140-70 Standard Method for Sampling Bituminous Materials in order to obtain a sample which represented an average composition of the residue. Because of the limited amount of the available residue the sample size was 2-3 g.

The elemental analysis of the residue was performed on the Control Equipment Corporation (CEC) elemental analyzer model 240-XA. Normally the samples of 1-3 mg were weighed with the accuracy of 100 ng. Analysis of samples with a small hydrogen content required sample weights of more than 3.7 mg (Section 7.2.4.4). In the C-H-N mode of the analyzer, the sample was combusted and then reduced to convert oxides of nitrogen to molecular nitrogen. The gases were passed through a series of thermal conductivity detectors for H, C, N which were isolated by appropriate traps. For oxygen and sulphur separate runs with different apparatus configurations were carried out. Because the residue contains metals which may remove oxygen from the sample, the oxygen analysis should only be considered an approximation. The analysis of sulphur includes the sulphur content in both organic and inorganic parts of the residue. According to the manufacturer of the 240-XA elemental analyzer errors associated with the method could be estimated as follows: error (±%) = ±(0.15 % absolute + 0.0015 · (reading in %) + error due to weighing in %). With the exception of oxygen, the error in elemental analysis is less than 0.30 %. The results are presented in

Table 5.1.

Table 5.1 Elemental Compositions of the CANMET Residue and the Feedstocks to the CANMET Process

element	CANMET residue (%)	Forestburg coal[3] (%)	Cold Lake vacuum[3] bottoms (%)
Carbon	74.71[1]	64.04	83.34
Hydrogen	6.60[1]	3.87	9.69
Sulphur	3.43[1]	0.53	5.84
Nitrogen	1.18[1]	1.65	0.45
Oxygen	4.10[1]	20.41[4]	0.68[4]
Ash	9.68[2]	9.50	-

[1] CEC model 240-XA elemental analyzer
[2] Ashed at 775 °C to constant mass
[3] From Rahimi *et al.* (1989)
[4] By difference

The elemental abundances in the CANMET residue are determined by the elemental composition of the Forestburg coal and the Cold Lake vacuum bottoms. Sulphur, nitrogen and oxygen are preferentially retained in higher boiling fractions from the CANMET process and in the remaining residue (Rahimi *et al.* 1989) The C/H ratio of the residue (0.94) is between those of Forestburg coal (1.37) and the Cold Lake vacuum bottoms (0.7[illegible]) It corresponds to the C/H ratio of hydrocarbons that distil between 205 and 525 °C, are soluble in methyl-tert-butyl ether and are characterised by high aromaticity and high nitrogen content; Rahimi *et al* (1989) denoted those compounds as Polars 1 Thus it appears that the organic part of the CANMET residue contains a highly condensed aromatic structure This could be corroborated further by investigating the solubility of the residue in different solvents

The ASTM D 2042-81 Standard Test Method which describes the solubility of asphalt materials in trichloroethylene may also be applied to other solvents Using this technique, the solubilities of the residue were found to be 72.1, 63.3 and 46.3 % in tetrahydrofuran (THF), toluene and pentane, respectively. THF is a powerful solvent for a wide spectrum of synthetic and natural materials (Mellan 1977) It dissolves not only aliphatic, alicyclic and aromatic hydrocarbons (as pentane) but also dissolves heterocyclic aromatic compounds more efficiently than does toluene. Moreover the aromaticity of toluene solubles is higher than pentane solubles and smaller than THF solubles. As reported by Rahimi *et al.* (1989) solubility of the Cold Lake vacuum bottoms in pentane was 76.2 % Therefore, the structure of the CANMET vacuum residue is more aromatic than the structure of the Cold Lake vacuum bottoms, especially since there is a substantial difference in the solubility of the residue in pentane and in toluene In fact, the CANMET residue can even be more aromatic than the original coal since simple aliphatic and alicyclic hydrocarbons elute first during the distillation. Moreover 8.8 % of the residue is soluble in THF but not in toluene and about 15 % of the organic part of the residue is not THF soluble at all Again this indicates that the residue contains high proportion of condensed and complex aromatic hydrocarbons which incorporate nitrogen, sulphur and oxygen in their structure.

The amount of ash in the residue was determined according to the ASTM D 482-80 Standard Test Method for Ash from Petroleum Products. A 2 g sample was placed in a crucible and ashed in a furnace at 775 °C to constant mass (±0 5 mg). The ashing of THF insolubles yielded 34 57 % ash, *i.e* 9 65 % on the basis of the original residue This may be compared with 9.68 % from Table 5 1 to show small error in those results

If the residue is ashed at 1000 °C for a few hours to a constant mass all metal oxides are transformed to their highest and known levels of oxidation Table 5 2 shows the analysis of the ashed CANMET residue performed by the X-ray fluorescence (XRF) in the Department of Geological Sciences at McGill University.

Rahimi *et al* (1989) report that the Cold Lake vacuum bottoms contain V (235 ppm), Ni (93 ppm) and Fe (18 ppm). Although the presence of some metals is beneficial in the hydrogenation process since they act as catalysts (e.g. nickel, vanadium, iron sulphate and chromium oxide) the assembly of the inorganic compounds in the residue has an overall negative effect on the conversion of the residue to acetylene in the plasma.

Table 5.2 Results from the XRF Analysis of the Ashed CANMET Residue

Compound	Content
SiO_2	36.99%
Fe_2O_3	22.57%
Al_2O_3	18.42%
CaO	15.57%
MgO	3.52%
Na_2O	0.68%
TiO_2	0.47%
K_2O	0.29%
MnO	0.17%
V	5302 ppm
Ni	3852 ppm
BaO	3512 ppm
P_2O_5	960 ppm
Cr_2O_3	622 ppm

(ppm = mass fraction • 10^{6})

It may expected that the mineral part of the coal and the catalyst would undergo small transformations during hydrogenation by the CANMET process. These include mainly pyrite converting to pyrrhotite and possible some dehydration. However, most minerals and the catalyst (iron sulphate) remain essentially unchanged (Russell and Rimmer 1973) and hence they occur in the residue. It should be emphasized that the amount of the high temperature ash is less than the amount of the inorganic part in the residue. Thus the amount of hydrocarbons in the residue that could be decomposed in plasma is less than derived from the carbon and hydrogen content in Table 5.1. In addition, the mineralogy of the original coal and the residue is much different from the mineralogy of the ash.

Some similar transformations occurring during ashing also occur initially during plasma decomposition of the residue. Carbonates will decompose with the loss of CO_2, clays will release water and sulphates will decompose releasing SO_2. Eventually, in the hydrogen plasma metal oxides will be reduced to metals by carbon (from the residue) and hydrogen (from the plasma), leading to the release of CO and H_2O. At plasma conditions carbon dioxide will be transformed to carbon monoxide, sulphur dioxide will produce H_2S and water vapour will react with carbon releasing hydrogen. All these processes will have a significant but detrimental influence on the production of acetylene.

To gain further insight into the mineralogical content of the residue the X-ray powder diffraction (XRD) study was performed. The mineral content of the residue was concentrated by dissolving a significant percentage of the organic part of the residue in THF. Subsequently, a small amount (below 0 1 g) of the THF insolubles was placed in a low temperature asher (LTA) for more than 50 hours at 100 W net RF power and 100 cm^3/min of oxygen flow LTA uses a low pressure (1-3 torr) radio frequency (RF) discharge to excite and ionize oxygen atoms which have temperature (*i e* heavy particles temperature) of around 150 °C (Jenkins and Walker 1978). In principle, only small changes in the mineralogical composition may take place during oxidation in the LTA at the mentioned above operational conditions For example pyrite could be oxidized to hematite or gypsum may be dehydrated to hemihydrate Removal of the carbonaceous material is a surface phenomenon thus a sample should be stirred. The complex aromatic structure of the THF insolubles resulted in a slow rate of oxidation.

The oxidized sample was deposited on a silver membrane in the special vacuum equipment; due to the low oxidizing rates in LTA it was impractical to collect sufficient amount of samples to use regular powder mounts Some amorphous carbonaceous material was not removed in LTA which resulted in high background as seen in Figure 7.4 a. The analysis was performed on the Phillips PW 1710 diffractometer using nickel filtered CuK_γ radiation generated at 40 kV and 20 mA The diffractometer was connected to a PDP 11 computer. Among the minerals present trigonal quartz was the easiest to identify and gypsum, anhydrite, hemihydrate (bassanite) and hematite were also seen. It is possible that hematite, anhydrite and to a certain extent bassanite are artifacts from the plasma ashing in LTA. Other iron minerals, such as siderite, pyrite and iron sulphate can be identified only with difficulty. In general carbonates (dolomite, calcite, ankerite) are possible but could not be definitely identified Similar conclusions may be drawn for feldspar (orthoclase, albite) and clay (kaolinite, illite) minerals (Figure 7 4 a). Jenkins and Walker (1978) listed minerals commonly found in coals.

6.0 TEMPERATURE MEASUREMENTS

6 1 Calorimetry

The mean exit temperature of the plasma stream at the torch nozzle, as well as the joint torch and the power supply efficiency may be conveniently determined from calorimetric experiments The calorimetric system consisted of the reactor, the heat exchanger and the water cooled flange between them, all connected in series To avoid heat losses, the calorimeter was insulated, and an asbestos gasket was placed between the reactor and the torch

K type thermocouples, with a digital meter having a precision of 0.1 K, were used to determine water inlet and outlet temperatures and the cold gas exhaust temperature (see section 6.4). The argon and the water flow rates were measured by high precision (±2% of the full scale) rotameters. The thermocouples were connected to a strip chart recorder to verify the existence of steady state conditions Normally, steady state was attained within six to ten minutes depending on the flow of the cooling water To reduce errors associated with the temperature measurements the water flow rate was maintained at around 1.3 l/min This corresponded to the minimum temperature gain of 10 K for the cooling water in the calorimeter The exhaust gas temperatures were between 7 and 10 °C

The power removed by the cooling water was obtained from the difference in the enthalpies of water entering and leaving the calorimeter. The mean exit temperature of the plasma was computed from heat capacities prepared by Lesiński and Boulos (1978)

The following independent variables determine the temperature of the exit gas and the joint efficiency of the torch and the power supply (1) nozzle diameter, (2) argon flow rate and the mode of its injection - axial or tangential, (3) number of coil turns, (4) grid setting, and especially (5) plate power The grid setting regulates the coupling of energy between the coil and the plasma gas whereas the plate power is the product of the plate current and the plate voltage delivered from the power supply The effect of the nozzle diameter and the argon flow rate, for the same apparatus, were investigated by other researchers (Munz 1974, Biceroglu 1978). In this study, the nozzle diameter was maintained at 2.54 cm, the argon flow rate was set at 58.03 g/min with 35.9 % of it injected axially, the grid setting was kept at 20.25. The optimum number of coil turns is four for monatomic and five for diatomic gases; however operating with hydrogen requires six turns. Hence, to avoid taking apart the torch frequently the experiments were performed with six coil turns.

The effect of the plate power on torch efficiency is illustrated in Figures 6 1 and 6.2. At powers below 4 kW the flame could not be sustained and above 15 kW the fireball increased in size resulting in breaking of the quartz tube which confined the flame. Increases in radiation and conduction losses from the fireball, at high power, are blamed for the decrease in torch efficiency This effect may be also seen in Figures 6.1 and 6.3 - the power removed by the cooling water and the temperature of the exit gas tend to level off as a function of the plate power. In order to start the discharge, the quartz tube was initially coated with a gold paint. The freshly baked layer of gold increased the losses, probably due to the direct coupling of RF energy to the gold coating. This effect was negligible after approximately 20 runs (Figure 6.1).

The mean exit argon temperature was best fitted with the second degree least squares polynomial:

$$T = b \cdot PP + c \cdot PP^2 \qquad (6.1)$$

where T is temperature in K, PP denotes plate power in kW, b is 570.7 ± 6.2, c is -18.18 ± 0 56 and R^2 is 0.994.

Hydrogen could be either injected to the torch or added to the argon tailflame. The effect of the latter was computed by heat balances and is shown in Figure 6.3. The heat capacity of hydrogen was taken from the JANAF Thermochemical Tables (1971) For example, the addition of up to 20% of cold hydrogen would decrease the argon flame temperature by 1100 K at 11 8 kW.

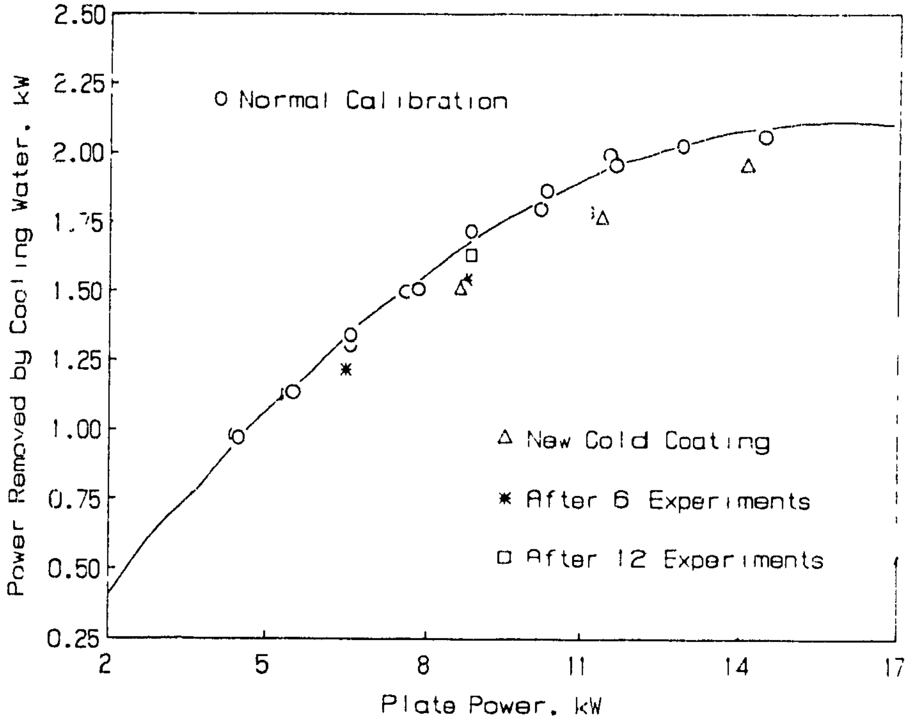

Figure 6.1 Power Removed by Cooling Water (Plasma Parameters. Nozzle Diameter = 2 54 cm, Coil Turns = 6, Grid = 20.25, Argon Flow = 20.81 g/min Axial and 37.22 g/min Swirl)

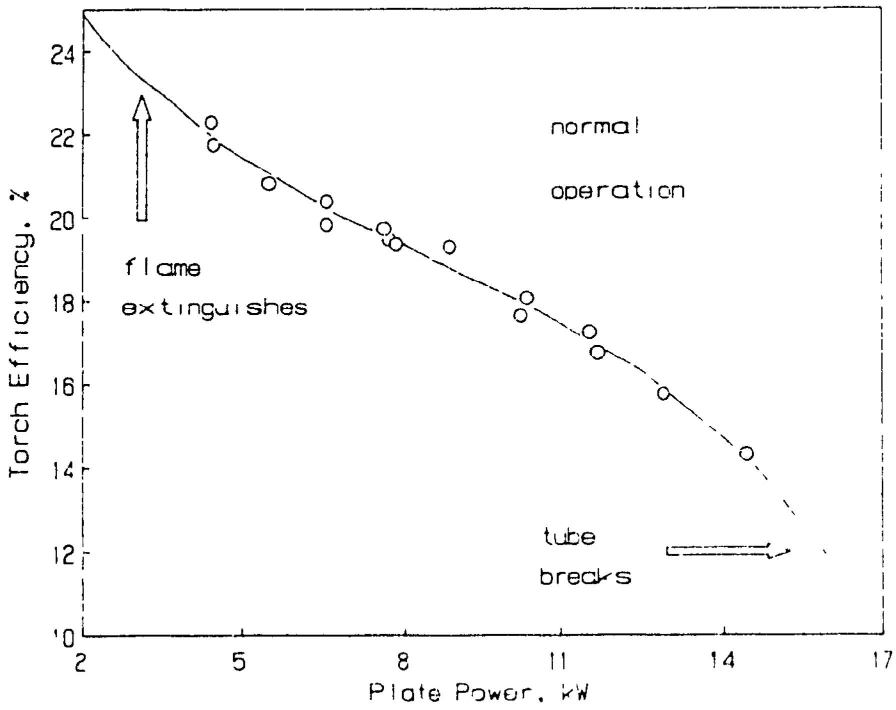

Figure 6 2 Torch Efficiency (Plasma Parameters Nozzle Diameter = 2.54 cm, Coil Turns = 6, Grid = 20 25, Argon Flow = 20 81 g/min Axial and 37 22 g/min Swirl)

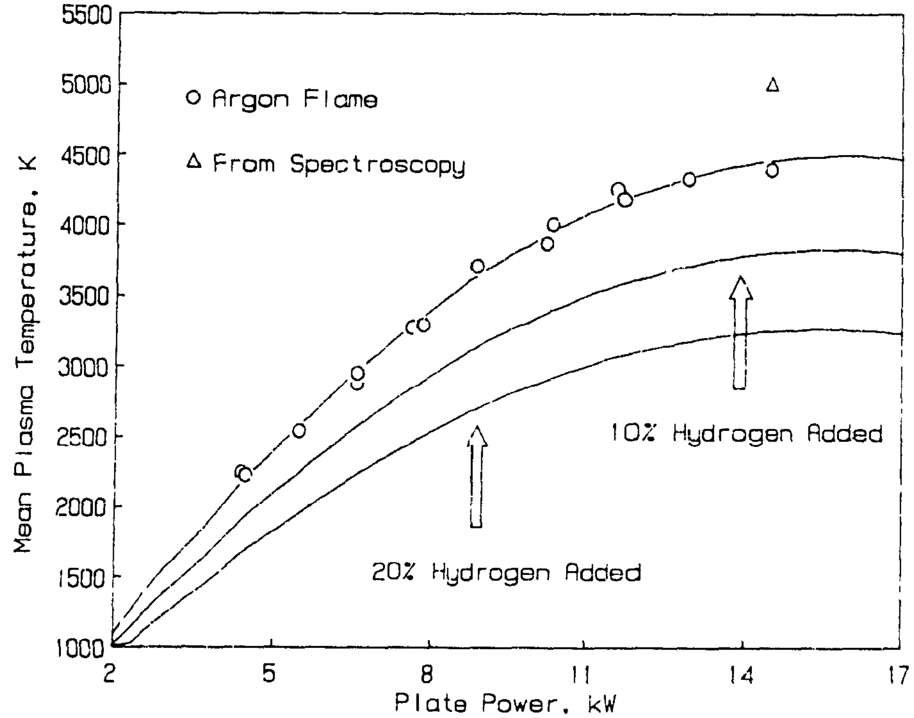

Figure 6.3 Mean Exit Gas Temperature (Plasma Parameters: Nozzle Diameter = 2.54 cm, Coil Turns = 6, Grid = 20 25, Argon Flow = 20.81 g/min Axial and 37.22 g/min Swirl)

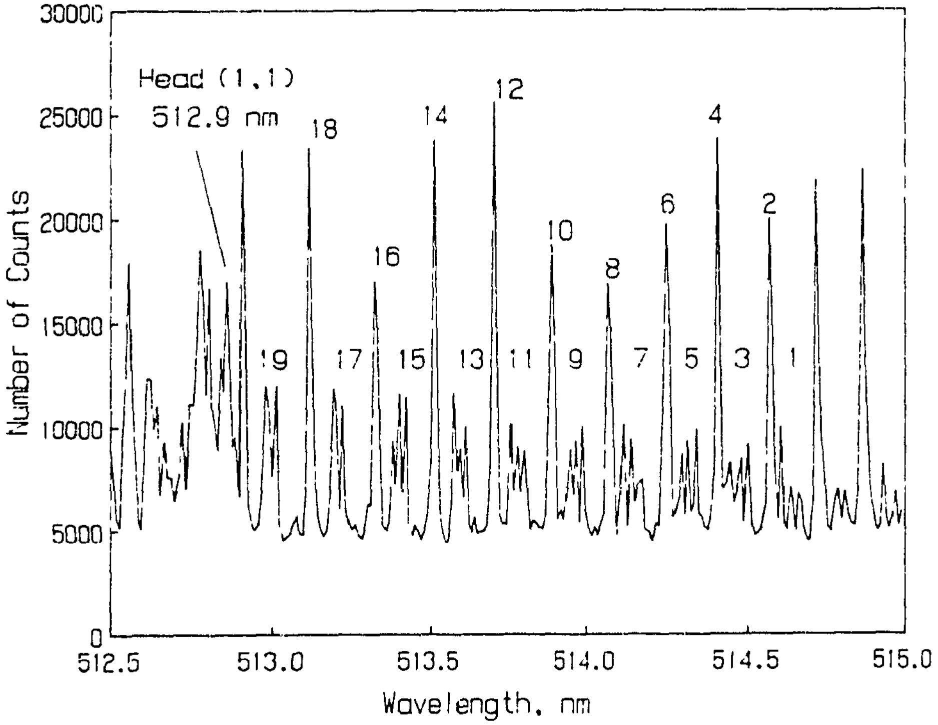

Figure 6.4 Thermometric Lines for Partially Resolved 516.5 nm C_2 Band (Plasma Parameters: Plate Power = 14.4 kW, Argon Flow = 20.81 g/min Axial and 37.22 g/min Swirl, Location = 8.8 cm below Coil and r = 0.7 cm)

6.2 Spectroscopy

A direct and a non-intrusive method to measure the local temperature in the plasma is to look at the intensity of the radiation coming out at specific wavelengths This was used to confirm the calculated temperature from the calorimetric experiments. Many different spectroscopic methods yield temperature, however, they all involve the assumption of the thermodynamic equilibrium between the particles (atoms, ions, molecules, electrons) giving rise to radiation For example, if one uses the intensity of a line emitted from an excited argon atom, calculation of temperature using this intensity involves the assumption that the "electron gas" and the "argon atom gas" in the plasma are in equilibrium with respect to collisions and have the same temperature This corresponds to local thermodynamic equilibrium (LTE) At the temperatures and electron number density we are dealing with here ($T < 6000$ K), the plasma is generally not in LTE because radiation becomes an important energy exchange mechanism as compared with collisions within the plasma However, we can consider the heavy particles (atoms, ions, molecules) to be in equilibrium at a temperature T_g that is different from the electron temperature T_e (usually $T_g < T_e$) Departures from LTE have only small effects on the plasma enthalpy but may be significant in spectroscopic measurements (Boulos *et al* 1986)

Because of this behaviour, two types of spectroscopic measurement are made to characterize the state of our plasma. The temperature of the heavy particles is the most important one to measure because they are the main source of energy transfer. This temperature will be deduced from the rotational emission spectra of the C_2 molecule around 516 5 nm Although it is recognised as a difficult measurement because of the high wavelength resolution required and the complex nature of molecular bands, it is the best method to obtain a meaningful temperature which can be compared to the calorimetric experiments. Furthermore it is only linked to heavy particle behaviour and is not affected by LTE consideration

The second diagnostic is to evaluate the electron number density profile using the half width of the $H\beta$ line (486 132 nm) This measurement also does not depend on LTE assumptions and gives a true value of the electron density profile whatever the type of equilibrium in the plasma. Two important types of information are deduced from the profile. Firstly, its shape will show homogeneity of the plasma in the neighbourhood of the crucible. Secondly, the density can be compared to the theoretical density needed to have LTE in the plasma.

All the spectroscopic measurements were taken at the maximum plate current of 3.0 A and the coinciding voltage of 4.8 kV. This corresponded to the plate power of 14.4 kW and the average flame temperature of 4450 K as determined from calorimetry. The flow of argon was maintained at 20.81 g/min (11.7 l/min) to the axial and 37.22 g/min (20.8 l/min) to the tangential injection ports in the torch.

The spectroscopic system was based on a one meter focal length Jobin-Yvon THR 1000 grating monochromator with a 1800 groves/mm grating Light from the plasma was collected by a lens with optical aperture of f/4 and brought to the monochromator by an optical fibre. A photomultiplier was used to record the light intensity. The resolution of the monochromator was 0.005 nm.

All measurements were performed through the circular reactor window with a radius of 1.27 cm and located centrally 7.5 cm below the torch coil The reactor radius was 2.54 cm. Horizontal and vertical profiles were taken across the window. The crucible, which was 1.9 cm long and 1.4 cm in diameter, was located 7.8 cm below the torch coil. It follows that the horizonal profiles of the temperature and the electron density were taken at the level of the middle line of the crucible.

6.2.1 Temperature Measurements

C_2 molecules are normally present during plasma decomposition of hydrocarbons as opposed to N_2 or N_2^+ which are often used for rotational temperature measurements. Moreover, the overlapping of C_2 bands with spectra emitted by other hydrocarbon radicals or by argon is negligible (Winkelmann *et al.* 1977). The 516.5 C_2 band (Swan band) will thus be used along with the spectroscopic data of Czernichowski (1987) and Czernichowski *et al.* (1987) This method could be used to determine gas temperature in a continuous reactor. In this study however, small amounts of carbon dioxide (less than 1% of the total flow) were mixed with argon before entering the torch to simulate the hydrocarbons and to generate the C_2 molecule. No residue was treated during these measurements.

The intensity of a spectral line at a given wavelength from a transition between upper energy level p to lower q per unit volume of the plasma unit solid angle and time is given by.

$$I = \frac{h \cdot c}{4 \cdot \pi \cdot \lambda} \cdot N_p(T) \cdot A_{pq} \qquad (6\text{-}2)$$

where Np(T) is the population density of the species in the excited upper level p, A_{pq} is the probability of the transition (in s^{-1}) and $h \cdot c/4 \cdot \pi \cdot \lambda$ is the energy of the emitted photons. Knowing the total density N(T) of the atoms, the population density in the different levels at equilibrium at temperature T can be obtained using the Boltzmann density distribution equation:

$$N_p(T) = \frac{N(T)}{Z(T)} \cdot g_p \cdot \exp\left(- \frac{E_p}{k \cdot T}\right) \qquad (6\text{-}3)$$

where E_p is the energy of the upper excited state, k is the Boltzmann constant, Z(T) is the partition function and g_p denotes the statistical weight of level p The partition function is a normalization function obtained by summing up the Boltzmann factor for all bounded levels of the atom. Taking the logarithm of (6.2) and substituting (6.3) one obtains the equation for the Boltzmann plot,

$$\ln\left(4\pi \frac{I}{S}\right) = - \frac{E_p}{k \cdot T} + C \qquad (6\text{-}4)$$

where $S = g_p \cdot A_{pq} \cdot h\nu_{pq}$ and $C = \ln(N(T)/Z(T)) =$ constant The slope of the line ln (I/S) is a function of E_p and thus yields the temperature

Figure 6.4 shows an example of the rotational band of the C_2 molecule measured at 7 mm from the central axis of the flame and 8.8 cm below the coil. Each peak numbered on this curve corresponds to one upper level E_r, its area is reported on a Boltzmann plot. An example of a Boltzmann plot is given in Figure 6.5 for r=6.4 mm from the mid point of the window and 8.8 cm below the coil. The slope of the least squares line yielded a temperature of 5000 ± 210 K.

The horizontal temperature profile deduced from these spectra is presented in Figure 6.6. The Abel inversion is a mathematical operation used to correct intensity measurements along a line of sight in the plasma into local emissivity measurement. It thus yields the true value of local temperatures however with a larger associated error. Since the intensity profile is relatively flat the Abel inversion does not yield significantly different results.

The flat profile in the centre part of the reactor indicates that the crucible is exposed to a constant temperature profile. Since the cold fringes of the plasma lie outside of the view of the reactor window the average temperature calculated from the calorimetric measurements (Figure 6.3) is lower than determined from the spectroscopic experiments.

6.2.2 Electron Density Measurements

Electric fields existing in the plasma have the effect of widening the spectral lines emitted by the atoms (Stark effect). These fields are generated by the charged particles (electrons, ions) and are proportional to their number density. Measurement of the line broadening thus yields the electron number density n_e. One can note that this line width measurement is independent of the line intensity and hence it does not depend on the assumption of LTE. Griem (1964) calculated the proportionality coefficients between the electron density and the width ($w_{1/2}$) of hydrogen lines measured at half of the maximum amplitude;

$$n_e = c \cdot (w_{1/2})^{3/2} \qquad (6.3)$$

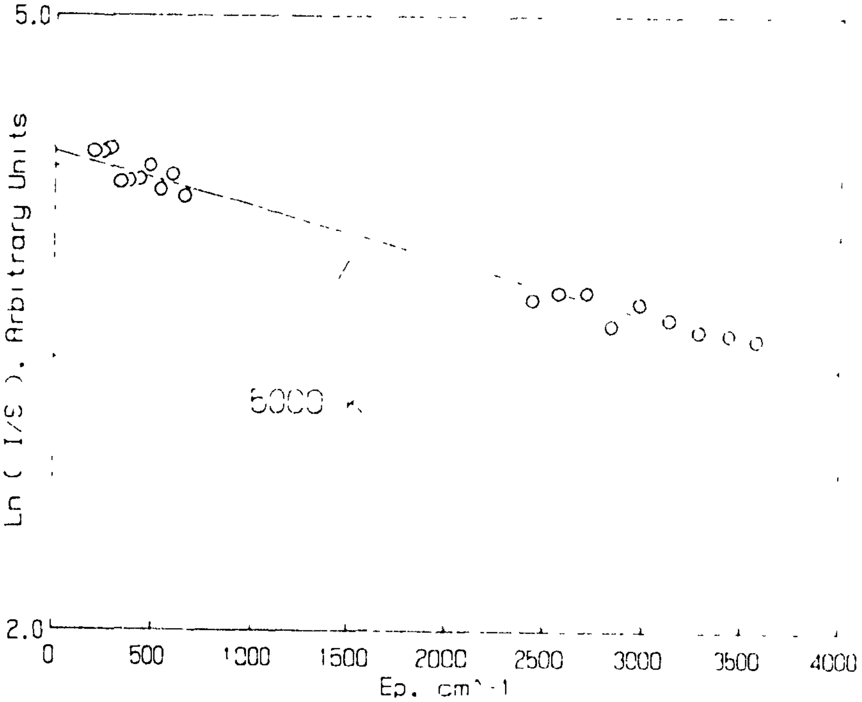

Figure 6.5 The Boltzmann Plot for Partially Resolved 516.5 nm C2 Band (Plasma Parameters: Plate Power = 14.4 kW, Argon Flow = 20.81 g/min Axial and 37.22 g/min Swirl. Location = 8.8 cm below Coil and r = 0.64 cm)

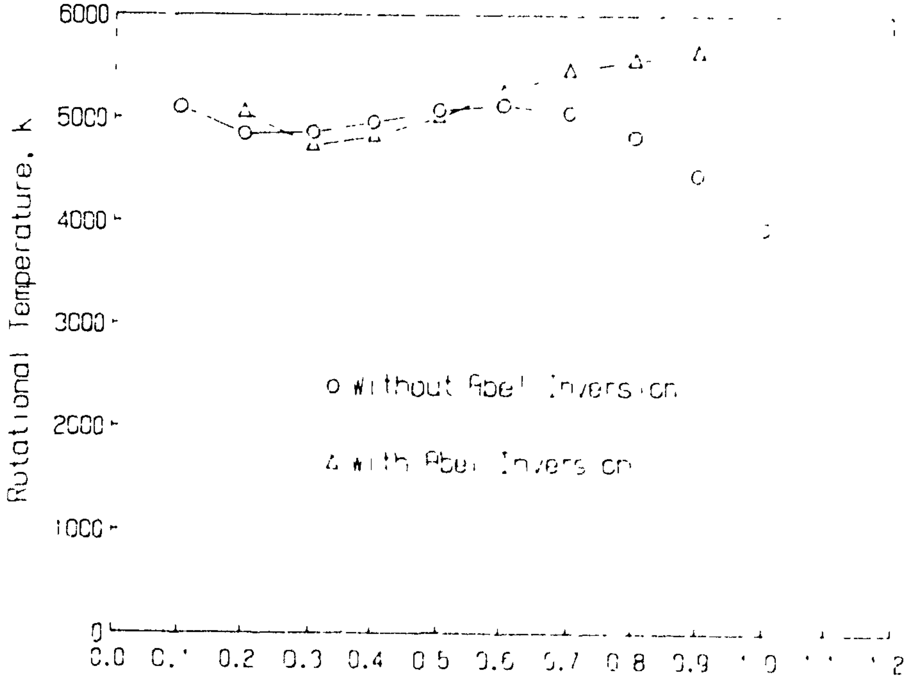

Figure 6.6 The Horizontal Rotational Temperature Profile from Partially Resolved 516.5 nm C2 Band (Plasma Parameters: Plate Power = 14.4 kW, Argon Flow = 20.81 g/min Axial and 37.22 g/min Swirl, Location = 8.8 cm below Coil and 0.0 cm < r < 1.5 cm)

with c being a weak function of n_e and T. The coefficient $c(n_e,T)$, corresponding to the experimental conditions, was taken as $c(n_e = 10^{14}cm^{-3}, T = 5000K) = 3.84 \cdot 10^{14}$ $\AA^{-3/2}$ cm^{-3} As in the case of C_2 rotational temperature the measurements were performed on the argon plasma. A very small amount of hydrogen (less than 0 5 %) was added to argon tail flame to ensure an insignificant change in thermal conductivity of the plasma gas The thermal conductivity of hydrogen is approximately ten times higher than the thermal conductivity of argon thus more energy is removed by the cooling water in the torch for an argon/hydrogen than for a pure argon plasma This results in changes in the temperature and in the electron density

Because of the relatively flat profile, and the large error associated with the Abel inversion, no inversion was made for this measurement Figure 6 7 shows that in this investigation the electron density in the centre of the argon flame ($0\ 0 \le r \le 1\ 0$ cm) remains approximately constant and equal to $1\ 2 \cdot 10^{14}$ cm^{-3} Again, this indicates that there should be no significant radial thermal gradients in the case of the argon flame The electron density profile along the vertical diameter of the window is presented in Table 6.1.

Table 6 1 Vertical Centre Line Profile of Electron Density

Position below the top of the window (cm)	Electron density (cm^{-3})
0 27	$1\ 94 \cdot 10^{14}$
0 77	$1\ 80 \cdot 10^{14}$
1 27	$1\ 54 \cdot 10^{14}$

Experimental criteria imply that in order to have LTE the electron density must be larger than 10^{16} cm^{-3} (Boffa *et al* 1971, Lochte-Holtgreven 1968, Kick *et al* 1984) The reported above measurements show that n_e stays far below this value, hence the electron temperature is not in equilibrium with the heavy particles temperature in the volume of interest This implies that

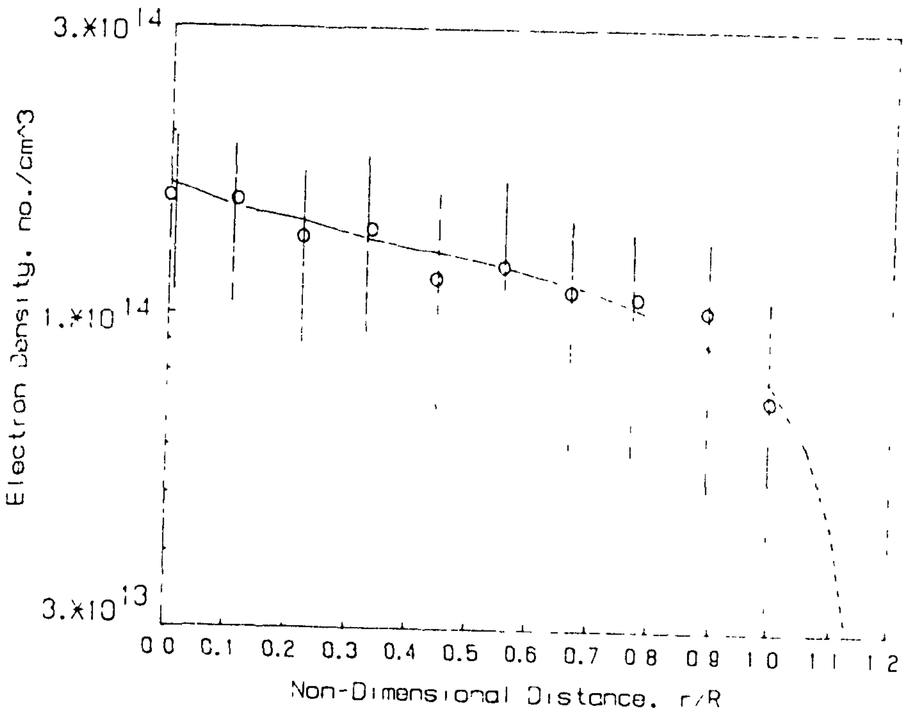

Figure 6.7 The Horizontal Electron Density Profile from Hβ Hydrogen Line without Abel Inversion (Plasma Parameters: Plate Power = 14.4 kW, Argon Flow = 20.81 g/min **Axial** and 37.22 g/min Swirl, Location = 8.8 cm below Coil and 0.0 cm ≤ r ≤ 1.3 cm)

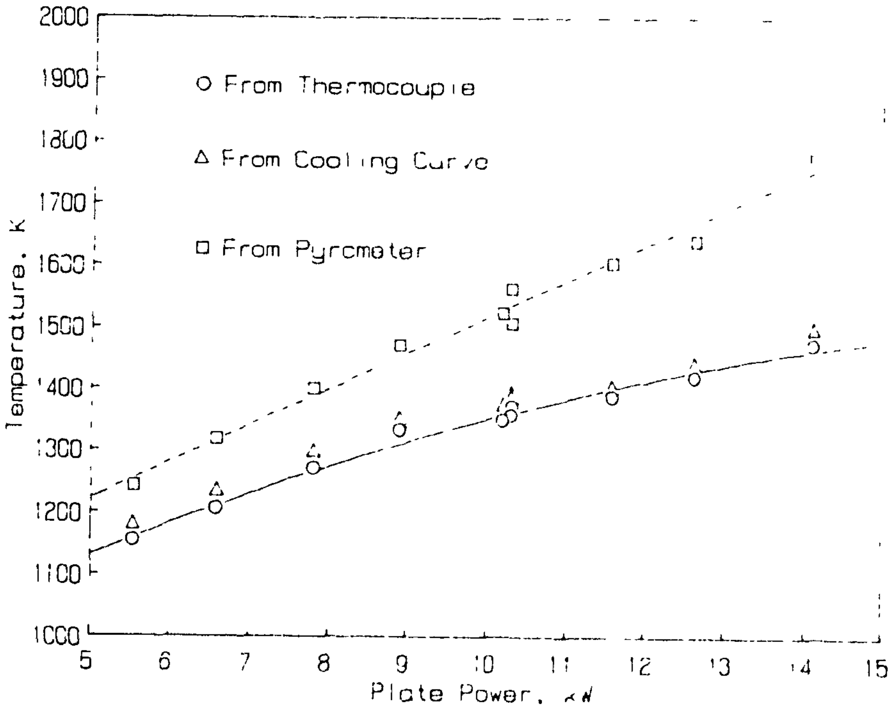

Figure 6.8 True and Apparent Surface Temperatures of the Carbon Cylinder in an Argon Plasma Jet (Plasma Parameters: Argon Flow = 20.81 g/min Axial and 37.22 g/min Swirl)

the heavy particles temperature had to be derived from an independent measurement

6 3 Pyrometry

In static systems, the temperature of the plasma gas is normally higher than the temperature of a reacting particle For the steady state conditions the heat transferred to a crucible by convection is removed by radiation to the cold reactor walls by conduction through the crucible support and is consumed during the endothermic reaction. This is especially important in the case of a plasma jet impinging on a crucible filled with hydrocarbons If the cracking temperature of hydrocarbons inside a crucible is substantially below the gas temperature the yield of acetylene may be affected. The cracking temperature could be approximated from the non-contact determination of the radiation emitted by the crucible walls

There are three types of radiation measuring instruments (DeWitt and Albright 1986) (1) total radiation pyrometer, (2) single-colour, optical or brightness pyrometer, and (3) two-colour also called two wavelength or ratio pyrometer (Themelis and Gauvin 1962) In short, total radiation and optical pyrometers require accurate values of total or spectral emissivities which may not be known with the adequate precision In addition, their performance is highly dependent on the size of a target and on the viewing conditions, as for example transmittance of the reactor window In contrast, two-colour pyrometer does not demand the knowledge of the absolute values of spectral emissivities at the two selected wavelengths However, it should be verified that the ratio of those emissivities is approximately unity or, in other words, that a target exhibits grey body characteristics.

In view of the above arguments the Ratio-Scope 8 two-colour pyrometer was used. The instrument was fabricated by Capintec Instruments and it was calibrated by the manufacturer between 1073 and 2273 K Its response time was 0 3 s and it measured the intensity of radiation emitted in narrow bands around two wavelengths 0 83 μm and 0.78 μm. Close-up lenses were mounted on the objective for small target measurements In experiments described in this chapter the pyrometer was focused on the central part of the crucible

Radio frequency interference was experienced between the magnetic field generated by the torch coil and the pyrometer which included the sensing head, the control readout unit and the connecting cable. Although Ratio-Scope 8 could be operated with no protection, the interference was severe with another two-colour pyrometer which was initially employed in the study. Since it was not feasible to remove the source of interference nor to deflect electromagnetic interference (EMI) field, two shielding aluminum boxes were built to enclose the head and the readout unit In theory, the boxes, often called Faraday cages, should not contain any gaps which would permit leakage of the external field (Breed 1986) As proven by Gauss, no electromagnetic radiation passes through an enclosure made out of a perfect conductor (Gomez 1988) In practice, however, there must be an opening for the objective lens and another for the digital readout The problem is somewhat alleviated by grounding. The braided copper strap, as suggested by Breed (1986), was used to diminish the impedance of the grounding connection at high frequencies The cable between the sensing head and the readout unit was also protected by a braided copper shield and grounded on both sides. Grounding on only one side resulted in poorer shielding, this conclusion was also reached by Rivenburg and Juba (1986)

In general, when a pyrometer is focused on a target it measures the incident flux density H(λ,T), which consists of the emission from the target surface, radiation from the plasma gas and radiation from the surroundings reflected from the target surface, where λ denotes wavelength and T is the absolute temperature

$$H(\lambda,T) = H_e(\lambda,T) + H_r(\lambda,T) + H_f(\lambda,T) \qquad (6.6)$$

In plasma systems, contributions from the last two terms may never be neglected To verify temperature readings taken by the pyrometer, a black body hole was drilled in a graphite cylinder and an W-5%Re/W-26%Re thermocouple (described in the next section) was inserted inside it The cylinder diameter and its length were identical to the actual molybdenum crucible. Once the plasma was extinguished the pyrometric cooling curve was recorded and the surface temperature was obtained by extrapolation of temperatures to time "zero" on the semi-log paper. This is illustrated in Figure 6.8 The temperatures measured from the cooling curves and by the thermocouple agree to within 3 %. The accuracy of the pyrometer was 1.5 % of the true temperature. The effect of radiation from the plasma gas may be reduced by selection of different wavelengths to avoid argon spectral lines. However for the system of reacting hydrocarbons it is virtually impossible to avoid the radiation from the plasma gas. As a matter of fact, the radiation from the soot, carried by the plasma gas, is so intense that the surface temperature of the crucible could not be measured during the reaction.

It should be added that a difference of up to 100 K was observed between the top and the bottom of the graphite cylinder

Once the amount of the volatile hydrocarbons in the crucible is depleted, the temperature of the crucible increases until it reaches the steady state According to Touloukian and Dewitt (1970-1972) the spectral emissivity of carbon, which is a grey body, is around 0 8 whereas that of molybdenum is between 0 07 and 0 65 depending on wavelength Thus the steady state temperature will be higher for the clean molybdenum crucible (because its emissivity is lower) than for a crucible with a layer of soot deposited on it during the reaction (since its emissivity is higher) Unfortunately this degree of "dirtiness" was not a reproducible function of the operational conditions Nevertheless, it may be concluded that the highest, temperature would be achieved for the clean molybdenum crucible and the lowest temperature for a crucible completely coated with soot Such a "dirty" crucible may be approximated by a graphite cylinder It follows from Figure 6.9 that for experiments in a hydrogen/argon plasma the maximum temperature may vary by up to 300 K, at the same operational conditions, depending on the amount of soot coating on the crucible walls For the reasons that will soon become apparent, the temperatures were measured by thermocouples rather than from the cooling curves

It may be recalled from Figure 6.8 that due to the constant spectral emissivity of graphite, the temperatures measured by the thermocouple and by the pyrometrically determined cooling curves, were essentially the same A similar conclusion may not be drawn for molybdenum For metals the

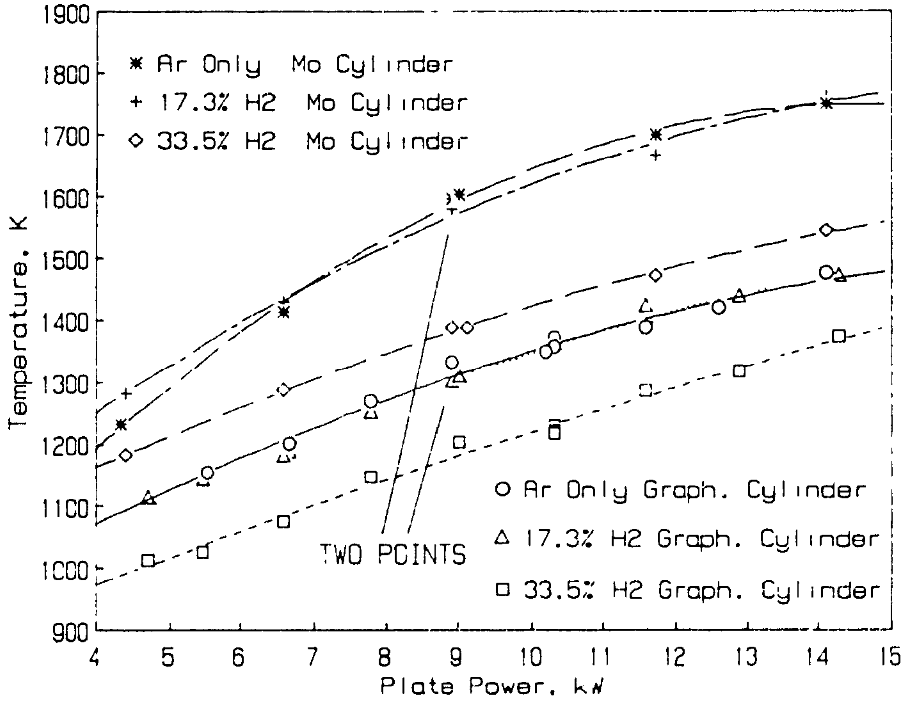

Figure 6 9 The Surface Temperature of the Carbon and Molybdenum Cylinders in Argon and Argon/Hydrogen Plasma Jets (Plasma Parameters Argon Flow = 20 81 g/min **Axial** and 37.22 g/min Swirl, Hydrogen Flow = 0 61 or 1 46 g/min to the Tail Flame)

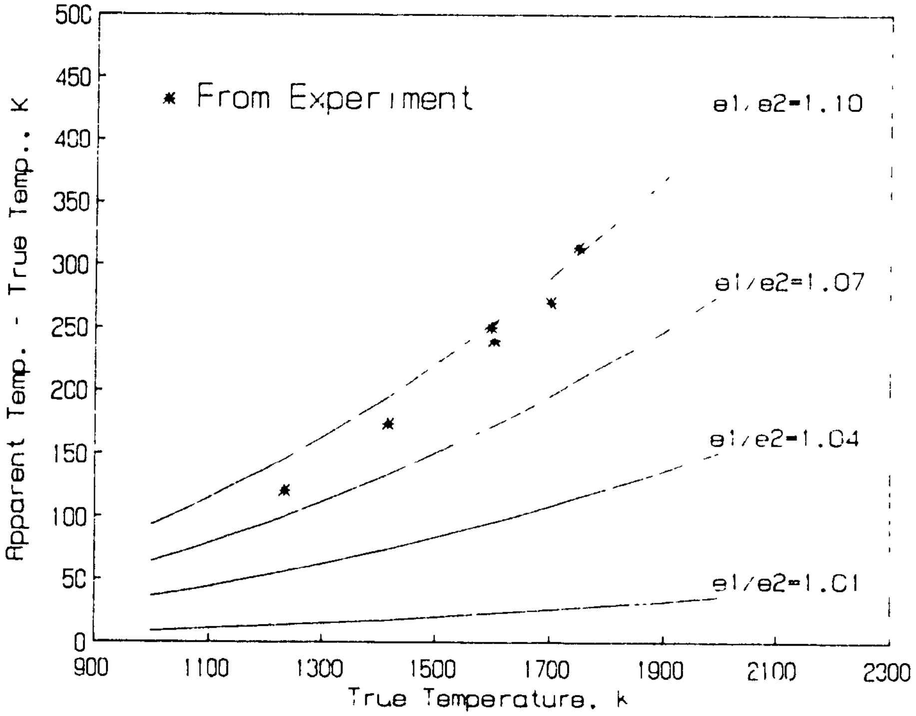

Figure 6 10 Verification of the Grey Body Assumption for Determination of Surface Temperature of Molybdenum Crucible by a Two-Colour Pyrometer emissivity at a smaller wavelength (e_1) is higher than emissivity at a larger wavelength (e_2) (Heimann and Mester 1975) Therefore a two-colour pyrometer tends to overestimate the temperature of a metal surface At time "zero" when plasma is extinguished, both $H_r(\lambda,T)$ and $H_f(\lambda,T)$ disappear (Equation 6.6), it follows from the Wien's law that (Wien's law is an approximation to Planck's law for $\lambda \cdot T < 0\ 3$ cm K),

$$E(\lambda,T) = c_1 \cdot \lambda^{-5} \cdot \exp\left(- \frac{c_2}{\lambda \cdot T} \right) \qquad (6\ 7)$$

where $E(\lambda,T)$ is the monochromatic emissive power of a black body, c_1 and c_2 are constants, $c_1=3\ 7415 \cdot 10^{-16}$ W m^2 and $c_2=1.4388 \cdot 10^{-2}$ m K. Further, taking the ratios of intensities at the two selected wavelengths it is possible to write,

$$\frac{e_1 \cdot E(\lambda_1,T_t)}{e_2 \cdot E(\lambda_2,T_t)} = \frac{E(\lambda_1,T_a)}{E(\lambda_2,T_a)} \qquad (6\ 8)$$

where T_t and T_a denote respectively true and apparent temperatures Substituting (6 7) into (6 8) and after some algebraic manipulation one obtains,

$$T_a = \left(\frac{1}{\lambda_2} - \frac{1}{\lambda_1}\right) \cdot \left[\frac{1}{c_2} \cdot \ln\left(\frac{e_1}{e_2}\right) + \frac{1}{T_t} \cdot \left(\frac{1}{\lambda_2} - \frac{1}{\lambda_1}\right) \right]^{-1} \qquad (6.9)$$

It is easy to see that for a grey body, when $e_1 = e_2$, $T_a = T_t$ Figure 6.10 presents the difference between true and apparent temperatures for different ratios of emissivities computed from equation 6 9, λ_1 and λ_2 were taken as 0 78 μm and 0 83 μm As the true temperature and the ratio of emissivities increase, readings of apparent temperature become associated with large errors From Touloukian and Dewitt's (1970-1972) compilation of data of spectral emissivities of molybdenum it follows that the ratio of

$e_{0\ 78\ \mu m}/e_{0\ 83\ \mu m}$ may vary, depending on the set of data, but it is never constant In Figure 6 10 the experimental points were obtained by subtracting the true temperature, measured by the thermocouple, from the apparent temperature determined from the cooling curves. It follows that for this investigation the ratio of spectral emissivities, at the mentioned wavelengths, is between 1.08 and 1.10.

6 4 Thermocouple Thermometry

In the induction plasma system the flame remains at a floating potential of around 1100 V, AC at 4 MHz, as measured by the Tektronix P6013 probe with 1000 times attenuation which was connected to an oscilloscope In order to maintain the plasma flame the reactor, the sampling probe and the heat exchanger were operated at the floating potential. An attempt was made to insert a non-conductive transite washer, that could withstand high temperature, between the reactor and the heat exchanger which was grounded The gas leaving the reactor was still partially ionized requiring a transite ring at least 5.0 cm wide to avoid discharges between the gas and the heat exchanger In principle this change allowed the measurement of temperature of the gas exiting the heat exchanger by a K type ungrounded thermocouple It was observed however, that the radio frequency interference (RFI) of the torch field with the thermocouple wire resulted in inaccurate temperature results. The inlet and outlet water temperatures were initially measured by bimetallic dial thermometers between 0 and 50 °C. Although accurate, during calorimetric experiments, they demanded long running times to verify the steady state conditions

In order to avoid these difficulties it was necessary to develop a technique to separate DC thermocouple signal, (few mV) from the RFI (hundreds of V, for a floating thermocouple inside the probe) Normal filters would attenuate the already weak DC signal but it is known that ferrite beads have high impedance to radio frequencies, above 1 MHz In addition they can substantially attenuate transient spikes which often occur in RF plasma systems due to arcing Ferrite beads consist of polycrystalline spinel structured - ceramic materials which may contain oxides of iron, nickel, zinc, or manganese. Since above a certain frequency their resistance increases and inductance decreases they may be described as frequency-sensitive resistors (Gigliotti 1975)

Ferrite beads were placed in two locations. (1) very close to the apparatus to eliminate transient spikes and to attenuate AC component of the signal - those beads were inclined to overheat and (2) just before the strip chart recorder to eliminate any RFI in the thermocouple cables Thus the cables did not have to be shielded with a copper strap. The strip chart recorder was not placed in the Faraday cage but was situated far away from the torch. Every thermocouple line was wrapped around three or four large beads or snap-on chokes to gain sufficient attenuation of the noise.

As opposed to the nickel-chromium vs. nickel-aluminum thermocouples used to measure water and exit gas temperatures it was necessary to employ tungsten rhenium thermocouples for measurements of gas temperature inside the reactor. Bare wire tungsten-5% rhenium vs tungsten-26% rhenium thermocouples could measure temperature up to 3000 K for short exposures in neutral or reducing atmospheres. They were supplied by Omega Engineering Inc. Burns and Hurst (1975) review other types of thermocouples for measurements of high temperatures

During the initial experiments soot tended to form a layer at the tip of the probe around the thermocouple junction Although gas flowed through this layer the flow rates through the probe were approximately 30 % lower than normal and the recorded temperature decreased dramatically. It is thought that the temperature of the soot layer was lower than the gas temperature due to the heat loss by radiation from the soot surface. Subsequently, in the following experiments the thermocouple was removed from the suction probe

An attempt was made to verify the calorimetrically determined flame temperature using the suction probe In principle, one can measure the temperature of the pure argon plasma flame at low power (below 7.0 kW) that corresponds to the average flame temperature of under 3000 K. However, under those conditions the plasma flame inverts (Chapter 4), and the temperature does not represent the average flame temperature. Moreover, it was noticed that the probe, after a few seconds of operation, was sucking a small stream of incandescent gas whose temperature was likely to be higher than the average flame temperature. Thus it may be concluded that those difficulties prevent the use of a suction probe to measure the temperature even in the colder region of the RF plasma flame.

7.0 RESULTS AND DISCUSSION

The objectives of this investigation were twofold; firstly to optimize the production of light unsaturated hydrocarbons (including liquids) as a function of average plasma temperature, plasma gas composition, and residence time, and secondly to characterize the unconverted residue in terms of elemental and mineralogical changes.

This chapter is divided into three sections. The qualitative aspects such as microscopy and X-ray diffraction are discussed first followed by the quantitative measurements. Finally the results from this study are compared with the existing data.

The residue before the plasma treatment will be referred to as the CANMET, the original or the fresh residue and after treatment as the unconverted or the unreacted residue.

7 1 Qualitative Results

7.1.1 Visual Observations

It was initially discovered that if the crucibles were fully filled before reaction, that much material overflowed (because of swelling), and reacted in an uncontrolled way The use of approximately 1.2 g, which occupied 50 % of the crucible volume, prevented this problem.

In the first few seconds of exposure to the plasma, the residue melted and expanded to the top of the crucible forming a porous dome. The hydrocarbon content of this layer was soon depleted and so it stabilized in this position. As the reaction progressed, the cracked gaseous hydrocarbon products flowed out of the crucible through the dome. Early during each experiment a layer of soot started to form on top of the dome and to a lesser extent on the external crucible walls. The mass of the soot layer was usually about 0.1 g or 11 % of the carbon initially present in the sample. It is believed that the source of this soot was the decomposition of acetylene produced in the reaction.

The height to which the dome rose depended on the temperature and composition of the plasma gas. High temperatures or the presence of hydrogen gave high heat transfer rates leading to rapid reaction within the crucible and thus a low dome. With a pure argon flame at low temperature the dome formed at the very top of the crucible.

The unconverted residue did not only form the dome, but it was always found adhering to the inside surface of the bottom and the walls of the crucible. The entire unconverted residue could be removed from the crucible and it had a hollow cylinder-like shape. This leads to the conclusion that the pyrolysis took place not only at horizontal interface between the residue and the plasma gas but also at the hot crucible walls.

During the reaction, the crucible was surrounded by the plasma gas, gaseous products and soot. The yellowish light radiated by the products was so intense that the crucible surface temperature could not be measured by the two wavelength pyrometer at this time. Visual observations showed that the crucible remained black (cooled) until the end of the reaction and only then did it achieve red heat. It may be concluded that the steady state crucible temperatures described in section 6.3 (Figure 6 9) were only achieved after the cracking reactions were essentially complete Nothing can be said concerning the temperature of the residue within the crucible which was exposed directly to the plasma flame.

The completion of cracking could also be inferred from the colour of the plasma flame which became blue and white respectively for pure argon and argon/hydrogen plasmas. Carbon whiskers of soot which had grown on the dome during reaction emitted intense red radiation because they were hotter that either the crucible or the dome. Their dimensions were, however, too small to allow a temperature measurement by the pyrometer

If the unconverted residue was re-exposed to the plasma in a second experiment, no further reaction was observed. This could be explained by the fact that the maximum crucible temperature was never higher than 1700 K (Figure 6.9). The vaporization rate of graphite at this temperature is practically zero (Clarke 1967). The reaction rate of graphite and hydrogen at the partial pressure of hydrogen of 10 kPa can be estimated as maximum 1 nmol/s or $4.3 \cdot 10^{-5}$ g of graphite/hr (Clarke 1967) which is too small amount to be detected by weighing

7.1 2 Microscopy

In this section, the changes in the mineral texture of the CANMET residue during the plasma treatment as determined by the optical and scanning electron microscopy are discussed.

7 1 2 1 Optical Microscopy

Thin sections were made of both fresh residue and unreacted residue by mounting ground particles in a resin and polishing the resin to a thickness of 30 microns on a glass plate. For fresh samples, the residue was first leached with THF and then ashed in the LTA to remove most of the organic carbon and concentrate the remaining minerals The unreacted residue (exposed to 17 3 % hydrogen plasma at 3110 and 3040 K) does not dissolve in THF and oxidizes only slowly in the LTA, and so it was simply ground

The size of the particles depended on the sample preparation, the shape, colour and other features could be examined at magnifications of 100 and 400x in transmitted and reflected light In transmitted light, the particles of the fresh residue were less angular then the particles of the unconverted residue In reflected light, particles before and after treatment displayed distinct colours Particles of the unconverted residue had no distinguishable structure and showed plenty of minute reddish internal reflections Single crystals were observed embedded in the matrix of the CANMET residue but they were not seen in the unconverted residue.

A few general conclusions may be drawn The residue after treatment is even more homogeneous since no crystals could be observed with 400x magnification However, the presence of internal reflections suggest the existence of very small and imperfect crystals with cracks and flaws The crucible temperature was sufficient to result in the partial melting of some minerals Since cooling of the hot crucible was fast (temperature decreased to below 800 °C in less than 15 s) complete recrystallization did not occur and the crystals formed were minuscule.

7.1 2.2 Scanning Electron Microscopy (SEM)

The fresh CANMET residue leached with THF and ashed in the LTA and the ground unreacted residue obtained from the upper part of the crucible (the dome) from an experiment in a 10 0 % hydrogen plasma at 3390 K were investigated on JSM-840A scanning electron microscope Samples of the unreacted residue were too small to permit the analysis of the same samples in both optical microscopy and SEM studies The samples were prepared by depositing a thin layer of the material dispersed in ethanol on graphite mounts.

Single crystals of 1 to 5 μm in size were observed at the magnification of 5000x on the surface of the carbonaceous particles of the THF leached CANMET residue Iron, calcium and silicon are contained in different minerals, such as iron sulphate, bassanite and silica Their distributions were mapped (at 5000x magnification) and it was confirmed that they were associated with different single crystals.

Figures 7.1 a, b and c show the unconverted residue magnified 50, 500 and 5000x. Because the residue was crushed after the reaction, the particles are angular Distributions of iron, calcium and silicon were mapped and these elements were uniformly disseminated in every particle shown in Figure 7 1 c X-ray spectra were taken by SEM at a magnification of 50x of the fresh and the unconverted residues (Figure 7 2 and 7 3) The low magnification ensures (Figure 7.1 a) that the composition is obtained from many particles and it may be considered as average This technique cannot show elements lighter than sodium thus carbon does not appear in Figures 7 2 and 7 3 Clearly, the plasma treatment does not preferentially remove any of the important metallic elements

Although some of the sulphur is converted to H_2S (Section 7 2 3), Figure 7.3 shows that most of the sulphur content is retained in the residue

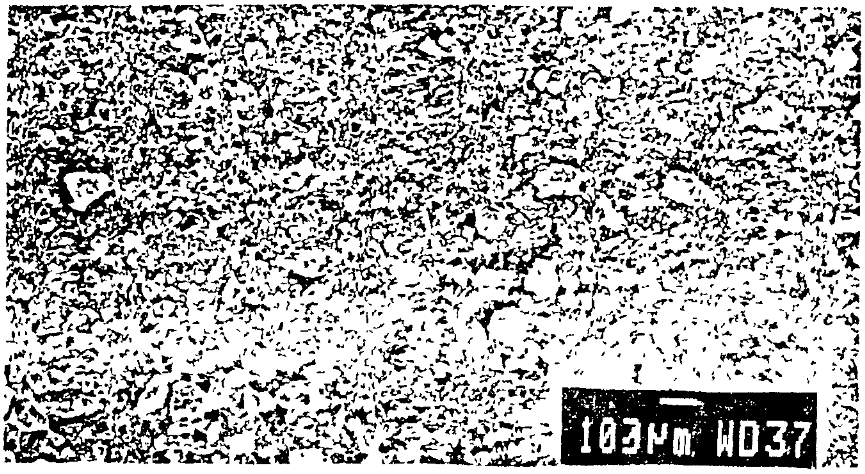

7.1a

71b

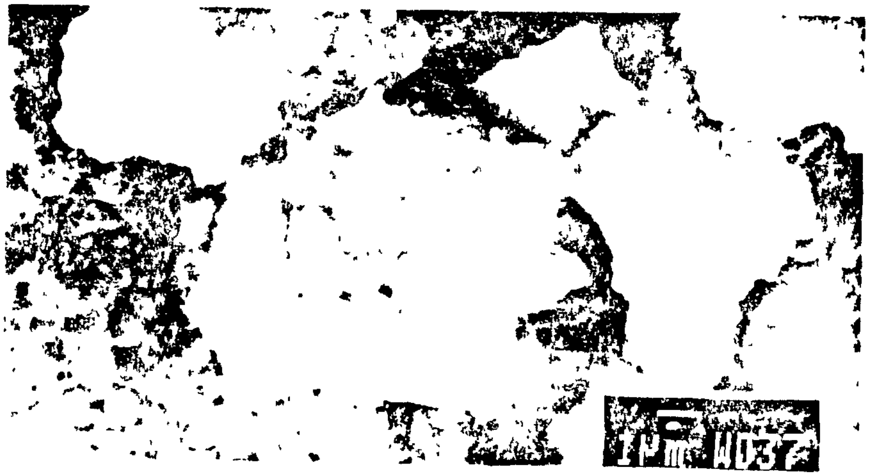

7.1c

Figure 7 1 a, b, c Micrographs of the Unconverted Residue in 10.0 % Hydrogen Plasma at 3400 K (magnification from the top 50, 500 and 5000x)

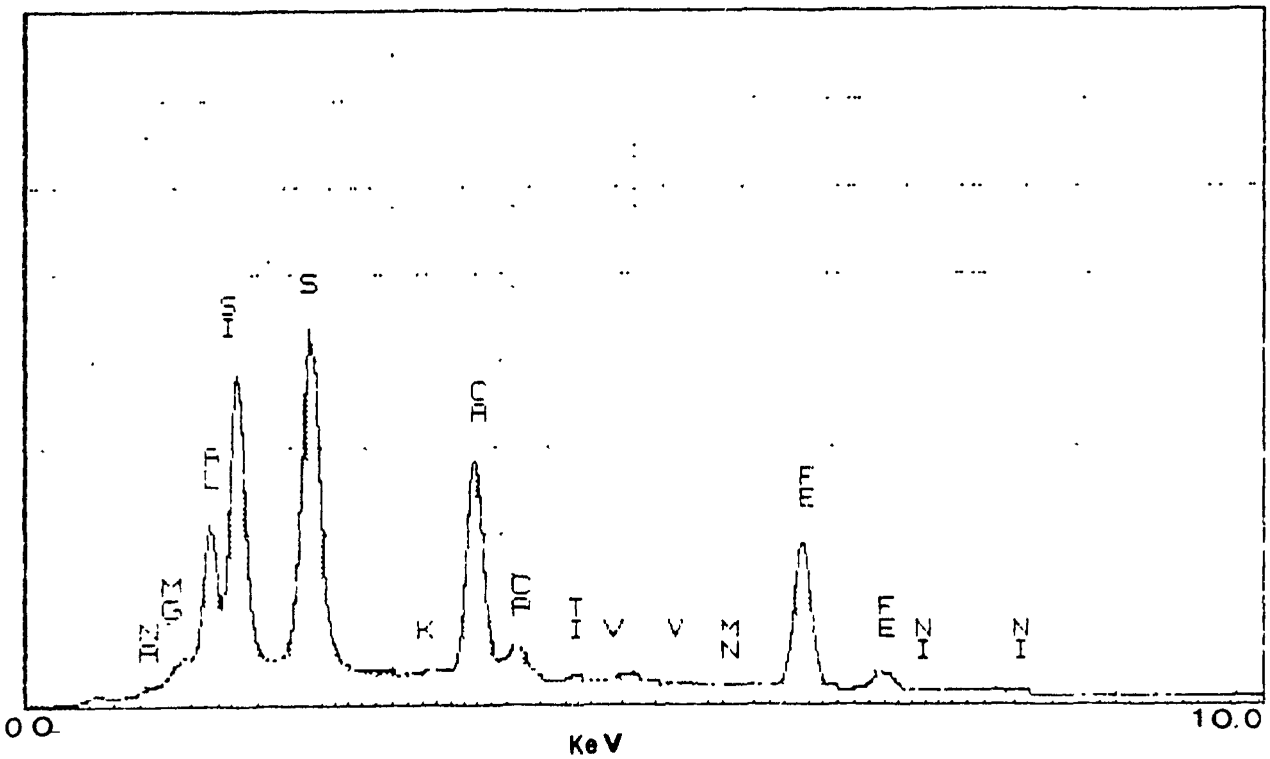

Figure 7.2 X-Ray Spectra of the CANMET Residue

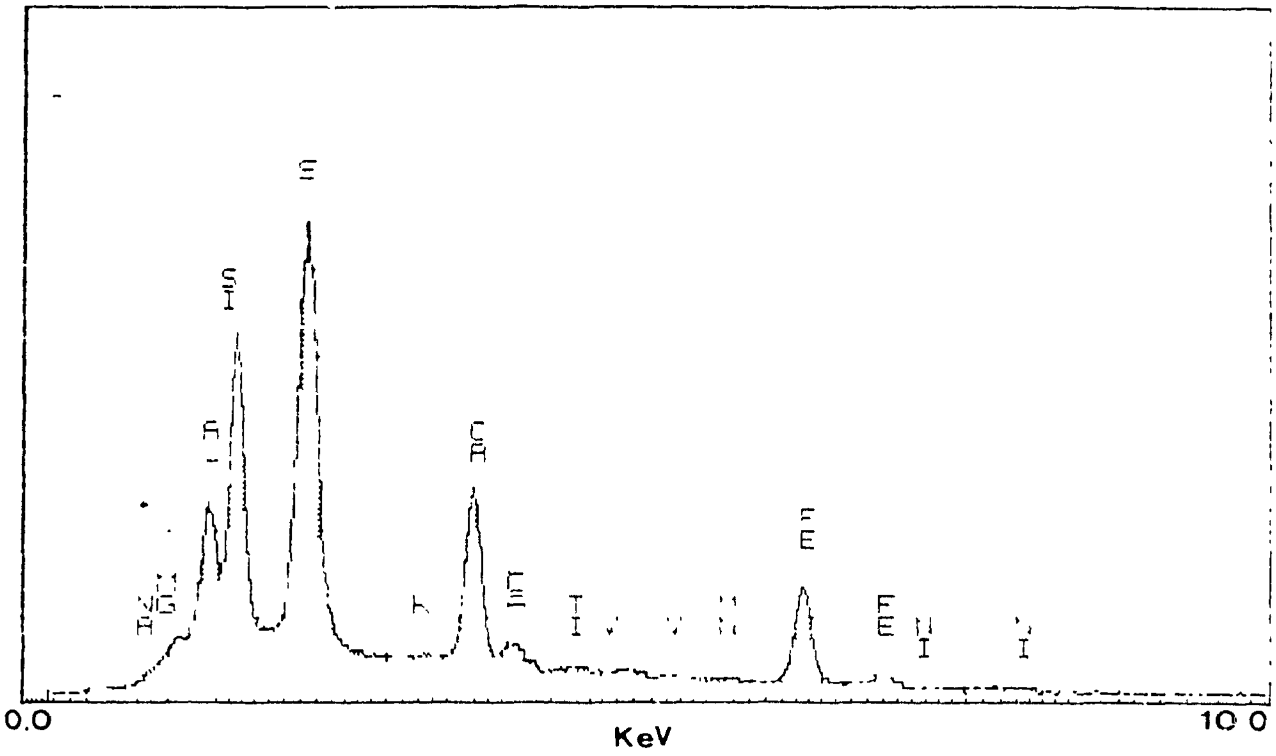

Figure 7.3 X-Ray Spectra of the Unconverted Residue

7 1 3 X-Ray Powder Diffraction (XRD)

Although coals are normally ashed in LTA, to remove their organic content before analysis by XRD, the unconverted residue was not ashed to avoid any chemical changes; the plasmas used were inert or reducing while the asher is strongly oxidizing

The minerals of the fresh residue are presented in Figure 7 4 a and described in Chapter 5 The changes, they undergo during the treatment in 33 5 % hydrogen plasma are presented in Figure 7 4 b c, d and e These experiments were conducted at the plasma average temperatures of 1570, 1920, 2320 and 2470 K respectively High background and small peaks in all graphs suggest a high content of amorphous carbon

As shown in Figure 7 4 b, gypsum ($CaSO_4 \cdot 2H_2O$) and bassanite ($CaSO_4 \cdot 1\ 5H_2O$) lose their hydration water converting to anhydrite ($CaSO_4$) A comparison of Figures 7.4 a to e shows that anhydrite decomposes at higher temperatures to calcium sulphide (CaS) However, the decomposition of anhydrite begins before CaS peaks could be recognized suggesting the existence of an intermediate compound The resolution of Figures b, c, and d is not sufficient to make a definite conclusion that such an intermediate stage is $CaSO_3$

To improve the resolution, the unconverted residues from two series of experiments in pure argon and 17 3 % hydrogen plasmas were oxidized in LTA and analyzed by XRD All ashings and analysis were conducted under the same conditions As expected, CaS was not identified since it was oxidized to $CaSO_4$ which was present on all XRD traces If LTA would first oxidize CaS to $CaSO_3$ and then to $CaSO_4$ one would expect to see $CaSO_3$ on all XRD traces (if the oxidation was not complete) or on none of them (if the oxidation was complete). However, $CaSO_3$ was identified only on the XRD traces taken from the lower temperature experiments; specifically, at 1660 and 2160 K in 17 3 % H_2 plasma and at 2240 and 3100 K in pure argon plasma $CaSO_3$ was not observed at 2920 and 3100 K in 17 3 % hydrogen plasma nor at 3680 and 4150 K in pure argon plasma, an example is given in Figure 7 4 f This proves that $CaSO_3$ is an intermediate compound and exist at the lower temperature only

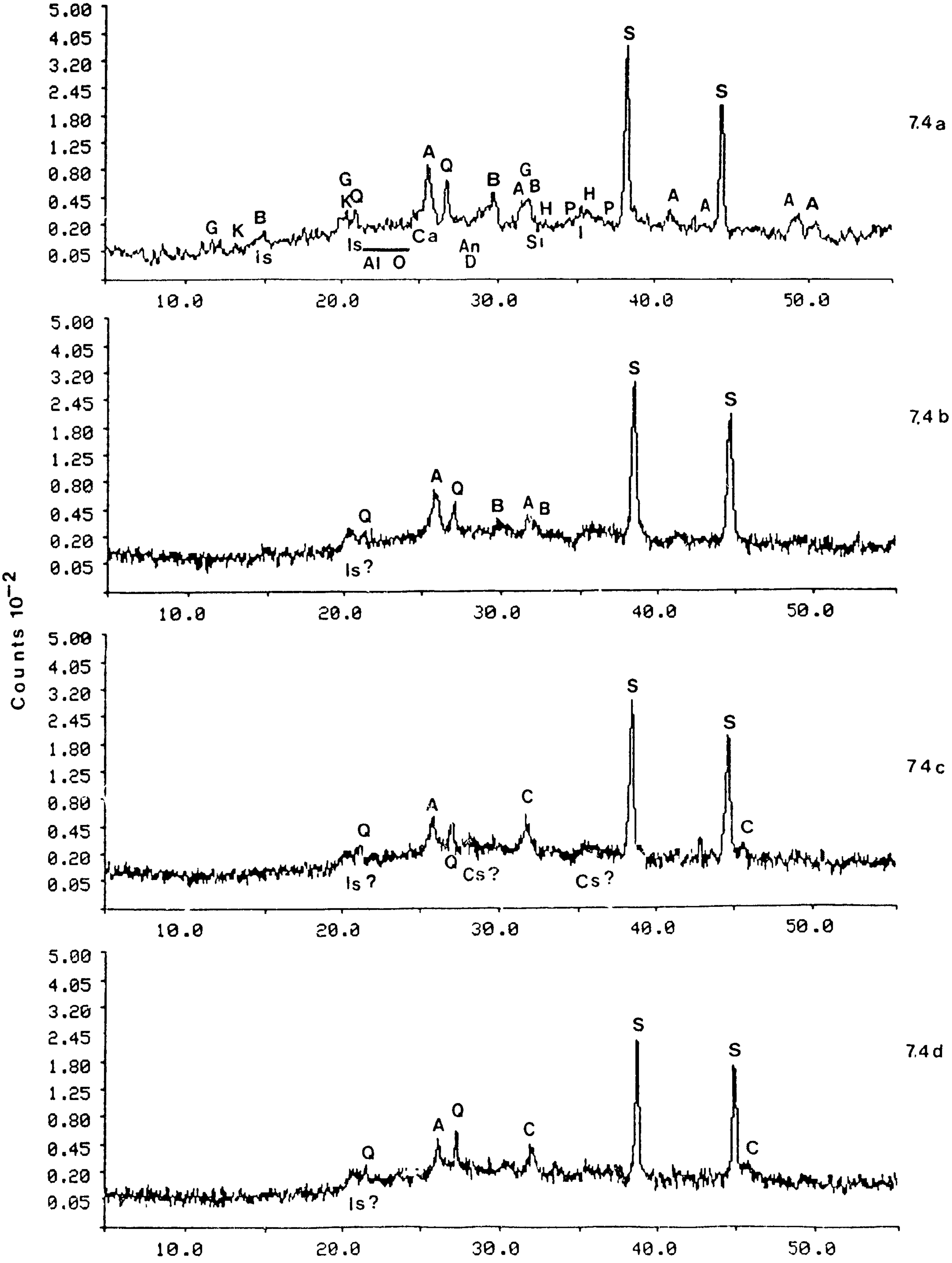
7.4 a
5.00
4.05
3.20
2.45
1.80
1.25
0.80
0.45
0.20
0.05
S
S
A
Q
B
G
A
B
G
K
Q
B
K
G
H
P
H
P
A
A
A
A
Is
Is
Al
O
Ca
An
D
Si
I
10.0
20.0
30.0
40.0
50.0
7.4 b
S
S
A
Q
B
A
B
Q
Is?
Counts 10^{-2}
7.4 c
S
S
C
A
Q
C
Q
Is?
Cs?
Cs?
7.4 d
S
S
Q
A
C
C
Q
Is?

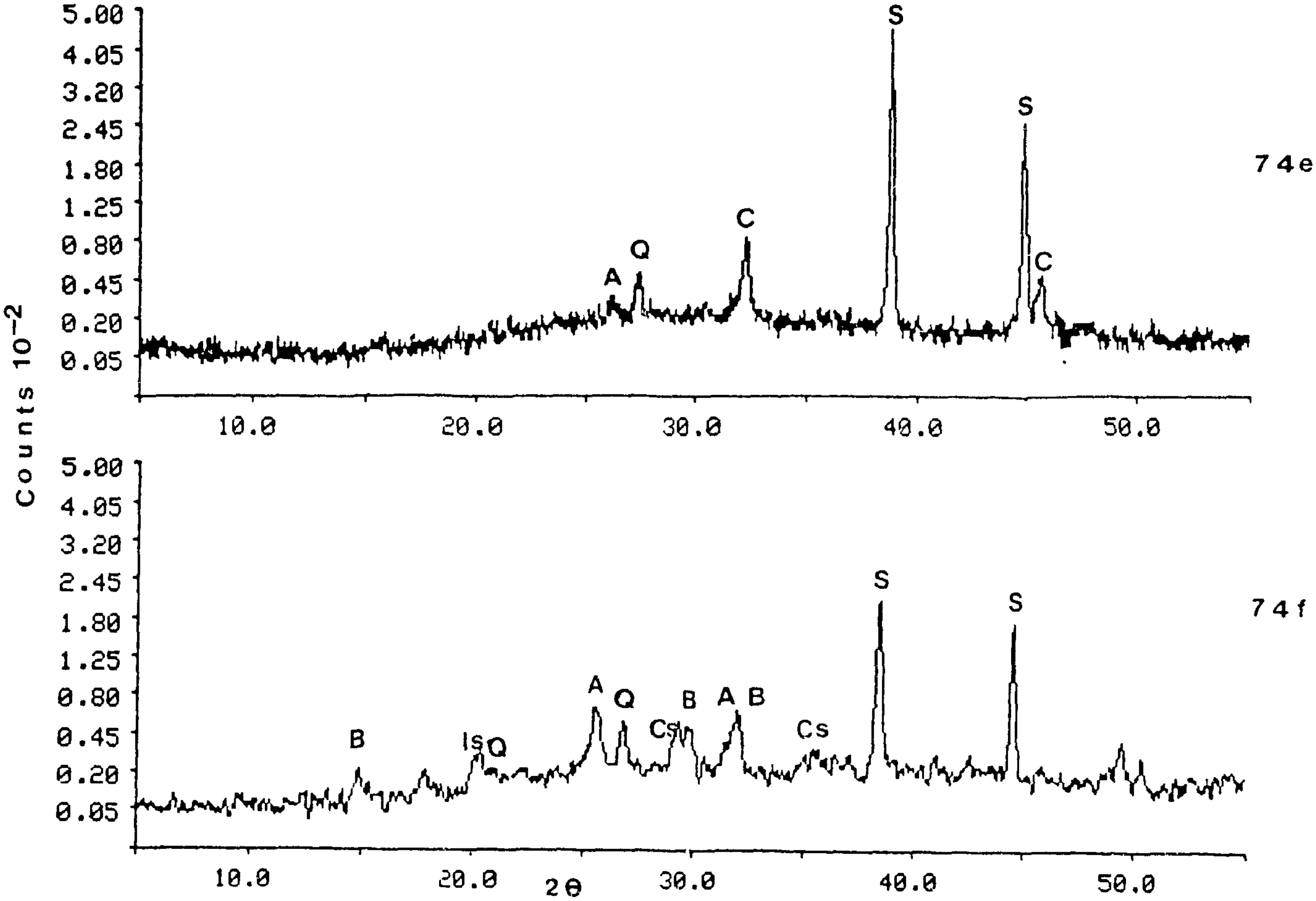

Figure 7.4 a XRD Trace of the CANMET Residue Dissolved in THF and Oxidized in LTA

Figure 7.4 b XRD Trace of the Unconverted Residue, 33.5 % Hydrogen Plasma at 1570 K

Figure 7.4 c XRD Trace of the Unconverted Residue, 33.5 % Hydrogen Plasma at 1920 K

Figure 7.4 d XRD Trace of the Unconverted Residue 33.5 % Hydrogen Plasma at 2320 K

Figure 7.4 e XRD Trace of the Unconverted Residue, 33.5 % Hydrogen Plasma at 2470 K

Figure 7.4 f XRD Trace of the Unconverted Residue Oxidized in LTA 17.3 % Hydrogen Plasma at 1660 K

(Description of Crystalline Phases Includes Code, Name, Nominal Composition and PDF Pattern A, anhydrite $CaSO_4$, 6-226, Al, albite $NaAlSi_3O_8$, 20-548, An, ankerite $Ca(Fe,Mg)(CO_3)_2$, 33-282, B, bassanite $CaSO_4 \cdot 1.5H_2O$, 14-453, C, calcium sulphide (oldhamite) CaS, 8-464, Ca, calcite $CaCO_3$, 5-586, Cs, calcium sulphite $CaSO_3$, 31-306, D, dolomite $CaMg(CO_3)_2$, 11-78, G, Gypsum $CaSO_4 \cdot 2H_2O$, 21-816, H, hematite Fe_2O_3, 33-664, I, illite $K_{1-1.5}Al_4(Si_{7-6.5}Al_{1-1.5}O_{20})(OH)_4$, 29-1496, Is, iron sulphate $Fe_2(SO_4)_3$, 33-679, K, kaolinite $Al_2Si_2O_5(OH)_4$, 29-1488, P, pyrite FeS_2, 6-710, O, orthoclase $KAlSi_3O_8$, 31-966, Q, quartz SiO_2, 33-1161, S, silver from the filter Ag, 4-783, Si, siderite $FeCO_3$, 29-696)

In conclusion, the following mechanism is suggested for the fixation of sulphur during the plasma treatment,

$$CaSO_4 \cdot 2H_2O \rightarrow CaSO_4 \cdot 1.5H_2O \rightarrow CaSO_4 \rightarrow CaSO_3 \rightarrow CaS$$

In addition, the carbonates (dolomite, calcite) which easily decompose to calcium and magnesium oxides during the plasma treatment may also fix inorganic and organic sulphur (Ibarra *et al.* 1989),

$$CaO + H_2S \rightarrow CaS + H_2O$$

In general, the transformations of the iron bearing compounds could not be resolved by X-ray powder diffraction. For example, it appears that iron sulphate decomposes only at higher temperatures (Figure 7.4 b and 7.4 e). Although the production of iron would be expected it could not be confirmed due to the low resolution of the unashed XRD traces and the oxidizing character of LTA.

7.1.4 Condensation of Liquid Hydrocarbons

The conversion of long chain paraffins and high molecular weight cycloalkanes and aromatics to light unsaturated hydrocarbons in the plasma is around 2.0 % and 12 % respectively (Baronnet *et al.* 1987). If a similar conversion is obtained from the CANMET residue then a sample of 12 g (i.e. 10 experiments run one after another) would produce at least 0.18 g of liquid hydrocarbons. A carbon dioxide (sublimation point at -56.6 °C) trap should be able to condense all liquid hydrocarbons since their equilibrium constants are small at low temperatures (Smith and van Ness 1975). The thermal efficiency of the constructed trap was confirmed by using liquid nitrogen (boiling point -195.8 °C) to condense argon (boiling point -185.7 °C). Since no liquid hydrocarbons were condensed, it may be concluded that the plasma treatment of the CANMET residue in the semi-batch reactor does not lead to the formation of liquid hydrocarbons.

7.2 Quantitative Results

7.2.1 Repeatability

Errors in the experimental data may have resulted from the uncertainty in process variables and from errors in individual measurements.

The plate current was adjusted to ±0.1 A which corresponded to ±0.56 kW of the plate power. Thus the average flame temperature was determined with the precision of ±150 K. The accuracy of the gas flow meters, pyrometer and thermocouples has been discussed previously.

The gas composition was measured by the gas chromatograph which had a detection limit of around 10 ppm (0.001 %) for all gases with the exception of hydrogen. Its precision varied depending on gas concentrations but it was usually around 100 ppm. The instrument readings were periodically compared with the calibration mixture and found that gas percentages agree to within 5 % throughout the work, during the same period the retention times decreased slightly by less than 0.1 min.

For every series of experiments, with different hydrogen concentration, at least one point was replicated. Five replicates were taken at 3390 K for 10 % hydrogen plasma. Table 7.1 presents the concentrations of hydrocarbons and carbon monoxide in the integral samples collected usually during first three minutes of every experiment (column 4). The gas stream was withdrawn through the suction probe whose tip was located 8.0 cm below the torch exit or 5.5 cm below the top of the crucible. In all experiments the flow of argon was maintained constant at 32.5 l/min; however, the flow of hydrogen was varied between 0.0 and 8.1 l/min.

Table 7.1 Composition of the Integral Samples of Product Gases

H_2 Flow (l/min)	Temp (K)	Residue (g)	Time (min)	C_2H_2 (%)	C_2H_4 (%)	CH_4 (%)	CO (%)
0.0	2190	1.1950	4.0	0.076	0.016	0.020	0.016
0.0	2990	1.2026	3.0	0.100	0.009	0.000	0.039
0.0	3370	1.2024	3.0	0.115	0.000	0.000	0.049
0.0	3670	1.2252	3.0	0.115	0.003	0.006	0.060
0.0	3670	1.1945	3.0	0.111	0.000	0.000	0.058

0.0	4110	1.2088	3.0	0.124	0.000	0.000	0.068
0.0	4440	1.2085	3.0	0.120	0.000	0.000	0.074
0.0	4450	1.1976	3.0	0.106	0.000	0.000	0.075
3.6	2890	1.2093	3.0	0.145	0.019	0.051	0.037
3.6	3160	1.2142	3.0	0.160	0.016	0.037	0.040
3.6	3390	1.1946	3.0	0.148	0.012	0.029	0.040
3.6	3390	1.2035	3.0	0.145	0.014	0.031	0.046
3.6	3390	1.2013	2.5	0.168	0.014	0.037	0.050
3.6	3390	1.2040	3.0	0.140	0.012	0.026	0.048
3.6	3390	1.1979	3.0	0.143	0.013	0.027	0.045
3.6	3590	1.2088	3.0	0.137	0.011	0.027	0.052
3.6	3740	1.2134	3.0	0.132	0.010	0.024	0.055
3.6	3810	1.1944	3.0	0.127	0.008	0.021	0.057
3.6	3810	1.2049	3.0	0.125	0.008	0.025	0.057
8.1	2500	1.2013	3.0	0.106	0.025	0.064	0.023
8.1	2720	1.2176	3.0	0.120	0.022	0.062	0.026
8.1	2920	1.2055	3.0	0.148	0.021	0.057	0.035
8.1	2940	1.1931	3.0	0.139	0.021	0.057	0.031
8.1	3080	1.2096	3.0	0.138	0.018	0.048	0.032
8.1	3190	1.1936	3.0	0.152	0.017	0.046	0.033
8.1	3260	1.1974	3.0	0.137	0.015	0.041	0.035

The spread in the acetylene concentration was between 0.140 and 0.148 % which corresponded to the difference in the conversion to acetylene of 6.6 % (relative). Similarly, the conversion to ethylene shows spread of between 1.54 and 1.80 %, to methane of between 1.67 and 2.00 % and to carbon monoxide of between 2.60 and 3.07 %. It should be pointed out that the acetylene results may be associated with an addition error due to the partial decomposition of acetylene in the suction probe (Section 7.2.2)

7.2.2 Quenching

Since acetylene may decompose during sampling, the design of the water cooled suction probe has an effect on the determination of the acetylene yield. Thus the probe inner diameter (1.6 mm) and the gas flow rates (250 cm^3/min of argon) were selected on the basis of the experimental work by Plooster and Reed (1959) and Baddour and Iwasyk (1962). This section will estimate the extent of the decomposition of acetylene inside the probe (used in this project) as a function of the quenching rate. Firstly, the theoretical quench rate will be given followed by the estimation of the quench rates in the probe. The average calculated quench rate between 1500 and 600 K will be verified by experiments, then a simple segregated flow model, based on the computed quench rates will be used to estimate the extent of the acetylene decomposition.

The quenching rate (dT/dt) necessary to preserve the whole amount of acetylene in the sampling gas was given by Bukhman *et al.* (1965) as,

$$\frac{dT}{dt} > \frac{T_o - T_f}{6 \cdot 10^{-7} \cdot \exp(15100/T_o)} \qquad (7.1)$$

where T_o is the sample temperature at the probe inlet, T_f is a temperature at which the decomposition of acetylene is negligible. For example, taking T_o=2500 K and T_f=600 K equation (7.1) yields $dT/dt > 7.5 \cdot 10^6$ K/s.

Expression (7.1) tends to overestimate the quenching rate (Khait 1965) since it assumes the same quenching rate at high (where the decomposition of acetylene is fast) and at low temperatures (where the decomposition of acetylene is slow).

In this study, the amount of acetylene present in the hot argon gas was always below 1 % and hence the transfer and thermodynamic properties of the hot gas were close to those of argon. Sundstrom and DeMichiell solved continuity, heat and momentum equations for the quenching of high temperature argon using a slightly bigger probe (3.2 mm in diameter) and higher flow rate of argon (650 cm^3/min). However, the heat transfer coefficient is expected to be higher for the probe used in this investigation, thus the Sundstrom and DeMichiell's calculations provide conservative evaluations of the quenching rates. These are as follows: $5.0 \cdot 10^6$ K/s between 2500 and 2000 K, $1.3 \cdot 10^6$ K/s between 2000 and 1500 K, $0.16 \cdot 10^6$ K/s between 1500 and 600 K and below 600 K the acetylene decomposition is negligible.

The last quenching rate was confirmed experimentally. The suction probe with K type thermocouple (0.8 mm in diameter) was used to withdraw the hot air from within the muffle furnace whose temperature was maintained above 1150 K. The conduction losses through the thermocouple were negligible since the same temperature was measured independently inside the furnace and by the thermocouple at the probe inlet The temperature profiles inside the probe were taken along first 100 mm (Figure 7.5). An error associated with a single temperature measurement was ±20 K. Knowing the air flow rate (500 cm^3/min at STP), the cross-sectional area for flow and using the ideal gas law the quenching rate was calculated as $0.4 \cdot 10^6$ K/s at the beginning of the cooling jacket at the probe inlet. This corresponds well with the average quench rate of $0.16 \cdot 10^6$ K/s obtained from the Sundstrom and DeMichiell results between 1500 and 600 K and the local quench rate of $0.31 \cdot 10^6$ K/s at 1150 K, however air has better heat transfer properties than argon.

In order to estimate the decomposition of acetylene, based on the quench rates calculated by Sundstrom and DeMichiell, the segregated flow model (in axial direction) was employed. At high temperatures the flow of argon is laminar however for this analysis good mixing in radial direction is assumed. Similar assumption was made by others (Amman and Timmins 1966). The first order rate expression (in acetylene) for the reaction $C_2H_2 \rightarrow 2C + H_2$ taken from Melamed *et al.* (1965) as (in s^{-1});

$$r = -1.57 \cdot 10^6 \cdot \exp(-\frac{15100}{T}) \qquad (7.2)$$

was used in conjunction with the mentioned quench rates to yield the decomposition of acetylene in the probe of 32 % This appears to be a conservative estimate especially since the quench rate of $7.5 \cdot 10^3$ K/s (no decomposition of acetylene according to Bukhman *et al* 1965) implies that only 85 % of acetylene is preserved. However, the model does not include the adiabatic quenching

It should be noted that some soot was collected on a filter which was attached to the probe exit, the soot could be also sucked from within the reactor.

Gas mixing is an efficient quenching technique with quenching rates that are twice as high as for the quenching by cold wall However, on laboratory scale a suction probe is a more flexible method than other quenching techniques Moreover, it is unlikely that in the industrial

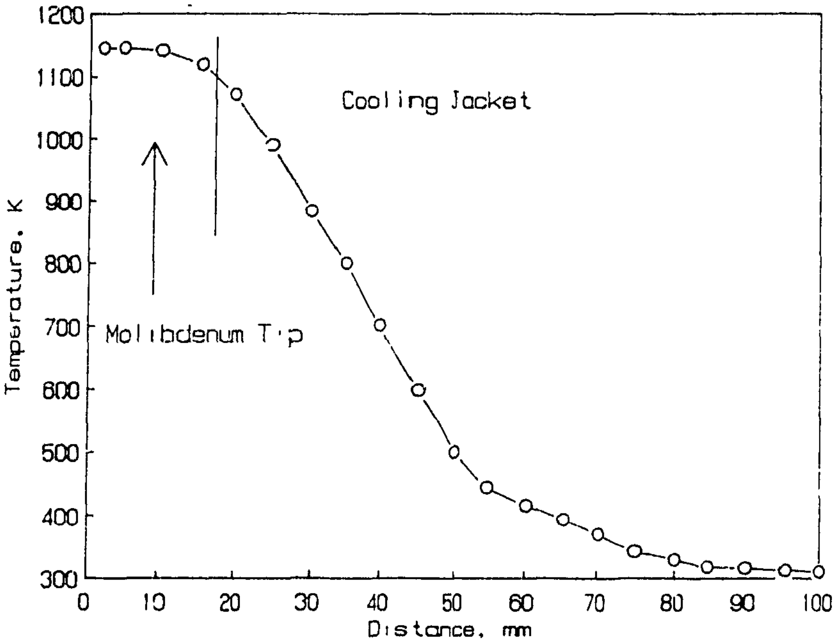

Figure 7 5 Temperature Profile inside the Probe (Air Flow = 0 5 l/min, Inlet Temperature = 1140 K)

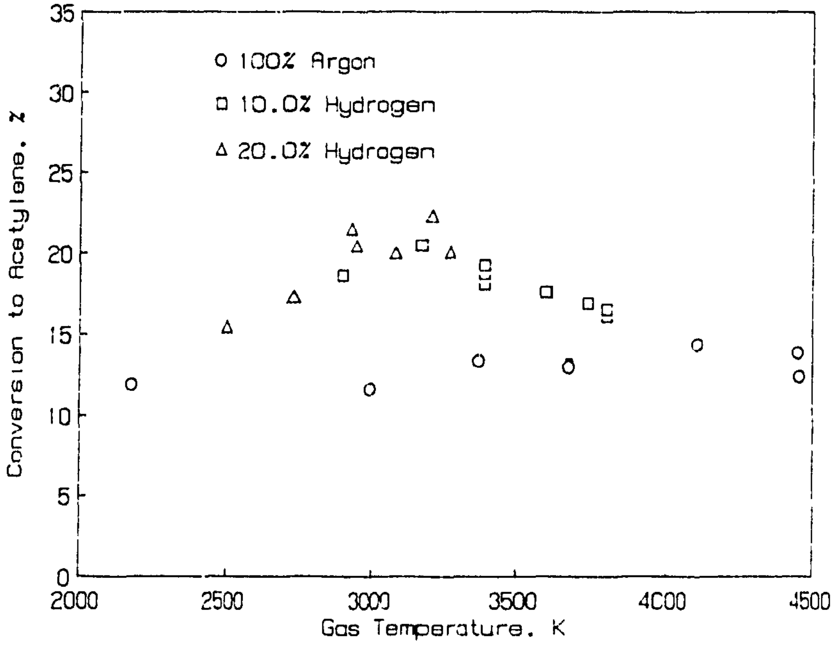

Figure 7 6 Conversion of Carbon in the CANMET Residue to Acetylene; five replicates at 3390 K for 20 % hydrogen plasma (Argon Flow = 20 81 g/min Axial and 37 22 g/min Swirl, Hydrogen Flow = 0.32 or 0 73 g/min to the tailflame) facility higher quench rates, than used in this study, can be obtained. Thus it is possible to minimize but not to avoid the acetylene decomposition.

7.2.3 Gas Composition and Conversion to Gaseous Products

Acetylene, ethylene, methane, carbon monoxide and hydrogen were the most important gases produced. However, the concentration of hydrogen was too small to be determined accurately. Small amount of ethylene was detected in a few samples but this gas was never observed in the integral sample. Since hydrogen sulphide was identified by its characteristic odour, but not detected on the TCD detector, its concentration was below 10 ppm. The concentration of nitrogen was between 0.4 and 4.0 % depending on the extent of the air leakage into the gas samples; thus the concentrations of other gases were adjusted to air free basis. Carbon dioxide (10 - 70 ppm) was detected only in injections which had high nitrogen content, and so it was not considered as a product gas.

7.2.3.1 Effect of Plasma Temperature and Hydrogen Concentration in Plasma Gas

The conversion of carbon in the residue to acetylene (Figure 7.6) is about twice as high in 10 and 20 % hydrogen plasmas (23 %) than in pure argon plasma (14 %). There is no increase in the acetylene production once the hydrogen content in the plasma gas reaches 10 %. Thus it is possible that similar results would be obtained in pure hydrogen plasmas. Moreover, the conversion to acetylene in argon/hydrogen plasmas as a function of temperature exhibits a broad maximum at around 3200 K. This trend agrees with the results of the thermodynamic calculations; however, the equilibrium conversion is much higher than experimental.

The conversion of carbon to ethylene (Figure 7.7) and methane (Figure 7.8) is higher in 20 % than in 10 % hydrogen plasmas. In general, the treatment in pure argon plasma does not lead to the production of ethylene and methane unless the temperatures are below 3000 K. In fact, the

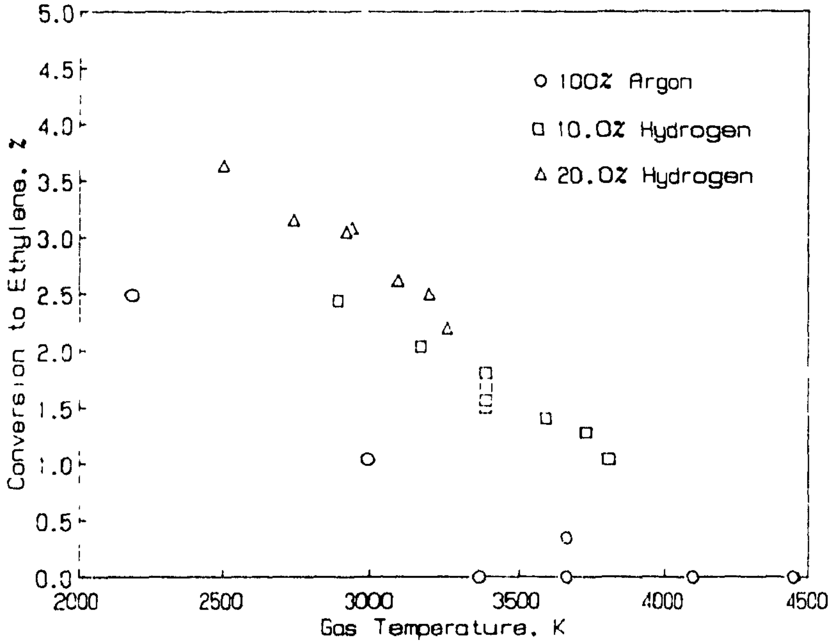

Figure 7.7 Conversion of Carbon in the CANMET Residue to Ethylene, five replicates at 3390 K for 20 % hydrogen plasma, two replicates at 3810 K for 10 % hydrogen plasma (Argon Flow = 20.81 g/min Axial and 37.22 g/min Swirl, Hydrogen Flow = 0.32 or 0.73 g/min to the Tailflame)

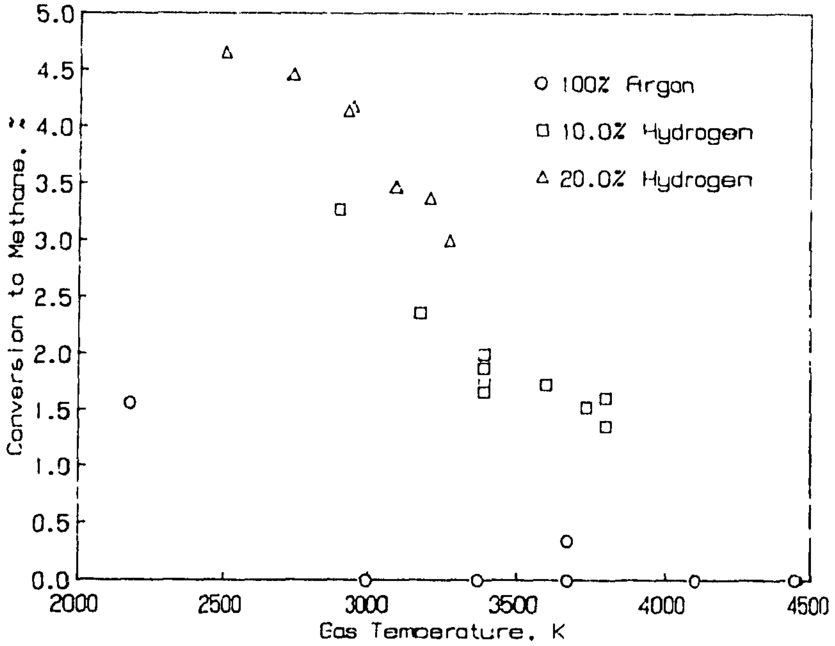

Figure 7.8 Conversion of Carbon in the CANMET Residue to Methane; five replicates at 3390 K for 20 % hydrogen plasma (Argon Flow = 20.81 g/min Axial and 37.22 g/min Swirl, Hydrogen Flow = 0.32 or 0.73 g/min to the Tailflame)

thermodynamic analysis predicted a small production of methane and ethylene in argon/hydrogen plasmas and no production in pure argon plasma. The conversion of carbon to ethylene and methane at 2500 K is 3.7 and 4.7 %, respectively, and it decreases to 1.0 and 1.5 % at 3800 K. The thermodynamic calculations anticipated slightly higher production of methane than ethylene (Figures 3.1 and 3.2).

On the other hand, the production of carbon monoxide (Figure 7.9) depends only on the temperature of the plasma gas. The conversion of oxygen to CO is 40 % at 2190 K, but it increases to 106 % at 4450 (Figure 7.10). This apparent inconsistency is explained by the fact the CEC 240-XA analyzer underestimated the total amount of oxygen in the sample due to the oxygen removal by metals (Chapter 5). The emission of CO may be divided into two stages. Below 2800 K the organic oxygen is removed by cracking and the conversion of oxygen to CO is approximately constant. Above the gas temperature of 2800 K the inorganic oxygen leaves the residue because of mineralogical transformations especially the removal of oxygen from calcium sulphate. At this stage, the extent of the carbon monoxide emission is directly proportional to the gas temperature. This is corroborated by the results from XRD study which showed that the extent of the calcium sulphate reduction to calcium sulphide increases with temperature

Figure 7.11 compares the amount of hydrogen present in acetylene, ethylene and methane with the amount of hydrogen initially present in the residue. The difference between pure argon and argon/hydrogen plasmas has resulted not only from the better removal of hydrogen from the residue by argon/hydrogen plasmas (Section 7.2.4.4) but also from the addition of hydrogen to the gaseous products of pyrolysis.

The time required for reaction depended somewhat on the plasma gas temperature but was less than 110 s for experiments with pure argon plasma (Figure 7.12) and 85 s for runs with 20 % hydrogen/argon plasma (Figure 7.13). For an experiment performed in an inverted flame (which implies colder plasma on the flame centre line than on the periphery) at 2190 K (Figure 7.12) it takes substantially more time for the residue to react. The production rates of acetylene were 2.1 mmol/s at 4450 K in pure argon plasma and 4.5 mmol/s at 3260 K in 20 % argon/hydrogen plasma.

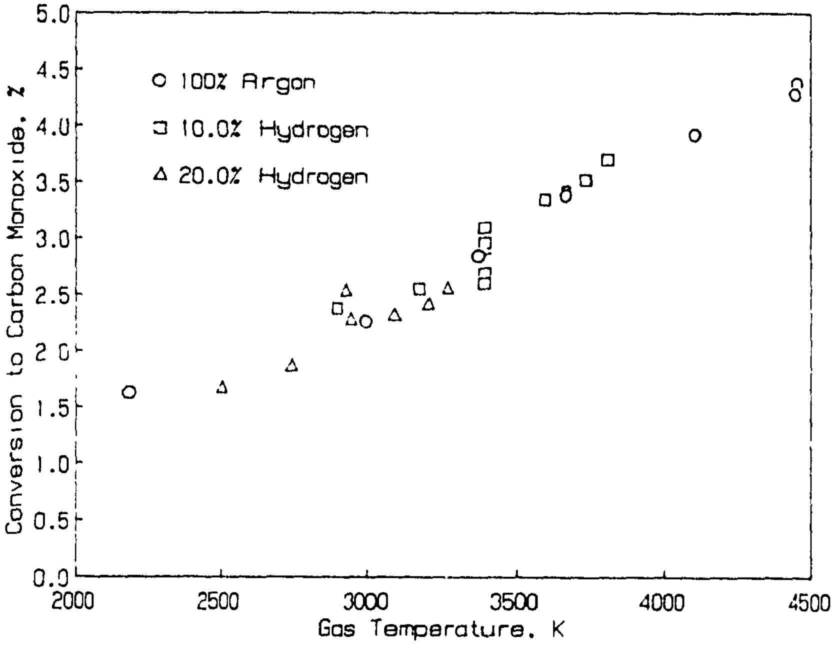

Figure 7.9 Conversion of Carbon in the CANMET Residue to Carbon Monoxide, two replicates at 3810 K for 10 % hydrogen plasma (Argon Flow = 20 81 g/min **Axial** and 37.22 g/min Swirl, Hydrogen Flow = 0 32 or 0.73 g/min to the Tailflame)

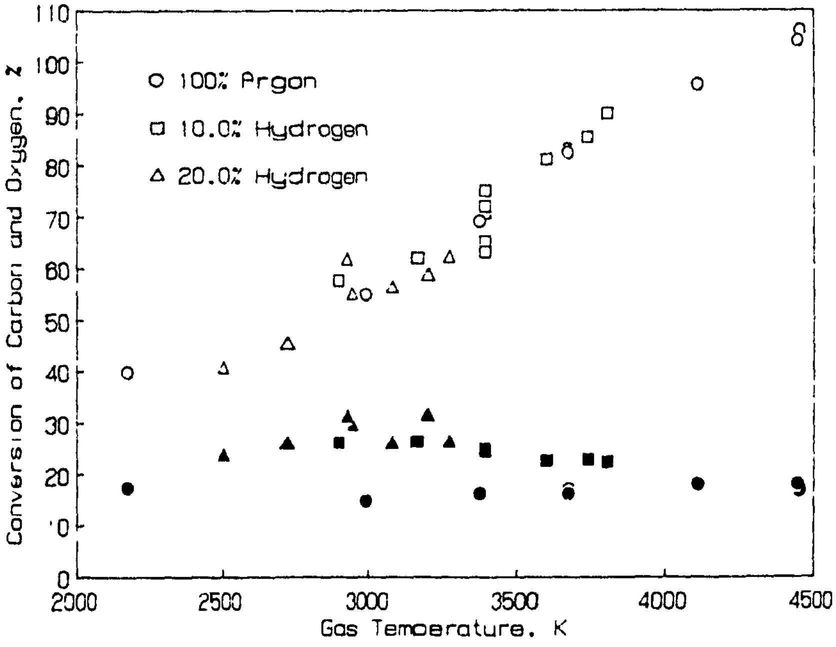

Figure 7.10 Conversion of Carbon and Oxygen in the CANMET Residue to Gaseous Products; oxygen - open symbols, carbon - closed symbols, five replicates at 3390 K for 20 % hydrogen plasma, two replicates at 3810 K for 10 % hydrogen plasma (Argon Flow = 20.81 g/min **Axial** and 37.22 g/min Swirl, Hydrogen Flow = 0.32 or 0 73 g/min to the Tailflame)

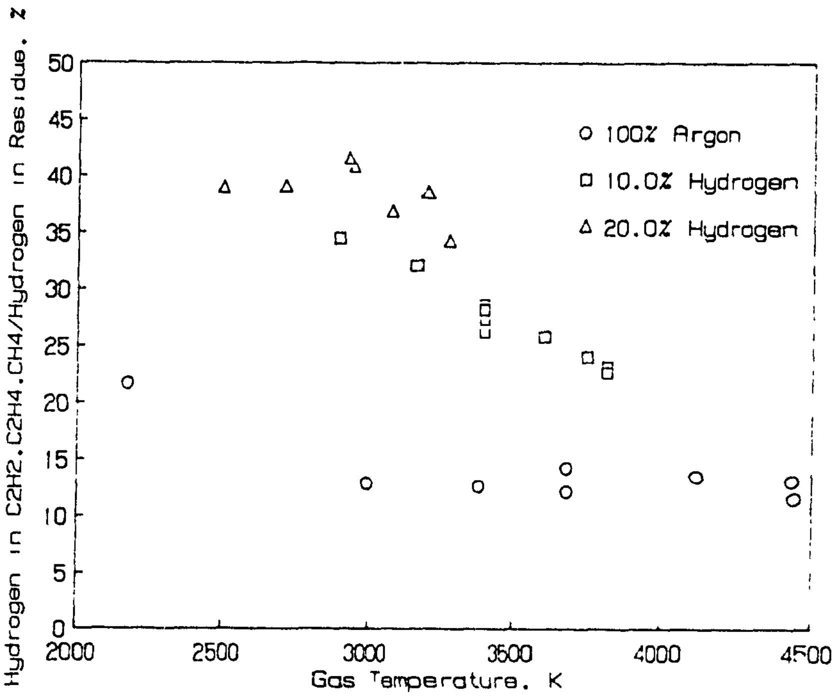

Figure 7 11 Ratio of Total Hydrogen in Acetylene, Ethylene and Methane to Hydrogen Initially Present in the CANMET Residue, five replicates at 3390 K for 20 % hydrogen plasma (Argon Flow = 20.81 g/min **Axial** and 37.22 g/min Swirl, Hydrogen Flow = 0 32 or 0 73 g/min to the Tailflame)

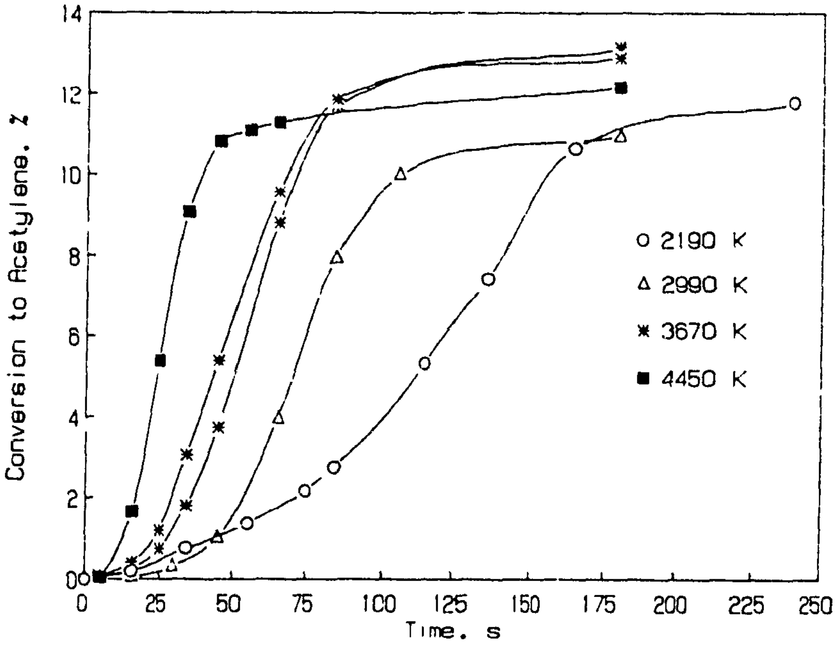

Figure 7.12 Conversion to Acetylene in Argon Plasma as a Function of Time (Argon Flow = 20.81 g/min **Axial** and 37 22 g/min Swirl)

In general, one may conclude that the conversion of carbon to light hydrocarbons is limited by the cracking of the CANMET residue; however, the effect of the plasma temperature and its hydrogen content on the product distribution may be approximately predicted from the thermodynamic considerations.

7 2 3.2 Effect of Residence Time

The residence time was calculated on the basis of the average flame temperatures at the torch exit and the reactor volume below the top of the crucible.

Gas samples were withdrawn from the exhaust gases at the reactor outlet and through the suction probe 0.5 and 5.5 cm below the top of the crucible. In addition an insert (2.54 cm in diameter) was placed inside the upper part of the reactor. This allowed to vary the residence time (between the crucible and the sampling points) between 0.36 and 52 ms

No difference in the conversion of carbon to acetylene (within the gas chromatography error) was observed which suggests that most of the decomposition of acetylene occurs at the top of the crucible and soot is swept to the lower part of the reactor and deposited on the reactor walls Thus it appears that the decomposition of acetylene results from the diffusion of the products from the pyrolysis through the porous dome.

Since the effect of the residence time, of a few milliseconds, on the decomposition of acetylene is within the gas chromatography accuracy the extent of the decomposition of acetylene inside the suction probe was likely overestimated.

7.2.4 Chemical Analysis of the Unconverted Residue

This section will examine the affect of the temperature and the hydrogen concentration in the plasma gas on the organic and inorganic materials which were left in the crucible after the treatment. During the experiments the CANMET residue was exposed to the plasma gas usually for 120 s (pure argon, 17 3 and 33.5 % hydrogen plasmas) or 180 s (pure argon

10 and 20 % hydrogen plasmas). In general, only small changes may be expected in the organic and inorganic parts after the pyrolysis of the hydrocarbons was completed For example, the emission of carbon monoxide suggests that the minerals are still undergoing some transformations, and the organic carbon may be consumed in the process. However, those changes are so small that they cannot be accounted for by the analytical techniques presented below.

7 2.4.1 Solubility in THF

The residue left in the crucible after the reaction accounts for between 40 and 50 % of the initial mass. The results, presented in Figure 7 14, are correlated with average gas rather than with crucible temperature The crucible temperature is substantially lower than the gas temperature, typical crucible temperatures were given in Figure 6.9.

The average measurement in Figure 7.14 is associated with an uncertainty of ±5 %. The amount of the residue decreases with temperatures but the effect of the plasma gas cannot be unequivocally determined

The unconverted residue contained practically no hydrocarbons which were soluble in tetrahydrofuran This implies that the aliphatic, alicyclic and part of aromatic hydrocarbons have been cracked and the organic part of the residue contains only condensed aromatic structure with heteroatoms which is not soluble in THF

7 2.4.2 Ashing

Since at 1600 K (Figure 7 14) around 50 % of the original residue is removed from the crucible, most of the pyrolysis takes place at lower temperatures However, the amount of ash left in THF insolubles increases slightly with temperature (Figure 7.14) reaching 25 % at above 4200 K. (Ash on THF insolubles = ash obtained from the unconverted residue / mass of the unconverted residue • 100 %.) This indicates that at higher gas temperatures inorganic elements become more concentrated in the crucible whereas carbon is preferentially removed into the gas phase. This is

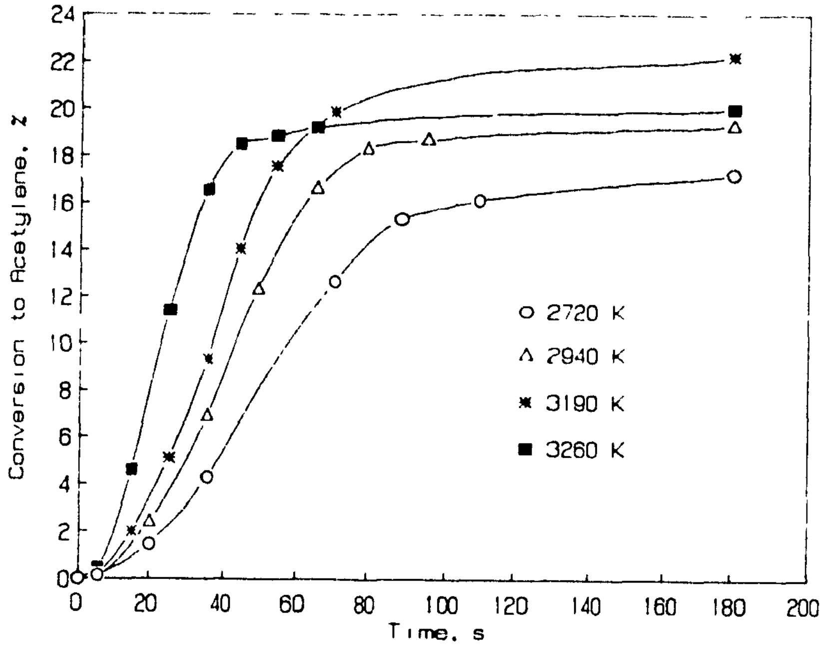

Figure 7.13 Conversion to Acetylene in 20 % Hydrogen Plasma as a Function of Time (Argon Flow = 20.81 g/min Radial and 37.22 g/min Axial Hydrogen Flow = 1.46 g/min to the Tailflame)

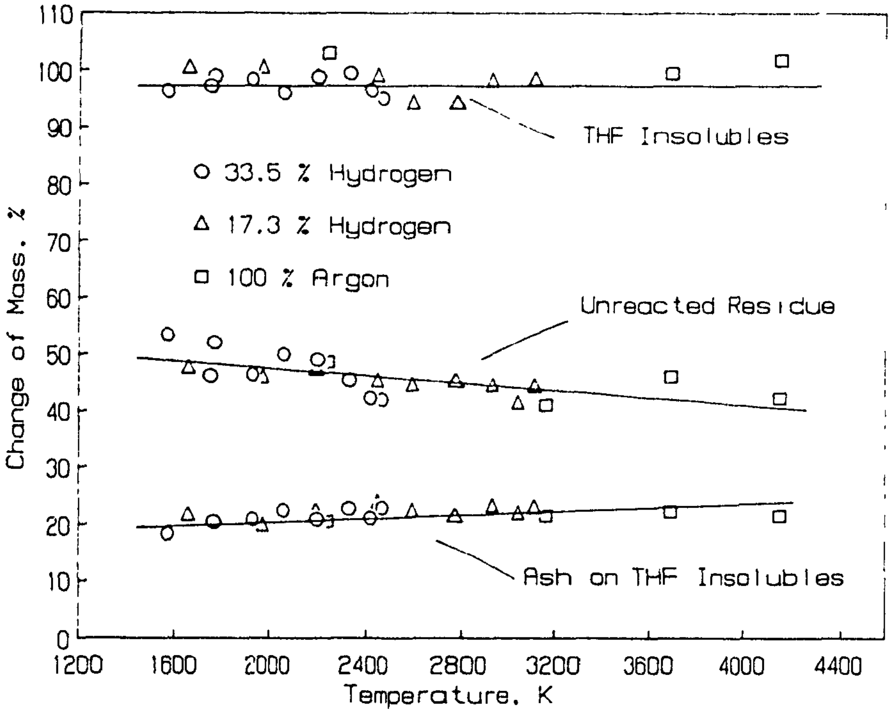

Figure 7.14 Analysis of the Unconverted Residue (Argon Flow = 20.81 g/min Axial and 37.22 g/min Swirl, Hydrogen Flow = 0.61 or 1.46 g/min to the Tailflame)

expected since increasing gas and crucible temperatures give faster and more complete pyrolysis.

7.2.4.3 Atomic Absorption

The unconverted residue, after ashing at 780 - 800 °C, was analyzed for iron, aluminum, vanadium and nickel on an atomic absorption apparatus (Figure 7.15) Vanadium, iron and nickel were selected for their potential to be used as catalysts in the CANMET process; therefore their recovery can be important. In addition, some researchers showed (Meubus 1975a&b, Moisyeyev *et al* 1986) that the presence of metal particles, such as Fe, Al and Ni in the reacting mixture of hydrocarbons in plasma may change the product distribution enhancing the production of acetylene

No significant variations in the contents of Fe, Al, V and Ni were observed as a function of temperature and composition of the plasma gas The results presented in Figure 7 15 may be compared with the analysis of the initial CANMET residue (Table 5.2) to show that no metals are removed from the crucible during the plasma treatment.

Two conclusions may be drawn: (1) since they do not volatilize the metals have no effect on the reactions in the gaseous phase and (2) to recover the catalyst further separation is required. Since the SEM results demonstrate that the metals are evenly distributed in the unconverted residue the separation should be performed by a chemical process.

7 2.4 4 C-H-N-S-O Analysis

The hydrogen content of the unreacted residue may vary greatly depending on the position of the unreacted residue in the crucible For the carbon and hydrogen analyses the unconverted residue was divided into two samples: one representing the top portion of the unreacted material (which was directly exposed to the plasma flame) and the bottom part (which remained at approximately crucible temperature). With the exception of experiments conducted under the inverted flame conditions (Figure 7.16), all results show that the top part of the unreacted material contains less

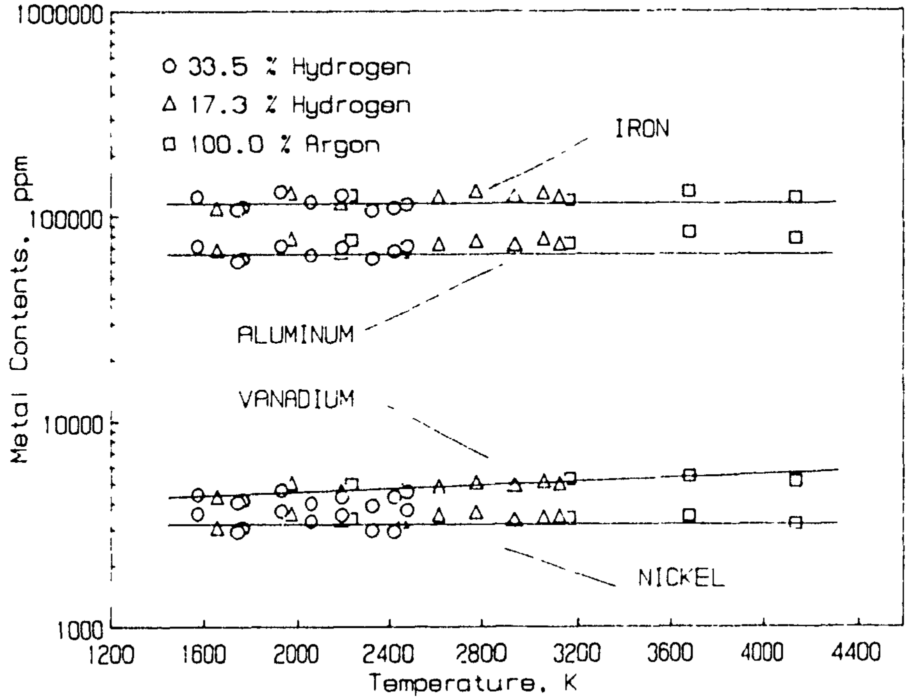

Figure 7.15 Analysis of the Ash Obtained from the Unconverted Residue, ppm = mass fraction • 10^5 (Argon Flow = 20.81 g/min **Axial** and 37.22 g/min Swirl, Hydrogen Flow = 0.61 or 1.46 g/min to the Tailflame)

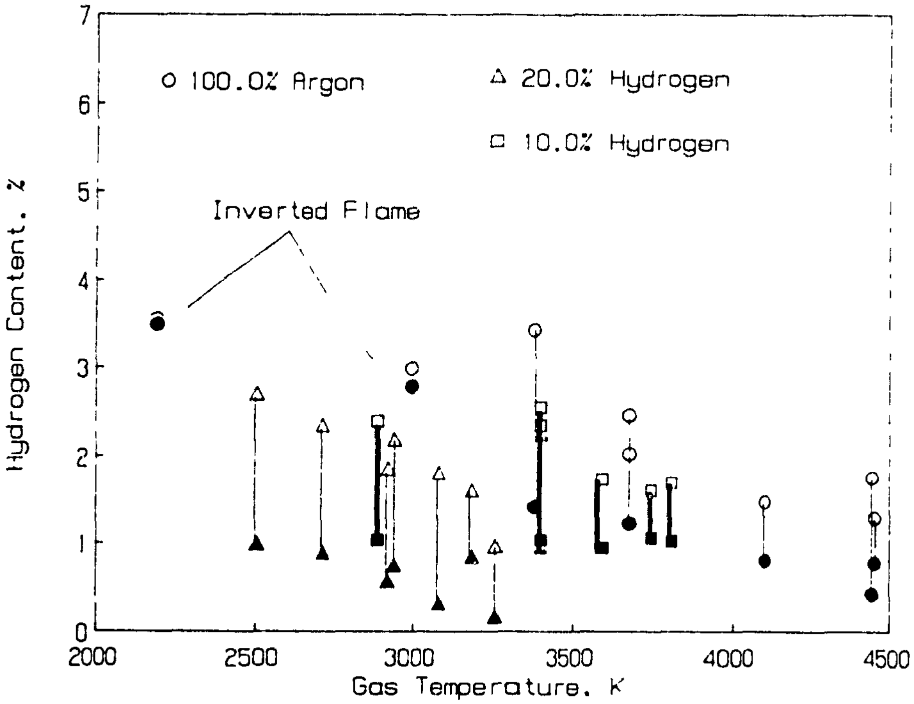

Figure 7.16 Hydrogen Content of the Unconverted Residue; open symbols - sample from bottom of crucible, closed symbols - sample from top of crucible (Argon Flow = 20.81 g/min **Axial** and 37.22 g/min Swirl, Hydrogen Flow = 0.32 or 0.73 g/min to the Tailflame)

hydrogen. There seems to be a decrease in residue hydrogen content as the plasma gas temperature is increased For the same average flame temperature, more hydrogen is removed from the residue in argon/hydrogen than in pure argon plasmas This may be due to a more efficient heat transfer from plasma to residue for argon/hydrogen plasmas. The fact that the residue in the lower (and colder) part of the crucible changes its hydrogen content suggest that there is some reaction even here

The sulphur content of the unconverted residue does not vary appreciably with the position inside the crucible. This is corroborated by the results shown in Table 7.2. The nitrogen and the sulphur content in the original CANMET residue was 1.18 and 3 43 % respectively (Table 5.2). Hence, nitrogen and sulphur become more concentrated in the unreacted residue This indicates that the aliphatic, alicyclic and aromatic hydrocarbons are pyrolysed first and those which contain heteroatoms, such as N and S, decompose during the later stages of pyrolysis and their decomposition may not be complete. In addition, the organic and inorganic sulphur is retained in CaS (Section 7.1.3).

Table 7.2 Nitrogen, Oxygen and Sulpnur Contents in the Unconverted Residue

Temp. K	Hydrogen in Plasma %	Upper part %	Lower Part %	Analyzed Element
4190	0.0	1.24, 1 24	1.46	N
3670	0.0	1 39	1.50	N
3370	0 0	1.35, 1 39	1 67	N
2190	0.0	1.68, 1.58	1.67	N
3390	10 0	1 32, 1.26	1.78, 1 73	N[1]
3390	10.0	1.41	1.60, 1.61	N[1]
3260	20 0	0.75	1.08	N
3190	20.0	1.32	1 56	N
3080	20.0	0.95	1.65	N
2920	20.0	0.98	1.56	N
3080	20.0	0 44	3.43	O
3590	20.0	4 37	4.19	S[2]

[1] Separate experiments

[2] Using LECO induction furnace and Metrohm titrator

On the other hand, the distribution of oxygen in the crucible, which is high in the lower part and low in the upper part, is similar to that of hydrogen. The inorganic oxygen is released from the calcium and magnesium salts by the thermal decomposition or during the fixation of sulphur and from kaolinite by dehydration. The presence of the organic oxygen may actually enhance the initial cracking since the oxygen would be preferentially removed from the hydrocarbon structure.

The soot which formed on the top surface of the porous layer of the unreacted residue (the dome) was scraped and analyzed for C-H-N content. Since soot may contain small amount of hydrogen (Table 7.3) it may be concluded that the decomposition of acetylene is a chain reaction, as shown in Section 2.3.3. Also soot may incorporate trace amounts of nitrogen.

Table 7.3 H-C-N Content of Soot, Carbon may be calculated by difference

Temp K	Hydrogen in Plasma %	Hydrogen %	Nitrogen %
4450	0.0	0.16	0.41
4440	0.0	0.54	0.62
4110	0.0	0.47	0.35
3670	0.0	0.75	0.21
3670	0.0	0.22	0.55
3370	0.0	0.53	0.61
2990	0.0	0.75	0.51
2190	20.0	3.10	1.56[1]
3260	20.0	0.48	0.38
3080	20.0	0.26	0.62
2940	20.0	0.91, 0.72	0.54, 0.74
2500	20.0	0.33, 0.47	0.57, 0.35

[1] Inverted flame

All analyses, described in this section with the exception of sulphur, were performed on CEC 240-XA elemental analyzer (Chapter 5) whose error was estimated to be below ±0.30 % (absolute). Tables 7.2 and 7.3 contain replicates which support this statement. The error associated with the determination of sulphur was ±0.20 % (absolute).

7.3 Comparison with Other Results

The treatment of pitches in argon/hydrogen plasmas has not yet been fully investigated. The only other study was performed by Nicholson and Littlewood (1972) who experienced similar problems in pyrolysing condensed aromatic structure of pitches. They obtained maximum conversion to acetylene of 34.5 % although they were able to attain conversion from methane to acetylene of 87 9 % and from coal to acetylene of 74 % (the highest ever reported).

Mazumdar *et al.* (1959) showed that the yield of pyrolysis gas depends on the percentage of alicyclic and aliphatic hydrocarbons which are volatile, and during pyrolysis they form condensable compounds called tars or primary volatiles (Baumann *et al*. 1988). In the plasma gas those primary volatiles undergo further cracking resulting in the production of acetylene However, pitches such as the CANMET residue contain high proportion of aromatic components which tend to retain their hydrogen content during pyrolysis. Thus the acetylene formation mechanism can be different, it may actually consist of only one step - the high temperature pyrolysis of aromatic compounds directly to acetylene and its radicals. The addition of hydrogen may then occur in the gaseous phase. Such mechanism would favour the production of soot rather than liquid hydrocarbons.

Because of their characteristic composition, no fair comparison can be made between conversion of pitches to acetylene and conversion of other carbonaceous materials to acetylene in plasma. However, the low conversion of the CANMET residue to acetylene would be expected by analyzing the compilation of the conversion data of coal to acetylene by Dixit *et al.* (1982).

8 0 CONCLUSIONS

The treatment of the CANMET residue in pure argon and argon/hydrogen plasmas was investigated in a stationary particle (semi-batch) reactor.

The conversion of carbon in the residue to light hydrocarbons such as acetylene, ethylene and methane has been shown to depend on the plasma parameters The conversion was limited by the composition of the CANMET residue

The conversion to acetylene in pure argon plasma was around 14 % and it did not change with the gas temperature, only trace amounts of ethylene and methane were observed The presence of hydrogen in the plasma gas improves the pyrolysis of the residue due to more efficient heat transfer between the plasma gas and the residue. Moreover, hydrogen takes part in the gaseous phase reactions improving, by almost twofold, the acetylene yield and enhancing the production of ethylene and methane The maximum conversion to acetylene and ethylene (together 24 %) was obtained between 2900 and 3400 K as predicted from the thermodynamic calculations The increase in the hydrogen concentration in the plasma, above 10 %, did not improve the acetylene yield but resulted in the higher production of ethylene and methane.

The low conversion to acetylene (and also to ethylene) is a result of the condensed heteroaromatic structure of the residue, its high oxygen content and the low cracking temperature. The cracking of aromatic and heteroaromatic compounds leads not only to the formation of acetylene and its radicals but also leaves the dehydrogenated residue in the crucible. Because of its low temperature such residue does not react with the hydrogen in the plasma gas

During the treatment in plasma, the inorganic minerals in the residue lose their crystallization water (sulphates, clays) or decompose (carbonates). Sulphur (organic and inorganic) is retained in the unconverted residue as calcium sulphide. The released oxygen reacts with carbon forming carbon monoxide. The conversion of carbon in the CANMET residue to CO is between 1.5 and 4.5 %. Nitrogen concentrates in the unconverted residue especially in the lower part of the crucible. No metals are removed from the residue during the treatment.

The crucible temperature was lower than the plasma gas temperature resulting in the slow pyrolysis and the incomplete cracking of the hydrocarbons in the lower part of the crucible. Thus hydrogen was removed preferentially from the residue in the upper part of the crucible. The formation of the porous layer of the unconverted material at the top of the crucible suggests that the production of the acetylene was controlled by the diffusion of the gaseous products from the pyrolysis through this porous layer. Since the residence time of acetylene (consisting of the time required for diffusion and the residence time in the reactor) was very long. a layer of soot formed on the surface of the unconverted residue as well as on the crucible and reactor walls

It can be concluded that the treatment of the CANMET residue consists of two stages: (1) reactions inside the crucible which include the pyrolysis of the hydrocarbons and the transformation of the mineral content of the residue and (2) reactions between the gas products from the pyrolysis and the plasma gas.

9.0 RECOMMENDATIONS

The conversion of the CANMET residue, to the light unsaturated hydrocarbons, is limited by the condensed aromatic structure of the residue and its high oxygen content. However, an improved yield may be realized if three technical limitations associated with the single particle system are avoided. Namely, (1) low crucible temperature, (2) uneven cracking of the CANMET residue in the upper and lower parts of the crucible and (3) decomposition of the acetylene during the diffusion through the porous dome at the top of the crucible and too long residence times.

The first constraint may be eliminated by surrounding the reaction chamber with a refractory material rather than a water jacket. One may use the continuous concurrent injection of atomized residue to eliminate the last two limitations. Countercurrent feeding of the molten residue may be attempted but the problem described in (3) may occur.

If the process is to be scaled-up it is important to obtain energy requirement (SER) data for the production of acetylene; hence the inductively coupled RF plasma torch should be substituted by a more efficient DC plasma jet.

Most of the sulphur and nitrogen is retained in the solid unconverted residue; therefore it is not necessary to construct a scrubber for a lab scale continuous reactor. It is sufficient to dilute the exhaust gases.

Finally, a few words of caution. Usually a high intensity arc is required to react solid carbon with hydrogen plasma to produce acetylene. Thus it is economically impractical to improve production of light unsaturated hydrocarbons by a direct reaction of the unconverted residue with hydrogen.

REFERENCES

Ammann P.R., Baddour R.F., Johnson M.M., Mix T.W., Timmins R.S., Coal Conversion in an Electric Arc, Chem. Eng Prog , vol. 60, no. 6, 1964, pp. 52-57

Ammann P.R., Timmins R.S., Chemical Reactions During Rapid Quenching of Oxygen-Nitrogen Mixtures from Very High Temperatures, AIChE J., vol 12, no. 5, 1966, pp. 956-963

Anderson J E , Case L.K , An Analytical Approach to Plasma Torch Chemistry, I&EC Proc. Des Devel , vol. 1, no. 3, 1962, pp. 162-165

Anderson L L., Hill G.R., McDonald E.H., McIntosh M.J , Flash Heating and Plasma Pyrolysis of Coal, Chem. Eng. Prog Symp. Ser , vol. 64, no. 85, 1968, pp. 81-88

Anonymous, Acetylene Output Rising, Chemical Week, June 7, 1989, p. 36; also Quarterly Chemical Output Report, Chemical Week, June 7, 1989, p. 37

Baddour R.F., Iwasyk J.M., Reactions between Elemental Carbon and Hydrogen at Temperatures above 2800 K, I&EC Proc Des. Devel., vol. 1, no. 3, 1962, pp. 169-176

Baddour R.F., Blanchet J.L., Reactions of Carbon Vapour with Hydrogen and with Methane in a High Intensity Arc, I&EC Proc. Des. Devel., vol. 3, no 3, 1964, pp. 258-266

Baddour R.F., Timmins R S , eds, Introduction, The Application of Plasmas to Chemical Processing, edited by R F. Baddour and R.S. Timmins, The M.I T. Press, Cambridge, Massachusetts 1967, pp. v-xiii

Bal S., Swierczek R., Musialski A., Perspectives for Coal Gasification in Plasmochemical Reactors, Koks-Smola-Gaz, vol. 16, no. 4, 1971, pp 96-100 (in Polish)

Baronnet J.M., Lesiński J , Sauvage B., Vandensteendam C., Meillot E., Hydropyrolysis of Heavy Oils in H_2/CH_4 Arc Plasma, Eighth Int Symp Plasma Chem., Tokyo, 1987, paper DI-06

Baumann H., Bittner D., Coal Conversion to Acetylene in a Plasma Jet, Erdol Erdgas Kohle, vol. 104, no 1, 1988, pp 37-44 (in German)

Baumann H., Bittner D., Beiers H.-G., Klein J., Juntgen H., Pyrolysis of Coal in Hydrogen and Helium Plasmas, Fuel, vol. 67, no. 8, 1988, pp. 1120-1123

Baumann P., Acetylene Production by an Electric Arc Process, Angew Chem , vol. B20, no. 10, 1948, pp. 257-259 (in German)

Beiers H.-G., Baumann H., Bittner D., Klein., Experiments on the Acetylene

Formation during the Pyrolysis of Coal in Arc-Heated Hydrogen, Seventh Int Conf. Plasma Chem , Eindhoven, 1985, Paper B-2-2

Beiers H.-G., Baumann H., Bittner D., Klein J., Juntgen H., Pyrolysis of Some Gaseous and Liquid Hydrocarbons in Hydrogen Plasma, Fuel, vol. 67, no. 7, 1988, pp. 1012-1016

Belov K.A., Romas' V.1., Production of Synthesis Gas from Gasification of Coal by Water Vapour in a Plasma Jet, Khim. Tvor. Topl., vol. 12, no.5, 1978, pp. 76-77 (in Russian)

Biceroglu O., Chlorination Kinetics of ZrO in an RF Plasma Tailflame, Ph.D. Thesis, McGill University, 1978

Bittner D., Baumann H., Klein J., Relation between Coal Properties and Acetylene Yield in Plasma Pyrolysis, Fuel, vol. 64, no. 10, 1985, pp 1370-1374

Boffa C., Heberlein J., Pfender E., Criteria for Establishing Deviations from the Local Thermodynamic Equilibrium at Atmospheric Pressure Plasma Jets, Warme u. Stoffubertragung, vol. 4, 1971, pp. 213-221

Bolouri S., Amouroux J , Acetylene Black Production in a Plasma Pilot Plant, Sixth Int Conf. Plasma Chem., Montreal, 1983, Paper A-8-1

Bond R.L., Galbraith I.F., Ladner I.F., McConnell G.I.T , Production of Acetylene from Coal, Using a Plasma Jet, Nature, vol. 200, 28 December, 1963, pp. 1313-1314

Bond R.L., Ladner W.R., McConnell G.I.T., Reactions of Coal in a Plasma Jet, Fuel, vol 45, no. 5, 1966, pp. 381-395

Bonet C., Thermal Plasma Processing, CEP, vol. 72, no. 12, 1976, pp 63-69

Borger I., Klotz H.-D , Spangenberg H.-J., Optimum Residence Time and Reaction Order for Methane to Acetylene Transformation at Temperatures between 1500 K and 3000 K, Z. Phys. Chemie (Leipzig), vol. 263, no. 2, 1982, pp. 257-268 (in German)

Boulos M , Fauchais P , Transport Processes in Thermal Plasmas, in Advances in Transport Processes, vol. 4, ed. by A.S Mujumdar and R A. Mashelkar, John Wiley & Sons, New York, 1986, pp. 274-385

Boulos M., Fauchais P , Pfender E., Diagnostic Techniques in Thermal Plasma Processing, U.S. Department of Energy, DOE/ER-0270 vol. 1-2, Feb. 1986

Bozzuto C.R., Acetylene from Coal and an Electric Arc, United States Patent 4,487,683, 11 December, 1984

Breed G.A., Grounding Techniques to Reduce RFI Susceptibility, R.F. Des., March 1986, p. 36

Brzeski J., Huczko A., Kurowski S., Lange H., Opalińska T., Plotczyk W.W., Podgorski A , Resztak A., Szymański A , Chemistry of Low Temperature Plasma, WNT, Warsaw, 1983 (in Polish)

Bukhman F.A., Melamed V.G., Polak L.C., Khait Yu L., Calculation of Some Parameters for Acetylene Quenching during its Production from Methane, in Kinetics and Thermodynamics of Chemical Reactions in Low Temperature Plasma, edited by L.S. Polak, Nauka, Moscow, 1965a, pp. 52-59 (in Russian)

Bukhman F A , Gulyaev G V , Melamed V.G., Polak L C , Khait Yu L , Temperature Control of a Plasma Jet as a Method for Improved Production of Acetylene from Methane, in Kinetics and Thermodynamics of Chemical Reactions in Low Temperature Plasma, edited by L.S. Polak, Nauka, Moscow, 1965b, pp 60-65 (in Russian)

Burns G.W., Hurst W.S., Thermocouple Thermometry, Inst. Phys Conf Ser , no. 26, 1975, pp. 144-161

Camacho S.L., Plasma Synthesis of Hydrogen-CO Gas from Steam and Carbonaceous Matter, Seventh Int Symp. Plasma Chem , Eindhoven, 1985, Paper B-1-2

Chakravartty S.C., Dutta D., Lahiri A , Reactions of Coals under Plasma Conditions· Direct Production of Acetylene from Coal, Fuel, vol 55, no 1, 1976, pp. 43-46

Chakravartty S.C., Dixit L.P., Srivastava S.K., Hydrogen Enriched Plasma for Direct Production of Acetylene from Coal, Indian J Technol , vol. 22, no. 4, 1984, pp. 146-150

Christofides C., Ibberson V.J , Processing of Hydrocarbons in a Thermal RF Plasma Reactor, Sixth Int Symp Plasma Chem., Montreal, 1983, Paper A-8-2

Clarke J.T , Reaction of Graphite and Hydrogen Above 2000 K, in The Application of Plasmas to Chemical Processing, edited by R.F. Baddour and R.S. Timmins, The M.I.T. Press, Cambridge, Massachusetts 1967, pp. 132-154

Cooke N.E., Ashraf F.A., Divanji H., Technical Opportunities for Converting Natural Gas to Acetylene-Based Chemicals, AIChE National Meeting (Chemicals from Natural Gas Session), Houston, March 29 - April 2, 1987

Czernichowski A., The Rotational Temperature Evaluation from Partially Resolved 516 5 nm C_2 Band, Eight Int Symp Plasma Chem., Tokyo, 1987, Paper P-032

Czernichowski A., de Izarra Ch., Lesueur H., Rotational Temperature Evaluation in a CO_2 + N_2 Arc from Partially Resolved CN and C_2 Molecular Bands, Eight Int Symp Plasma Chem , Tokyo, 1987, Paper P-033

Dessau L., Borger I , Spangenberg H.-J., Termination of Chemical Reactions in a Hydrocarbon Plasma by Means of Adiabatic Expansion Nozzle, Z. Phys. Chem (Leipzig), vol 266, no. 2, 1985, pp. 212-224 (in German)

DeWitt D.P., Albright L.F., Measurement of High Temperatures in Furnaces and Processes, AIChE Symp. Ser., vol. 82, no. 249, 1986, pp. 1-100

Dixit L.P., Srivastava S.K., Chakravartty S.C., Bandopadhyay A.K., Theoretical Maximal Yield of Acetylene from Coals by Plasma Pyrolysis, Fuel Proc Tech., no. 6, 1982, pp. 85-91

Dobal V , Gasification of Carbonaceous Matter in a Water Vapour Plasma, Khim Tvor Topl , vol 12, no.3, 1978, pp. 97-101 (in Russian)

Drost H , Plasma Chemistry, Akademie-Verlag, Berlin, 1978 (in German)

Drost H., Klotz H.-D., Spangenberg H.-J., Sensibilization of Plasmochemical CH_4 Conversion by C_2H_6 Addition at Pyrolytical Conditions in a Shock Tube, Seventh Int Conf. Plasma Chem., Eindhoven, 1985a, Paper P-3-1

Drost H., Behlke H., Klotz H.-D., Plasmopyrolytical Conversion of Oil Substrates to Light Hydrocarbons in a Rotating Arc Reactor, Seventh Int. Conf Plasma Chem., Eindhoven, 1985b, Paper P-3-2

Duff R.E , Bauer S H., Equilibrium Composition of the C/H System at Elevated Temperatures, J. Chem Phys., vol. 36, no. 7, 1962, pp. 1754-1767

Endyus'kin P.N , Volodin N.L., Polak L.S., Acetylene Production during Plasma Pyrolysis of Hydrocarbons, Khim Prom., no. 8, 1974, pp. 568-573 (in Russian)

Fauchais P., Bourdin E , Aubreton J , Amouroux J., Plasma Chemistry and its Applications to the Synthesis of Acetylene from Hydrocarbons and Coal, Int Chem. Eng , vol 20, no 2, 1980, pp 289-305

Fedoseyev S D., Shteiner E V., Pyrolysis of Kerosene Using a Plasma Jet, Tr Mosk Khim -Techn Inst , vol 48, 1965, pp 172-174 (in Russian)

Fey M.S., Meyer T.N., Reed W.H., Philbrook W.O , Thermal Plasma Systems for Industrial Processes, in Radio Frequency/Radiation and Plasma Processing, edited by P.N. Chereminisoff, O.G Farah and R.P Ouellette, Technomic Publishing Comp., Lancaster, Pennsylvania, 1985, pp. 117-134

Foster T , Liu G., Plasma Arc Heater Design Techniques for Commercial Process Applications, in Radio Frequency/Radiation and Plasma Processing, edited by P.N. Chereminisoff, O G. Farah and R P Ouellette, Technomic Publishing Comp., Lancaster, Pennsylvania, 1985, pp. 155-170

Frenklach M., Clary D., Gardiner W C , Stein S.E., Detailed Kinetic Modelling of Soot Formation in Shock-Tube Pyrolysis of Acetylene, Twentieth Int. Symp Comb , 1984, pp. 887-901

Gauvin W.H., Munz R J., Grosdidier de Matons P., Stuart P., The Gasification of Peat with Plasma Superheated Steam, Sixth Int. Symp. Plasma Chem , Montreal, 1983, Paper A-9-1

Gehrmann K., Schmidt H., Pyrolysis of Hydrocarbons Using a Hydrogen Plasma, Eighth World Petroleum Congress, Moscow, 1971, pp. 379-388

Gigliotti O.V., Ferrite Beads, the Noise Fighters, R.F. Des., July/August, 1983, pp. 38-45

Gladisch H., Acetylene Production in an Electric Arc, Chemie-Ing.-Techn., vol. 41, no. 4, 1969, pp. 205-208 (in German)

Goldberger W.M . Oxley J.H., Quenching the Plasma Reaction by Means of the Fluidized Bed, AIChE J., vol. 9, no 6, 1963, pp 778-782

Gomez M., Shielding - An Overview, R F. Des., July 1988, pp. 48-51

Graves R.D., Kawa W., Hiteshue R.W., Reactions of Coal in a Plasma Jet, I&EC Proc Des Dev, vol 5, no 1, 1966, pp 59-62

Griem H R., Plasma Spectroscopy, McGraw Hill, New York, 1964

Gulyaev G V., Kozlov G.I., Polak L.S , Khitrin L.N , Khudyakov G.N , The Conversion of Methane to Acetylene in a Plasma Jet, Int Chem Eng, vol 3, no. 4, 1963, pp. 531-532

Gulyaev G V , Polak L.C , Production of Acetylene from Methane in a Plasma Jet, in Kinetics and Thermodynamics of Chemical Reactions in Low Temperature Plasma, edited by L.S. Polak, Nauka, Moscow, 1965, pp. 72-99 (in Russian)

Heimann W., Mester U., Non-Contact Determination of Temperatures by Measuring the Infrared Radiation Emitted from the Surface of a Target, Inst. Phys. Conf Ser, no. 26, 1975, pp. 219-237

Hoffmann H , Kohler D., Spangenberg H -J., Conversion of a Liquid or Liquefiable Hydrocarbon Mixture into Gaseous Products, East German Patent 159081, 16 February, 1983, pp 1-10 (in German)

Honda T., Kanzawa A., Anekawa H., Gasification of Coal in the Thermal Argon Plasma, J. Chem Eng Jap., vol. 18, no.5, 1985, pp 414-419

Huczko A , Plotczyk W W., Opalińska T., Resztak A., Thermal Plasma Pyrolysis of Carbonaceous Matters, Eighth Int Symp Plasma Chem., Tokyo, 1987, paper P-063

Hunter D., OXY Joins Ethylene Plant Planners Crowd, Chemical Week, February 1, 1989, p. 8

Ibarra J V , Palacios J M., de Andrés A.M., Analysis of Coal and Char Ashes and Their Ability for Sulphur Retention, Fuel, vol. 68, no. 7, 1989, pp. 861-867

Ibberson V.J., Christofides C., Methane Pyrolysis in a Thermal Radio Frequency Electric Discharge Reactor, Third Int. Symp. Plasma Chem., Limoges, 1977, Paper G.1.4

Il'in D.T., Eremin E.N., Pyrolysis of Gasoline Vapour to Acetylene and Olefins in a Hydrogen Plasma, Int. Chem Eng , vol. 2, no. 4, 1962, pp. 524-525

Il'in D.T., Eremin E.N., Pyrolysis of Gasoline Vapour to Acetylene and Olefins in a Water Vapour-Water Plasma, Int. Chem. Eng., vol. 3, no. 2, 1963, pp. 229-230

Il'in D.T., Eremin E N., Pyrolysis of Pure Hydrocarbons and Gasoline Vapours in a Hydrogen Plasma Generated in an Electric Arc, Zh Prikl Khim , vol. 38, no. 12, 1965, pp 2786-2896 (in Russian)

JANAF Thermochemical Tables, project directors: D.R. Stull and H. Prophet, National Bureau of Standards, Washington D.C., NSRD6-NBS37, June 1971

Jenkins R G , Walker P L , Analysis of Mineral Matter in Coal, in Analytical Methods for Coal and Coal Products, ed by C. Karr, Academic Press, New York, 1978, vol. 2, pp. 265-292

Kassel L S., The Thermal Decomposition of Methane, Am Chem Soc J , vol. 54, no. 10, 1932, pp 3949-3962

Kassel L.S , The Role of Methyl and Methylene Radicals in the Decomposition of Methane, Am Chem. Soc J., vol. 57, no. 5, 1935, pp. 833-834

Kawana Y , Makino M., Kimura T., Formation of Acetylene from Coal by Argon Plasma, Int Chem Eng , vol. 7, no 2, 1967, pp 359-367

Kerker L , Muller R , The Plasma Reforming Process for the Production of Reducing Gases, Stahl u Eisen, vol 104, no. 22, 1984, pp 1137-1142 (in German)

Kevorkian V , High Temperature Chemistry of the Light Hydrocarbons, in Advances in Petroleum Chemistry and Refining, vol 5, 1962, pp 369-438

Khait, Yu. L., A Possible Mechanism of Quenching for Chemical Reactions in a Plasma Jet, in Kinetics and Thermodynamics of Chemical Reactions in Low Temperature Plasma, edited by L.S. Polak, Nauka, Moscow, 1965, pp 167-195 (in Russian)

Klotz H.-D., Drost H , Schulz G., Model Investigation of the Kinetics of the Plasmopyrolytical Conversion of CH_4/H_2 - Mixtures in a Single Pulse Shock Tube, Sixth Int Symp Plasma Chem , Montreal, 1983, Paper A-9-2

Koike T., Morinaga K., Shock Tube Studies of the Acetylene and Ethylene Pyrolysis by UV Absorption, Bull. Chem Soc Jpn , vol. 54, no. 1, 1981, pp. 530-534

Kolev K., Georgiev I., Plasma Gasification of Coal, Eighth Int. Symp Plasma Chem., Tokyo, 1987, Paper P-055

Kolobova E.A., Krukovskii V K., Popov V.T., Use of Criterial Equations for Predicting the Results of The Plasma Gasification of Irsha-Borodino Coal in Steam, translated from *Khim. Tvor. Topl.*, vol 18, No. 6, 1984, pp. 111-114

Kolobova E.A., Krukovskii V.K., Lar'kina L.T., Engel'sht V.S., Gasification of Pulverized Coal in a Water Plasma, *Izv. Akad Nauk Kirg S S R* , no 5, 1985, pp. 13-19 (in Russian)

Kozlova S.G., Kukhto V A , A Study on Conversion of Coal in an Inert Plasma, *Khim. Tvor Topl* , vol 10, no 2, 1976, pp. 82-89 (in Russian)

Kozlova S G , Kukhto V A , Lebedev V V , Krukovskii V K , Investigation of High Temperature Transformation of Mineral and Organic Parts of Coals, *Khim Tvor. Topl* , vol. 11, no 4, 1977, pp. 84-85 (in Russian)

Kovener G.S , Use of an RF Plasma for Thermal Pyrolysis of CH_4 and Heavy Oils, *Sixth Int Symp Plasma Chem* , Montreal, 1983, Paper A-8-3

Krukonis V.J., Schoenberg T., Formation of Acetylene from Coal Reacted in High-Intensity Arc, *Seventh Int. Conf. Coal Sc.*, Praha, 1968, Paper 5 132

Krukonis V.J , Gannon R.E., Deuterium and Carbon-13 Tagging Studies of the Plasma Pyrolysis of Coal, *Adv Chem Ser* , vol 131, 1974, pp. 29-41

Kubanek G., Munz R.J , Gauvin W.H , Heavy Oil Processing in Steam and Hydrogen Plasmas, *Seventh Int. Symp Plasma Chem* , Eindhoven, 1985, Paper B-2-1

Kubanek G., Munz R.J., Gauvin W.H., Heavy Oil Processing in Steam and Hydrogen Plasmas, *Can J. Chem Eng* , vol. 64, no. 10, 1986, pp 803-807

Kulczycka J., Coal and Coal Extracts Hydrogenation in an Argon-Hydrogen Plasma, *Second Polish Symp. Plasma Chem* , Czestochowa, 1974, pp. 159-168 (in Polish)

Kulczycka J., Fast Pyrolysis of Coals in a Hydrogen Plasma, *Khim Tvor Topl* , vol 12, no. 3, 1978, pp 102-108 (in Russian)

Kurowski S., Lesiński J , Mathematical Models for the Freezing Processes of the Chemical Reactions in Low Temperature Plasma Jets, *Third Polish Symp. Plasma Chem* , Lódź, 1978, pp. 229-240 (in Polish)

Kushner L.M., Plasma Technology in Acetylene Production in the US, *in Radio Frequency/Radiation and Plasma Processing*, edited by P N. Chereminisoff, O.G. Farah and R.P Ouellette, Technomic Publishing Comp., Lancaster, Pennsylvania, 1985, pp. 193-208

Lesiński J , Boulos M.I , *Thermodynamic and Transport Properties of Argon, Nitrogen and Oxygen at Atmospheric Pressure over the Temperature Range from 300 to 20 000 K*, University of Sherbrooke, Department of Chemical Engineering, Internal Report, December 1978

Lesiński J , Baronnet J.M., Meillot E., Debbagh Nour G., Modelling of Plasma Entrained-Bed Coal Gasifiers, Seventh Int. Symp Plasma Chem , Eindhoven 1985, Paper P-3-3

Leutner H.W., Stokes C.S., Producing Acetylene in a Plasma Jet, Ind & Eng Chem , vol. 53, no. 5, 1961, pp. 341-342

Lochte-Holtgreven W., Evaluation of Plasma Parameters, in Plasma Diagnostics, ed. by W. Lochte-Holtgreven, North-Holland Publishing Company, Amsterdam, 1968, pp. 134-213

Marynowski C W , Phillips R.C., Phillips J.R., Hiester N K , Thermodynamics of Selected Chemical Systems Potentially Applicable to Plasma Jet Synthesis, I&EC Fund , vol. 1, no 1, 1962, pp 52-61

Mazumdar B K , Chakrabartty S K , Lahiri A., Pyrolysis and Its Relation to the Structural Parameters of Coal, Symp on the Nature of Coal, India, 1959, paper no. 33, pp. 253-260

Melamed V.G., Mukhtarova T.A , Polak L.C., Khait Yu. L., A Method for Calculation Kinetics of Chemical Reactions in Plasma Jets (Example of Methane Conversion into Acetylene), in Kinetics and Thermodynamics of Chemical Reactions in Low Temperature Plasma, edited by L S Polak, Nauka, Moscow, 1965, pp 12-51 (in Russian)

Mellan I., Industrial Solvents Handbook, Noyes Data Corp , Park Ridge, 1977

Melik-Zade M.M., Ec'man V I., Melik-Aslanova T A., Aleperov G A , Acetylene Production from Low Octane Gasoline in a Plasma Jet, Dokl Akad Nauk Azer S S R , vol. 31, no. 11, 1975, pp 11-12 (in Russian)

Menzies M.A , Silva A.E., Denis J.M., Hydrocracking without Catalysis Upgrades Heavy Oil, Chem Eng , vol. 88, no. 4, 1981, pp. 46-47

Meubus P., Metal Vapour Effects on Chemical Reactions in an Argon Plasma, J Electrochem Soc , vol 122, no 2, 1975a, pp 298-305

Meubus P , High Temperature Propane Cracking in an Argon Plasma with the Presence of Aluminum Vapour and Tungsten Particles, Can J Chem Eng , Vol. 53, no. 10, 1975b, pp 653-658

Meubus P , Propane Cracking in an Argon Plasma Gas Irradiated by UV Light, Seventh Int. Symp Plasma Chem , Eindhoven, 1985, Paper P-3-4

Moisyeyev Yu. A., Gafarova N A , Popov V T , Pyrolysis of Hydrocarbons in a Hydrogen Plasma Jet in the Presence of Nickel Particles, Izv Akad Nauk Kaz. S.S R (Chemistry Series), no. 1, 1986, pp 69-72 (in Russian).

Mosse A.L , Menkh V A., Zabrodin V.K., Krylova I.A , Study of Several Reactor Construction Designs in Application to the Process of Oil Pyrolysis in a Plasma Jet, translated from Inz -Fiz. Zh., vol. 20, No 3, 1971, pp.

462-466

Muller R., Peuckert C., Recent Developments for the Production of Acetylene from Coal by the Huls Arc Process, Sixth Int. Symp Plasma Chem , Montreal, 1983, Paper A-8-5

Muller R., Kaske G , The Use of Plasma Chemical Processes for Chemical Reactions, Erdol Kohle Erdgas Petrochemie, vol. 37, no. 4, 1984, pp 149-155

Muller R., Kaske G., Kerker L., Huls Plasmareforming Process for the Production of Basic Chemicals, Eighth Int Symp Plasma Chem , Tokyo, 1987a, Paper P-059

Muller R. Kerker L., Proß G., Peuckert C., New Improvements and Applications for Huls Plasma Technology, Eighth Int. Symp Plasma Chem., Tokyo, 1987b, Paper DI-04

Muller R., Peuckert C., Krebs W , Praefke J., Bittner D., Brachhold H., Production of Acetylene from Coal by the Huls Plasma Process Different Operating Conditions and their Consequences for the Process, Eighth Int Symp Plasma Chem , Tokyo, 1987c, Paper P-060

Munz R.J., The Decomposition of Molybdenum Disulphide in an Induction Plasma Tailflame, Ph.D. Thesis, McGill University, 1974

Nicholson R , Littlewood K., Plasma Pyrolysis of Coal, Nature, vol 236, 21 April, 1972, pp. 397-400

Nick K.-P., Helbig V., Non-LTE Diagnostic of an Argon Arc Plasma, J. Quan. Spec. Rad Trans , vol 32, no 1, 1984, pp.1-8

Novikova G.A., Shoikhedbrod S.P., Valibekov Yu. V., Decomposition of Hydrocarbonaceous Matter into Carbon in Plasma, Dokl Akad. Nauk Tad S.S R , vol. 27, no. 9, 1984, pp. 513-516 (in Russian)

Nursultanov O.S., Polak L.S., Popov V.T., Pyrolysis of Oil Shales in a Plasma Jet, Khim Vys Ener , vol. 8, no. 5, 1974, pp. 395-400 (in Russian)

Ostroff N., Miller I F , The Kinetics of Benzene Pyrolysis in a Plasma, Chem Eng Prog Symp Ser , vol 67, 1971, pp. 109-116

Patrick A.J., Jr., Gannon R.E., A 1 MW Prototype Arc Reactor for Processing Coal to Chemicals, in Radio Frequency/Radiation and Plasma Processing, edited by P.N. Chereminisoff, O G. Farah and R.P. Ouellette, Technomic Publishing Comp., Lancaster, Pennsylvania, 1985, pp. 144-154

Peuckert C., Muller R , Acetylene from Coal by the Huls Plasma Process; Different Operating Conditions and their Consequences for the Process, Seventh Int Symp Plasma Chem , Eindhoven, 1985, Paper P-3-5

Plooster M.N., Reed T B., Carbon-Hydrogen-Acetylene Equilibrium at High

Temperatures, J. Chem. Phys , vol. 31, no. 1, 1959, pp 66-72

Plotczyk W.W., Effect of Quenching Temperature on the Synthesis of Acetylene from Methane in a Hydrogen Plasma Jet, Sixth Int Symp Plasma Chem., Montreal, 1983, Paper A-9-5

Plotczyk W.W , Thermodynamic Models for Acetylene Synthesis in an Argon Plasma Jet, Seven Int Symp. Plasma Chem., Eindhoven, 1985, Paper P-3-6

Plotczyk W W., Szymański A., Trepczyński J., Methane Pyrolysis in a Hydrogen Plasma Jet with a Liquid Hydrocarbons Quench, Przem Chem , vol. 65, no 10, 1986, pp. 543-545 (in Polish)

Polak L.S., Scientific, Technical and Financial Basis for Plasmochemical Conversion of Petroleum and Natural Gas, Seventh World Petroleum Congress, Mexico, 1967, pp 283-292 (in French)

Polak L.S., Endyus'kin P N., Uglev V.N., Volodin N.L., Acetylene and Olefins Production by Crude Oil Pyrolysis in a Hydrogen Plasma Jet, Khim Vys Ener., vol. 3, no. 2, 1969, pp. 184-185 (in Russian)

Polak L.S., Plasmochemical Pyrolysis of Gaseous and Liquid Hydrocarbons, Eight World Petroleum Congress, Moscow, 1971, pp. 367-370

Pustovoytenko A I., Thermodynamic Analysis of Product Distribution from the High Temperature Pyrolysis of Fossil Fuels, Khim. Tvor Topl , vol. 13, no. 5, 1979, pp 103-109 (in Russian)

Rahimi P M., Fouda S.A , Kelly J.F , Malhotra R , McMillen D F., Characteristics of CANMET Coprocessing Distillates at Different Coal Concentrations, Fuel, vol. 68, no 4, 1989, pp. 424-429

Resztak A., Plotczyk W W., Evaluation of Usefulness of a Modified Method for Volatiles Determination in Studies on Coal Pyrolysis in Plasma, Koks-Smola-Gaz, vol. 30, no. 1, 1985, pp 12-15 (in Polish)

Rice F.O., Dooley M D., The Thermal Decomposition of Organic Compounds from the Standpoint of Free Radicals. XII. The Decomposition of Methane, Am Chem. Soc J , vol. 56, no. 12, 1934, pp. 2747-2749

Rivenburg H.C., Juba J , Simple Approaches to Limiting Radiation from Foil-Shielded Computer Cables, R.F Des., February 1986, pp 72-76

Rozanova M.V., Sidorov V.I., Pyrolysis of Gasoline and Diesel Fuel at High Temperatures, Khim. Prom-St , no. 2, 1976, pp. 100-102 (in Russian)

Russel S.J , Rimmer S.M., Analysis of Mineral Matter in Coal, Coal Gasification Ash, and Coal Liquefaction Residues by Scanning Electron Microscopy and X-Ray Diffraction, in Analytical Methods for Coal and Coal Products, ed. by C Karr, Academic Press, New York, 1978, vol 3, pp. 133-162

Sennewald K , Schallus E., Pohl F., Acetylene Production from Thermally Cracked Hydrocarbons Using Very Hot Hydrogen, Chemie-Ing -Techn., vol. 35, no. 1, 1963, pp. 1-6 (in German)

Shantarovich P.C., Pavlov B.V., Mechanism of Methane Decomposition, Zh Fiz Khim , vol. 30, no. 4, 1956, pp. 811-820 (in Russian)

Sheer C., Korman S., Arc Synthesis of Hydrocarbons, Adv. Chem Ser , vol. 131, 1974, pp. 42-53

Sitting M, Handbook of Toxic and Hazardous Chemicals and Carcinogens, Moyes Publications, Park Ridge, 1985

Smith W R , Missen R W., Chemical Reaction Equilibrium Analysis Theory and Algorithms, John Wiley & Sons, New York, 1982

Smith J M , Van Ness H C., Introduction to Chemical Engineering Thermodynamics, third edition, McGraw-Hill, New York, 1975

Spangenberg H -J., Borger I., Schirmer W., Thermodynamic Functions for Different Carbon-Hydrogen-Nitrogen Compounds and Radicals at High Temperatures and Composition of CHN Plasmas, Z. Phys Chem (Leipzig), vol. 255, no. 1, 1974, pp. 1-15 (in German)

Spangenberg H.-J , Borger I , Hoffmann H., Mogel G., Formation of Acetylene Derivatives from Hydrocarbons during Plasma Pyrolysis and the Role of C_2H Radicals, Z Phys. Chem. (Leipzig), vol. 259, no. 3, 1978, pp 531-544 (in German)

Spangenberg H.-J., Formation and Decomposition of Acetylene in Thermal Plasma, Z Chem , vol. 21, no 5, 1981, pp. 165-175 (in German)

Spangenberg H.-J., Borger I., Lachmann J., Is there a Relationship between the Number of Primary Carbon Particles and Ion Density in the Thermal Plasma Pyrolysis of Hydrocarbon Gas ?, Ber Bunsenges Phys Chem , vol 87, no 12, 1983, pp. 1217 - 1222 (in German)

Spangenberg H -J , Borger I., Lachmann J., Physicochemical Conditions during the Pyrolysis of Hydrocarbons in a Plasma Jet, Seventh Int Symp. Plasma Chem., Eindhoven, 1985, Paper P-3-8

Spangenberg H.-J , Borger I , Drost H., Klotz H.-D., Measured and Calculated Distributions of Chemical Species during the Pyrolysis of Methane in Plasma Jets and behind Reflected Shock Waves, Z Phys Chem. (Leipzig), vol. 267, no. 6, 1986, pp. 1081-1097

Stuart P R., Munz R.J., Gauvin W.H., Synthesis Gas Production Using a Steam Plasma, Plasma Chem Plasma Proc , vol. 4, no. 4, 1984, pp. 297-313

Sundstrom D W , DeMichiell R.L., Quenching Process for High Temperature Chemical Reactions, I&EC Proc Des Devel , vol. 10, no. 1, 1971, pp. 114-122

Szymański A., Galska-Krajewska, Coal Pyrolysis in Various Plasmochemical Reactors, First Polish Symp Plasma Chem., Warsaw, 1971, pp. 306-311 (in Polish)

Szymański A , An Energy Criterion for the Processes Occurring in a Chemical Plasma Reactor, Third Int Symp Plasma Chem., Limoges, 1977, Paper G.1.16

Szymański A., Chemical Processes in the Low-Temperature Plasma Jet, Third Polish Symp. Plasma Chem , Lódź, 1978, pp. 193-206 (in Polish)

Szymański A , Resztak A., Plotczyk W.W , Reactions of Liquid Hydrocarbons in an Argon Plasma, Third Polish Symp. Plasma Chem., Lodź, 1978a, pp. 386-395 (in Polish)

Szymański A., Resztak A., Podgórski A., Brzeski J., Effect of Process Parameters on the Effectiveness of Plasma Pyrolysis of Coal, Third Polish Symp Plasma Chem , Lodź, 1978b, pp 381-386 (in Polish)

Szymański A , Resztak A , Trepczyński J , A Method for Forecasting Thermal Efficiency of a Chemical Plasma Reactor during Acetylene Production from Methane in a Hydrogen Plasma Jet, Third Polish Symp. Plasma Chem , Lodź, 1978c, pp. 409-418 (in Polish)

Szymański A., Effect of Some Parameters on Process of Plasma Pyrolysis of Coal, Khim. Tvor Topl , vol. 13, no. 1, 1979, pp 84-86 (in Russian)

Szymański A., Plotczyk W.W., Resztak A., Huczko A., Brown Coal Pyrolysis in a Hydrogen Plasma Jet, Sixth Int Symp. Plasma Chem , Montreal, 1983, Paper A-9-4

Szymański A , Plotczyk W.W., Resztak A., Brzeski J., Opalińska T., Plasma Pyrolysis of Brown Coal in a Flow Reactor, Seventh Int. Symp Plasma Chem., Eindhoven, 1985, Paper P-3-7

Tanzawa T., Gardiner W.C. Jr., Thermal Decomposition of Acetylene, Seventeenth Int. Symp Comb., University of Texas at Austin, 1978, pp. 563-573

Themelis N.J., Gauvin W.H., A Two-Wavelength Pyrometer for Temperature Measurements in Gas-Solid Systems, Can. J. Chem Eng., vol. 40, no. 8, 1962, pp. 157-161

Thorpe M L , Production of Superheated Hydrogen Plasma Using Induction Heating of Cold Plasma and DC Plasma Enhancement, NASA Contractor Report CR-657, 1966

Thorpe M.L , Induction Plasma Heating: System Performance, Hydrogen Operation and Gas Core Reactor Simulator Development, NASA Contractor Report CR-1143, 1968

Thorpe M.L., Scammon L.W., Induction Plasma Heating: High Power, Low

Frequency Operation and Pure Hydrogen Heating, NASA Contract NAS 3-9375, 1968

Touloukian Y.S., DeWitt D.P., Thermal Radiation Properties, in Thermophysical Properties of Matter, ed by Y.S. Touloukian and C.Y. Ho, IFI/Plenum, vol. 7-9, New York, 1970-1972

Towell G.D., Martin J.J., Kinetic Data From Nonisothermal Experiments: Thermal Decomposition of Ethane, Ethylene, and Acetylene, AIChE J, vol 7, no. 4, 1961, pp. 693-698

Tsentsiper A.B, Eremin E N., Kobozev N.I., A Comparative Study of Reaction Kinetics in Batch Conversion of Various Hydrocarbons to Acetylene Using an Electric Arc Torch, Int. Chem Eng., vol. 2, no. 3, 1962, pp. 412-415

Venugopalan M., Roychowdhury U.K., Chan K., Pool M.L., Plasma Chemistry of Fossil Fuels, in Topics in Current Chemistry, vol. 90, Plasma Chemistry II, edited by S. Veprek and M Venugopalan, Springer-Verlag, Berlin 1980, pp. 1-57

Vurzel F.B., Polak L.S, Acetylene and Olefins Production from Some Hydrocarbons and Gasoline in a Plasma Jet, in Kinetics and Thermodynamics of Chemical Reactions in Low Temperature Plasma, edited by L.S Polak, Nauka, Moscow, 1965a, pp. 100-117 (in Russian)

Vurzel F.B., Polak L.S, Chemical Processes in Plasma and in Plasma Jets (Literature Review), in Kinetics and Thermodynamics of Chemical Reactions in Low Temperature Plasma, edited by L.S. Polak, Nauka, Moscow, 1965b, pp. 238-253 (in Russian)

Vurzel F B., Polak L S., Plasma Chemical Technology - the Future of the Chemical Industry, Ind & Eng. Chem, vol. 62, no 6, 1970, pp. 8-22

Vurzel F.B., Polak L.S, Epshtein I.L., Kinetics of Plasma Pyrolysis of Hydrocarbons, Second Soviet Symp. Plasma Chem, Riga, 1975, pp 156-159 (in Russian)

White W.B, Johnson S.M., Dantzig G.B., Chemical Equilibrium in Complex Mixtures, J Chem. Phys, vol. 28, no. 5, 1958, pp. 751-755

Winkelmann G., Lachmann J., Spangenberg H.-J., Spectroscopic Determination of Temperature Profiles during Methane Pyrolysis in Nitrogen Plasma Jet, Ber. Bunsen-Ges., vol. 81, no. 4, 1977, pp. 432-437 (in German)

Yakovlev E A, Plastinin B.G., Polak L.S., Popov V.T., High Temperature Conversion of Liquid Hydrocarbons in Water Vapour/Air Atmosphere, Khim Vys Ener., vol. 16, no. 5, 1982, pp. 454-457 (in Russian)

Zabrodin V.K., Krylova I.A., Mosse A.L., Ermolayeva I.M., Crude Oil Pyrolysis in a Methane - Hydrogen Plasma Jet in a Counter Flow Reactor, Khim Vys. Ener, Vol. 7, no. 6, 1973 (in Russian)

Zeleznik F.J., Gordon S., Equilibrium Computations for Multicomponent Plasmas, Can J. Phys., vol 44, 1966, pp. 877-893